

**Physical chemistry and engineering  
of membranes  
for fat/fatty acid separations**

CENTRALE LANDBOUWCATALOGUS



0000 0424 2034

BIBLIOTHEEK  
LANDBOUWUNIVERSITEIT  
WAGENINGEN

Promotor: dr. ir. K. van 't Riet  
hoogleraar in de levensmiddelenproceskunde

Co-promotor: dr. M. A. Cohen Stuart  
universitair hoofddocent in de fysische- en kolloïdchemie

Jos Keurentjes

# Physical chemistry and engineering of membranes for fat/fatty acid separations

## Proefschrift

ter verkrijging van de graad van  
doctor in de landbouw- en milieuwetenschappen,  
op gezag van de rector magnificus,  
dr. H. C. van der Plas,  
in het openbaar te verdedigen  
op woensdag 6 maart 1991  
des namiddags te vier uur in de aula  
van de Landbouwniversiteit te Wageningen.

## STELLINGEN

---

1. In tegenstelling tot de klassieke methoden ter bepaling van de kritische oppervlaktespanning van vaste oppervlakken is oppervlakteruwheid juist bevorderlijk wanneer de "plakkende luchtbel" methode wordt gebruikt.

Dit proefschrift, hoofdstuk 4

2. Gelet op het feit dat de rejectie over het algemeen sterk varieert met de concentratie, is het gebruik van "de rejectie" als maat voor het scheidend vermogen van een membraan misleidend.
3. Maruyama et al. schrijven enantiomeerscheiding met behulp van een met (n-nonylphenoxy)-oligo(oxyethyleen) gederivatiseerd poly(L-glutamaat) membraan toe aan het ontstaan van een geordende vloeibaar kristallijne structuur en gaan ten onrechte voorbij aan het feit dat een membraan van louter poly(L-glutamaat) ook zou hebben geresulteerd in enantioselectiviteit.

A. Maruyama, N. Adachi, T. Takatsuki, M. Torii, K. Sanui and N. Ogata, Enantioselective permeation of  $\alpha$ -amino acids isomers through poly(amino acid)-derived membranes, *Macromolecules*, 23 (1990) 2748-2752

4. De conclusie van Vocel en Ryan, dat geadsorbeerde polymeerlagen geen zwichtspanning zouden vertonen, is wat voorbarig, omdat in het gebied waarin zij afschuifspanningen hebben aangelegd ook geen zwichtspanning te verwachten zou zijn.

J. Vocel and J.T. Ryan, Surface rheological properties of polymer-surface active agent solutions, *Can. J. Chem. Eng.* 49 (1971) 425-429

5. Door voorbij te gaan aan mogelijke conformatieveranderingen is de door van Oss et al. voorgestelde methode ter bepaling van de oppervlaktespanning van eiwitten niet correct.

C.J. van Oss, D.R. Absolom, A.W. Neumann and W. Zingg, Determination of the surface tension of proteins I. Surface tension of native serum proteins in aqueous media, *Biochim. Biophys. Acta* 670 (1981) 64-73

6. De resultaten van Koster en Cramer betreffende de remming van methanogeen korrelslib door langketenige vetzuren worden vertroebeld door voorbij te gaan aan de maximale oplosbaarheid van de calciumzouten van deze vetzuren.

I.W. Koster and A. Cramer, Inhibition of methanogenesis from acetate in granular sludge by long-chain fatty acids, Appl. Environ. Microb. 53 (1987) 403-409

7. Ook sociale systemen kunnen uitstekend beschreven worden met de Maxwell-Stefan theorie.
8. Het opzetten van een adequaat openbaar vervoersysteem in Nederland zal gepaard moeten gaan met een verdergaande urbanisatie.
- 9a. Het spelen van oude muziek op authentieke instrumenten is niet zinvol, omdat in het geval de desbetreffende componisten de beschikking hadden gehad over hedendaagse instrumenten, zij hun muziek daarop hadden laten spelen.
- b. Wil men echter toch op authentieke wijze spelen dan dient het geproduceerde dienovereenkomstig vals te zijn.
10. Gezien de kwaliteit van het Rijnwater is eau de Cologne meer dan eau de toilette.

Jos Keurentjes

Physical chemistry and engineering of membranes for fat/fatty acid separations

Wageningen, 6 maart 1991

*Voor Hanneke*  
*Voor mijn ouders*

## VOORWOORD

---

Onderzoek kan geen solowerk zijn en de resultaten zoals beschreven in dit proefschrift zijn dan ook tot stand gekomen dankzij de inspanningen van een groot aantal personen, van wie ik er hier een aantal met name wil bedanken.

Klaas van 't Riet, met bewondering heb ik gekeken naar jouw enthousiaste manier om een meute onderzoekers op het spoor te zetten en te houden. De vrijheid die je daarbij geeft voor een persoonlijke invulling van het onderzoek heb ik uitermate gewaardeerd.

Martien Cohen Stuart, hoewel het bij aanvang van dit onderzoek niet als zodanig in de planning stond ben je er steeds meer bij betrokken geraakt. Naast het verschaffen van enig inzicht in de grensvlakchemie heb je ook mijn Engels ontdaan van de grootste kronkels.

Albert van der Padt, we zijn samen in het diepe bad van het onderzoek gedoken en onze schier eindeloze discussies hebben mij doen inzien dat twee meer is dan één plus één. Intussen hebben we allebei een beetje leren zwemmen.

Doctoraalstudenten Karin Bosklopper, Anja Janssen, Jos Sluijs, Jolan Harbrecht, Dick Brinkman, Astrid van Triet, Ferry Sommerdijk, Arnold Broek, Robert-Jan Franssen, Karin Schroën, Victoire de Wild, Leonie Linders, John Kruijtzter en Freek Verhoeven, jullie hebben een geweldige berg werk verzet en het was mij een genoegen om met jullie samengewerkt te hebben.

Gésinda Doornbusch en in een later stadium Birgit Hasenack, jullie hebben met eindeloze reeksen proefjes de nodige gaten gestopt.

Kamergenoten, mijn dank voor de sfeer, inhoudelijke discussies en de koffie.

Wim Beverloo en Gerrit Meerdink, door jullie inspanningen ben ik toch een beetje procestechnoloog geworden.

Jan-Henk Hanemaaijer, jij hebt me enig inzicht gegeven in het wat en hoe van membranen en vanuit het NIZO en later TNO met raad en materiaal bijgestaan.

Medewerkers van de werkplaats, tekenkamer en fotolokatie van het Biotechnion, jullie wil ik hartelijk bedanken voor de behulpzaamheid en de geleverde kwaliteit van apparaten, tekeningen en foto's.

Alle medewerkers van de sectie Proceskunde, door de goede sfeer en collegialiteit was er op elke vraag wel een antwoord voorhanden. Bedankt voor deze geweldige vier jaar.

Jos Keurentjes



## CONTENTS

---

|                  |  |     |
|------------------|--|-----|
| Chapter 1        | Introduction   | 1   |
| Chapter 2        | The removal of fatty acids from edible oil; removal of the dispersed phase of a water in oil dispersion by a hydrophilic membrane  | 11  |
| Chapter 3        | Multicomponent diffusion in dialysis membranes   | 29  |
| Chapter 4        | Hydrophobicity measurements of MF and UF membranes   | 53  |
| Chapter 5        | Surfactant-induced wetting transitions: role of surface hydrophobicity and effect on oil permeability of ultrafiltration membranes | 67  |
| Chapter 6        | Extraction and fractionation of fatty acids from oil using an ultrafiltration membrane   | 89  |
| Chapter 7        | Membrane cascades for the separation of binary mixtures  | 113 |
| Chapter 8        | Concluding remarks; the improvement of membrane performance  | 133 |
| Summary          |  | 147 |
| Samenvatting     |  | 151 |
| Curriculum Vitae |  | 155 |

## INTRODUCTION

---

### 1.1 MEMBRANE PROCESSES

In the past two decades the range of conventional separation techniques such as distillation, crystallization and extraction has been extended with membrane separation processes. Several authors have given definitions of a membrane. In 1975 Hwang and Kammermeyer [1] defined a membrane as "a region of discontinuity interposed between two phases". Later, in 1984 Lakshminarayanaiah [2] defined a membrane as a "phase that acts as a barrier to prevent mass movement but allows restricted and/or regulated passage of one or more species through it". In 1986, the European Society of Membrane Science and Technology defined a membrane as "an intervening phase separating two phases and/or acting as an active or passive barrier to the transport of matter between phases adjacent to it" [3]. From these definitions it will be obvious that a membrane can be solid, liquid or gaseous and that it provides a separation.

Membrane separation processes may vary in their mode of operation and in their application. They are often more efficient and more economical than the conventional separation techniques mentioned above (distillation, crystallization and extraction) [4]. Many applications in the food and pharmaceutical industry and in biotechnology often require the processing of temperature-sensitive products. Since most membrane processes are performed at ambient temperatures, they can offer clear advantages as compared to the conventional separation processes.

In table 1 some of the technically relevant membrane separation processes are summarized. In reverse osmosis (RO), ultrafiltration (UF) and microfiltration (MF) a hydrostatic pressure difference is the driving force. In these processes the membrane acts as a sieve and retains molecules or particles larger than the pore diameter. Gas separations use the same pressure difference as a driving force, and a difference in solubility in the membrane material results in a separation. In electrodialysis, ion-exchange membranes are used and applying an electrical potential difference results in the separation of charged components. In dialysis and liquid membrane processes, a combined exclusion/extraction mechanism is used. Exclusion is used to avoid the passage of molecules or particles which are soluble in the extraction phase, and a

concentration gradient causes transport of the required component.

**Table 1.** *Some technically relevant membrane separation processes and some of their applications*

| Process               | Driving force                      | Applications  |
|-----------------------|------------------------------------|---|
| RO                    | pressure difference                | -desalination of sea/brackish water [5]<br>-concentration of whey and fruit juice [6,7,8]<br>-waste water treatment [9,10,11]   |
| UF                    | pressure difference                | -purification/concentration juices and polymer solutions [12]<br>-protein recovery [13]<br>-waste water treatment [14]          |
| MF                    | pressure difference                | -filtration of cell suspensions [15]<br>-blood plasma recovery [16]<br>-filtration of particles and cells from air streams [17] |
| Gas separation        | pressure difference                | -oxygen enriched air [18]<br>-purification natural gas [19]   |
| Electro-dialysis      | electric potential difference      | -demineralization [20]<br>-removal of metals from waste water [21,22]   |
| Dialysis              | concentration difference           | -purification polymer solutions [23]<br>-hemodialysis [24]  |
| Liquid membrane       | solubility difference              | -metal recovery [25,26]   |
| Membrane extraction   | solubility difference              | -L-L extractions [27]<br>-metal extraction [28,29]  |
| Membrane distillation | partial vapour pressure difference | -desalination of sea/brackish water [30,31]<br>-boiler feed water production [32]   |
| Pervaporation         | partial vapour pressure difference | -separation azeotropic mixtures [33]<br>-dewatering organic liquids [34]  |

Finally, membrane distillation uses a partial vapour pressure difference as a driving force, and pervaporation uses, in addition to this partial vapour pressure difference, a difference in solubility in the membrane material.

## 1.2 MEMBRANES IN TWO-PHASE SYSTEMS

From the processes mentioned in table 1, only a few apply to two phase systems. There are RO and UF applications for the separation of emulsions, although only the removal of the water phase from oil in water (o/w) emulsions is considered. The membrane should then preferentially be wetted by the water phase and applying a static pressure difference over the membrane results in the permeation of this phase. Most of these applications are found in industrial waste water treatment, mainly in the metal-finishing industry [35,36,37]. The removal of water reduces the volume of the o/w emulsion. The concentrated emulsion can then be reused or can be incinerated [5,12].

In processes such as membrane extraction, liquid membranes and membrane distillation two phases are involved. In the first process (figure 1) a porous membrane is used to keep two liquid phases separated and it provides a defined liquid-liquid interface, thus avoiding emulsification [38,39]. This is a clear advantage in the case of extraction with liquids having a low interfacial tension. In the case of liquid membranes, the membrane is a thin liquid film that is stabilized by a microporous polymer membrane in the case of a so-called immobilized liquid membrane (figure 2) [25,26]. In the case of membrane distillation the membrane phase is a vapour (figure 3) [30,31,32].

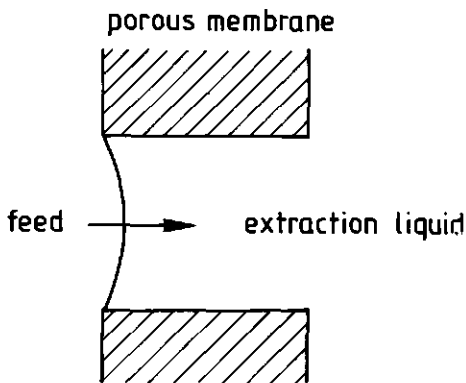


Figure 1. Membrane extraction

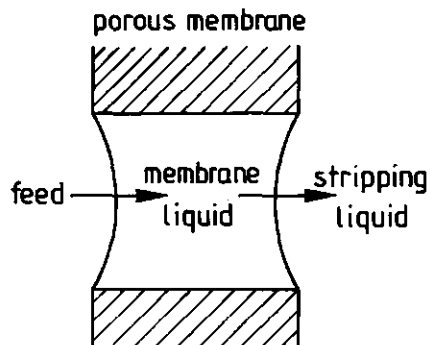


Figure 2. Solid-supported liquid membrane

The use of a membrane to keep two phases separated may serve other purposes as well. In some

biotechnological applications membranes are used as a bioreactor in which the membrane acts as a carrier for enzymes (mainly lipases) that require substrates from two phases. The same conversions can be carried out in an emulsion system, however, this results in the formation of a stable emulsion that has to be broken in order to obtain the products. Using a membrane, the formation of emulsions can be avoided, and since the enzyme can be immobilized, reuse of the enzyme can be achieved [40,41,42,43]. In all these processes, the membrane is preferentially wetted by one of either two phases, and the polymer membrane merely acts as a (non-separative) carrier to obtain a stable system. Besides, it will also prevent solid particles to pass through the membrane, which usually results in a rather pure product stream [44].

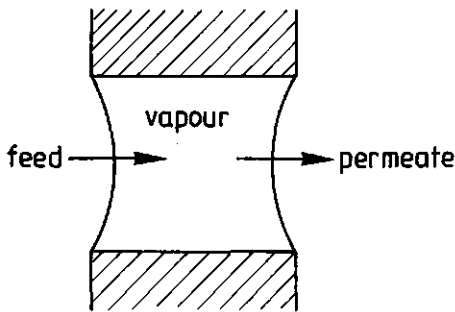


Figure 3. *Membrane distillation;  $T_{\text{feed}} > T_{\text{permeate}}$*

Whenever two-phase systems are studied, wetting of the polymer matrix by these two phases plays an important role. As stated above for the separation of emulsions, one of the two phases should preferentially wet the membrane (i.e. exhibit a contact angle with the surface  $< 90^\circ$ ), so that it will penetrate into the pores. The other phase cannot enter the pores as a result of the adverse Laplace pressure, which is for cylindrical pores:

$$\Delta P = \frac{2\gamma \cos \alpha}{R} \quad (1)$$

in which  $\Delta P$  is the pressure difference over the interface,  $\gamma$  the interfacial tension,  $\alpha$  the contact angle of the non-wetting phase with the surface and  $R$  the pore radius. Wettability of the membrane is determined by both the membrane characteristics (hydrophobicity and pore size) as well as the liquid properties (e.g. surface tension [45]). For the application of supported liquid membranes it is important that the polymer membrane is not wetted by one of the two liquid phases outside the membrane (i.e. they exhibit a contact angle larger than  $90^\circ$ ), otherwise the

liquid inside the pores will be displaced by one of the liquids outside the membrane.

### **1.3 FAT/FATTY ACID SEPARATION**

The separation of fatty acids from non-mineral oil is a process applied worldwide on a large scale in the refinery of edible fats and oils [46,47]. The conventional separation method (the so-called caustic refining) consists of the addition of an aqueous alkali solution to the oil at a temperature of around 90°C, resulting in the formation of the sodium salts of the fatty acids. The thus formed soapstock is separated from the oil by centrifugation. The application of this process, however, has one major drawback: the soapstock leaving the system contains considerable amounts of triglycerides (usually about 50% [48]), which are considered as a loss. For this reason, the caustic refining of oils containing high concentrations of fatty acids (e.g. rice bran oil) is not an economical process.

In the enzymatic hydrolysis of fats in a membrane bioreactor, the reaction rate rapidly decreases with an increase in fatty acid content of the oil phase [41]. To maintain a high reaction rate, the fatty acids have to be removed from the oil stream. Obviously, the classical caustic refining procedure can not be used for this purpose for two reasons. Firstly, the elevated temperature and the added alkali will inactivate the enzyme. Secondly, the poor quality of the product, as the soapstock only contains 50% fatty acids.

Alternative process designs are known [49,50,51,52], of which steam distillation is the one in which losses of triglycerides can be avoided. However, in the proposed extraction processes only a partial separation is achieved. Membrane separations can be an alternative when the requirements of selectivity, low temperature and economics are met [53].

### **1.4 MEMBRANE PROCESSES FOR THE SEPARATION OF FATTY ACIDS FROM EDIBLE OIL AND OUTLINE OF THIS THESIS**

Reports on the application of membranes in oil refining are only concerned with the filtration of one or more constituents from the oil [53,54,55]. The application of such a filtration step for the removal of fatty acids from the oil stream may result in a reduction of the triglyceride losses with 60% [53,54]. For the refining of edible oils this may be sufficient to make the process viable, however, this still implies a significant loss for removing fatty acids from the oil stream in the

enzymatic hydrolysis of oils. In this thesis two possible process schemes for the separation of fatty acids from oil without losses of triglycerides are presented, the two having in common that membranes are used in a two-phase environment. It is the aim of this thesis to study the engineering and physico-chemical phenomena that are relevant for the operation of these processes.

In the first system [56,57] (figure 4), an aqueous alkali solution is added to the oil, thus forming the sodium salts of the fatty acids. Subsequently, 2-propanol is added in order to solubilize the soaps and to form a system of two immiscible liquids. The water phase contains water, 2-propanol and the soaps, whereas the oil phase contains triglycerides and a trace amount of 2-propanol. This two-phase system can be separated into the two separate phases by a hydrophilic and a hydrophobic membrane in series, where the water phase permeates through the hydrophilic and the oil phase through the hydrophobic membrane. It appears to be impossible to detect triglycerides in the water phase, nor fatty acids in the oil phase (provided sufficient sodium hydroxide is added), indicating that the separation is complete in this respect.

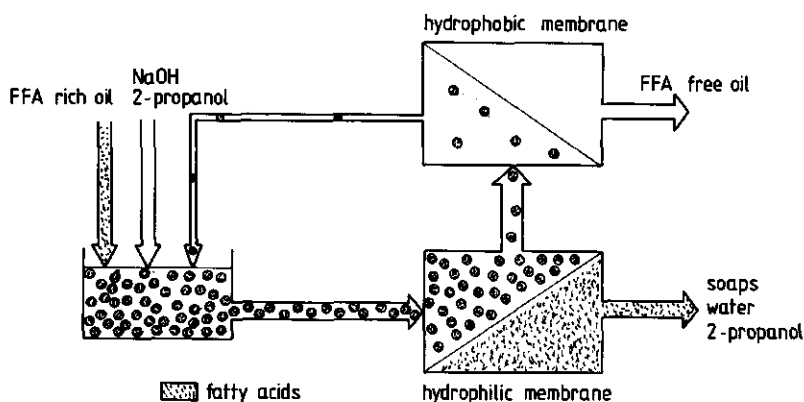


Figure 4. Two-membrane system for the removal of fatty acids from oil

In chapter 2 of this thesis this two-phase system will be characterized and the factors affecting the performance of the hydrophilic membrane will be investigated. In chapter 3 multicomponent transport phenomena through a hydrophilic homogeneous cellulose membrane will be described. On the basis of this description an enhanced permeation rate of the aqueous phase can be achieved. In chapter 4 a method is described for the measurement of hydrophobicity of membrane materials, since this will influence the wettability of the material by each of the phases. In chapter

5, the effect of adsorption of sodium oleate on the wetting behaviour is studied as a function of surface hydrophobicity, resulting in the design of a membrane for the separation of the oil phase from the two-phase system.

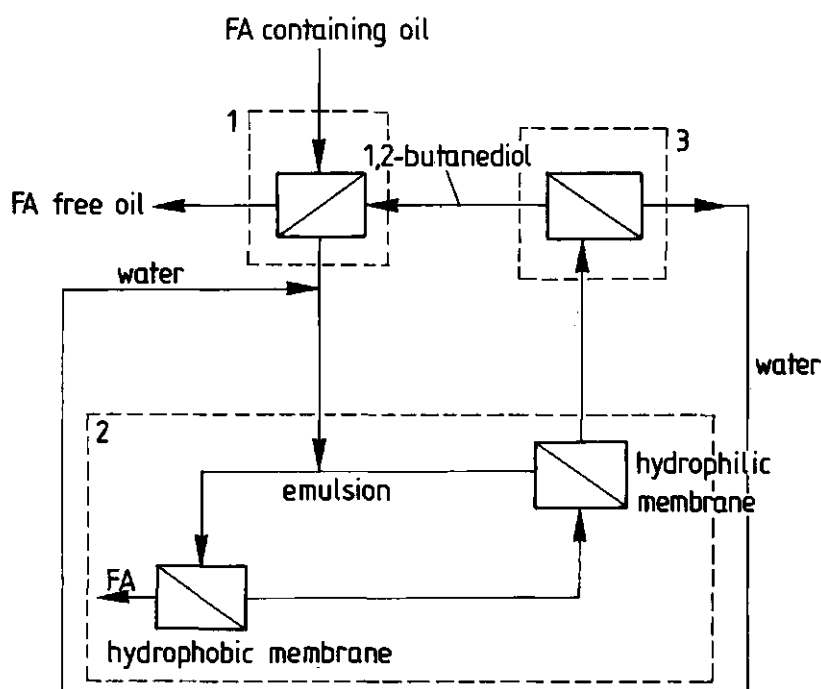


Figure 5. 3-step fatty acid removal from oil; step 1 is extraction, step 2 is emulsion separation and step 3 is dewatering

A second possible system for the separation of fatty acids from edible oil is depicted in figure 5. In the first step the fatty acids are extracted from the oil using a 1,2-butanediol/water (20:1 v/v) mixture. Subsequently, water is added to the system, which demixes as a result of the water addition, forming a dispersion of fatty acids in a 1,2-butanediol/water (6.5:3.5 v/v) mixture. The thus formed dispersion can be separated by centrifugation or by the two-membrane system as described above. Finally, excess water has to be removed from the 1,2-butanediol/water mixture. This can, for example, be achieved using reverse osmosis membranes.

In chapter 6 the extraction of fatty acids from oil using cellulosic membranes is described, a method that can also be used for the fractionation of fatty acid mixtures. Using membranes for



the separation of the water/1,2-butanediol mixture a multistage process will be required, since it is only possible to achieve a partial separation. In chapter 7 calculations are made on membrane cascades for the separation of binary mixtures, using a butanediol/water mixture as an example.

Obviously, the three steps involved in this system (extraction, emulsion separation and dewatering) can be performed by classical processes like liquid-liquid extraction, centrifugation and evaporation, respectively, and can be combined with the membrane processes in the most economical configuration. This thesis provides the engineering data and models to make a thorough costs analysis for the evaluation of the viability of any of these three steps.

## REFERENCES

- 1) Hwang, S.T. and K. Kammermeyer, *Membranes in Separations*, Wiley-Interscience Publications, John Wiley and Sons, New York, 1975
- 2) Lakshminarayanaiah, N., *Equations of Membrane Biophysics*, Academic Press, New York, 1984
- 3) Gekas, V., *Terminology for Pressure Driven Membrane Operations*, European Society of Membrane Science and Technology, 1986
- 4) Strathmann, H., *Synthetic Membranes and their Preparation*, in: *Synthetic Membranes: Science, Engineering and Applications*, P.M. Bungay, H.K. Lonsdale and M.N. de Pinho (eds.), NATO ASI Series, Series C: Mathematical and Physical Sciences Vol. 181, D. Reidel Publishing Company, Dordrecht, 1986
- 5) Sourirajan, S. and T. Matsuura, *Reverse Osmosis/Ultrafiltration, Process Principles*, National Research Council Canada, Ottawa, 1985
- 6) Kimura, S. and S. Sourirajan, Transport characteristics of porous cellulose acetate membranes for the reverse osmosis separation of sucrose in aqueous solutions, *Ind. Eng. Chem. Proc. Des. Dev.* 7 (1968) 548-554
- 7) Pereira, E.N., T. Matsuura and S. Sourirajan, Reverse osmosis separations and concentrations of food sugars, *J. Food Sci.* 41 (1976) 672-680
- 8) Baxter, A.G., M.E. Bednas, T. Matsuura and S. Sourirajan, Reverse osmosis concentration of flavor components in apple juice- and grape juice- waters, *Chem. Eng. Comm.* 4 (1980) 471-483
- 9) McDermott, G.N., M.A. Post, B.N. Jackson and M.B. Ettinger, Nickle in relation to activated sludge and anaerobic digestion processes, *J. Water Pollut. Control Fed.* 37 (1965) 163-177
- 10) Spatz, D.D., Reclaiming valuable metal wastes, *Pollut. Eng.* 4 (1972) 24-26
- 11) Liu, T., T. Matsuura and S. Sourirajan, Effect of membrane materials and average pore sizes on reverse osmosis separation of dyes, *Ind. Eng. Chem. Prod. Res. Dev.* 22 (1983) 77-85
- 12) Cheryan, M., *Ultrafiltration Handbook*, Technomic Publishing Company, Inc., Lancaster, 1986
- 13) Cheryan, M. and K.P. Kuo, Hollow fibers and spiral wound modules for ultrafiltration of whey: energy consumption and performance, *J. Dairy Sci.* 67 (1984) 1406-1413
- 14) Hayward, M.F., Ultrafiltration and reverse osmosis: a survey of industrial applications, *Proc. 3<sup>rd</sup> World Filtration Congress* (1982) 572-583
- 15) Defrise, D and V. Gekas, Microfiltration membranes and the problem of microbial adhesion, a literature survey, *Process Biochemistry* 23 (1988) 105-116
- 16) Solomon, B.A., F. Castino, M. Lysaght, C.K. Colton and L. Friedman, Continuous flow membrane filtration of

## chapter 1

- plasma from whole blood, *Trans. Am. Soc. Artif. Internal Organs* 24 (1978) 21-26
- 17) Koslow, E.E., System for removing contaminant particles from a gas, US patent 4,537,608, 1985
  - 18) Weller, S. and W.A. Steiner, Engineering aspects of separation of gases: fractional permeation through membranes, *Chem. Eng. Progress* 46 (1950) 585-590
  - 19) Agrawal, J.P. and S. Sourirajan, High flux freeze-dried cellulose acetate reverse osmosis membranes as microporous barriers in gas permeation and separation, *J. Appl. Polym. Sci.* 14 (1970) 1303-1321
  - 20) Audinos, R., Fouling of ion-selective membrane during electrodialysis of grape must, *J. Membrane Sci.* 41 (1989) 115-126
  - 21) Raghawa Rao, J., B.G.S. Prasad, V. Narasimkhar, T. Ramasami, P.R. Shah and A.A. Khan, Electrodialysis in the recovery and reuse of chromium from industrial effluents, *J. Membrane Sci.* 46 (1989) 215-224
  - 22) Sridhar, S., Desalination and recovery of catalysts by electrodialysis, *Proc. 6<sup>th</sup> International Symposium on Synthetic Membranes in Science and Industry*, Tübingen, F.R.G., September 4-8, 1989, 137
  - 23) Rautenbach, R. and G. Schock, Ultrafiltration of macromolecular solutions and cross-flow microfiltration of colloidal suspensions. A contribution to permeate flux calculations, *J. Membrane Sci.* 36 (1988) 231-242
  - 24) Dorson, W.J. and J.S. Pierson, Controlling factors in hemofiltration, *J. Membrane Sci.* 44 (1989) 35-46
  - 25) Neplenbroek, A.M., Stability of supported liquid membranes, Thesis, Twente University, 1989
  - 26) Liquid Membranes, Theory and Applications, ACS Symposium Series 347, R.D. Noble and J.D. Way (eds.), Denver, USA, 1986
  - 27) D'Elia, N.A., L. Dahuron and E.L. Cussler, Liquid-liquid extractions with microporous hollow fibers, *J. Membrane Sci.* 29 (1986) 309-319
  - 28) Alexander, P.R. and R.W. Callahan, Liquid-liquid extraction and stripping of gold with microporous hollow fibers, *J. Membrane Sci.* 35 (1987) 57-71
  - 29) Keurentjes, J.T.F., Th.G.J. Bosklopper, L.J. van Dorp and K. van 't Riet, The removal of metals from edible oil by a membrane extraction procedure, *J. Am. Oil Chem. Soc.* 67 (1990) 28-32
  - 30) Drioli, E., V. Calabro and Y. Wu, Microporous membranes in membrane distillation, *Pure and Appl. Chem.* 58 (1986) 1657-1662
  - 31) Jonsson, A.-S., R. Wimmerstedt and A.-C. Harrysson, Membrane distillation-a theoretical study of evaporation through microporous membranes, *Desalination* 56 (1985) 237-249
  - 32) Schneider, K. and T.J. van Gassel, Membrane distillation, *Chemie Ing. Technik* 56 (1984) 514-521
  - 33) Mulder, M., Pervaporation, separation of ethanol-water and of isomeric xylenes, Thesis, Twente University, 1984
  - 34) Tusel, G.F. and H.E.A. Bruschke, Use of pervaporation systems in the chemical industry, *Desalination* 53 (1985) 327-338
  - 35) Lipp, P., C.H. Lee, A.G. Fane and C.J.D. Fell, A fundamental study of the ultrafiltration of oil-water emulsions, *J. Membrane Sci.* 36 (1988) 161-177
  - 36) Kutow, O., W.L. Thayer, J. Tigner and S. Sourirajan, Tubular cellulose acetate reverse osmosis membranes for treatment of oily wastewaters, *Ind. Eng. Chem., Prod. Res. Dev.* 20 (1981) 354-361
  - 37) Vigo, F., C. Uliana and P. Lupino, The performance of a rotation module in oily emulsions ultrafiltration, *Sep. Sci. Technol.* 20 (1985) 213-230
  - 38) Kiani, A., R.R. Bhave and K.K. Sirkar, Solvent extraction with immobilized interfaces in a microporous hydrophobic membrane, *J. Membrane Sci.* 20 (1984) 125-145
  - 39) Prasad, R. and K.K. Sirkar, Dispersion-free solvent extraction with microporous hollow fiber modules, *AIChE J.* 34 (1988) 177-188
  - 40) Padt, A. van der, M.J. Edema, J.J.W. Sewalt and K. van 't Riet, Enzymatic acylglycerol synthesis in a membrane bioreactor, *J. Am. Oil Chem. Soc.* 67 (1990) 347-352
  - 41) Pronk, W., P.J.A.M. Kerkhof, C. van Helden and K. van 't Riet, The hydrolysis of triglycerides by immobilized

## chapter 1

- lipase in a hydrophilic membrane reactor, *Biotechnol. Bioeng.* 32 (1988) 512-518
- 42) Molinari, R., E. Drioli and G. Barbieri, Membrane reactor in fatty acid production, *J. Membrane Sci.* 36 (1988) 525-534
- 43) Hoq, M.M., M. Koike, T. Yamane and S. Shimizu, Continuous hydrolysis of olive oil by lipase in microporous hydrophobic hollow fiber bioreactor, *Agric. Biol. Chem.* 49 (1985) 3171-3178
- 44) Franken, A.C.M., Membrane distillation, a new approach using composite membranes, Thesis, Twente University, 1988
- 45) Franken, A.C.M., J.A.M. Nolten, M.H.V. Mulder, D. Bargeman and C.A. Smolders, Wetting criteria for the applicability of membrane distillation, *J. Membrane Sci.* 33 (1987) 315-328
- 46) Applewhite, T.H., Fats and fatty oils, in: *Kirk-Othmer Encyclopedia of Chemical Technology*, 3<sup>rd</sup> edition, M. Grayson (ed.), vol. 9, 795-830, J. Wiley and Sons, New York, 1980
- 47) Edible Oils and Fats, Developments since 1978, *Food Technology Review* 57, S. Torrey (ed.), Noyes Data Corp., Park Ridge NJ, 1983
- 48) Braae, B., Degumming and refining practices in Europe, *J. Am. Oil Chem. Soc.* 53 (1976) 353-357
- 49) Tiegs, C. and S. Peter, Zur Trennung von Öl-/Stearinsäure-Gemischen durch Extraktion mit einem überkritischen Lösungsmittel, *Fette Seifen Anstrichmittel* 87 (1985) 231-235
- 50) Forster, A. and A.J. Harper, Physical refining, *J. Am. Oil Chem. Soc.* 60 (1983) 265-271
- 51) List, G.R., T.L. Mounts, K. Warner and A.J. Heakin, Steam refined soy bean oil: Effect of refining and degumming methods on oil quality, *J. Am. Oil Chem. Soc.* 55 (1978) 277-279
- 52) Gloyer, S.W., Furans in vegetable oil refining, *Ind. Eng. Chem.* 40 (1948) 228-236
- 53) Köseoglu, S.S. and D.E. Engelgau, Membrane applications and research in the edible oil industry: an assessment, *J. Am. Oil Chem. Soc.* 67 (1990) 239-249
- 54) Iwama, A., New process for purifying soybean oil by membrane separation and an economical evaluation of the process, *Proc. World Conf. Biotechnology for the Fats and Oils Industry*, T.H. Applewhite (ed.), Hamburg, 1986, 244-250
- 55) Gupta, A.K.S., Neuere Entwicklungen auf dem Gebiet der Raffination der Speisöle, *Fette Seifen Anstrichmittel* 88 (1986) 79-86
- 56) Keurentjes, J.T.F., W. Pronk, G.I. Doornbusch and K. van 't Riet, Downstream processing of fatty acid/lipid mixtures using membranes, *Proc. Second Annual Meeting of the North American Membrane Soc.*, Syracuse, New York, June 1-3, 1988
- 57) Keurentjes, J.T.F., G.I. Doornbusch and K. van 't Riet, The removal of fatty acids from edible oil; removal of the dispersed phase of a water in oil dispersion by a hydrophilic membrane, accepted for publication in *Sep. Sci. Technol.*

## THE REMOVAL OF FATTY ACIDS FROM EDIBLE OIL; REMOVAL OF THE DISPERSED PHASE OF A WATER IN OIL DISPERSION BY A HYDROPHILIC MEMBRANE

---

### SUMMARY

Fatty acids can be extracted from an oil phase by forming a dispersed phase of saponified fatty acids/water/isopropanol in oil. This dispersion can be separated in the two phases by two membranes of opposite polarity in series. In this study the separation of the water phase from the dispersion by a hydrophilic membrane and the mechanisms underlying the flux characteristics have been investigated. The permeation flux through a PAN ultrafiltration membrane has been optimized with respect to the fatty acid/water/isopropanol ratio. It appears, that a 1:6.5:3 (v/v) ratio gives the highest flux ( $95 \text{ l}/(\text{m}^2 \cdot \text{h} \cdot \text{bar})$ ). The dispersion at these conditions consists of a continuous oil phase as well as a continuous water phase between 20% and 65% water phase hold up. The flux/pressure curve shows a linear increase of the flux with pressure at low pressures (determined by the membrane resistance), followed by a maximum flux value for the case that the volume of the water phase present in the inflow is limiting. It is not possible to remove the water phase with membranes, below a water phase hold up of 20%. At this hold up value also the transition between a bicontinuous and a discrete dispersion occurs.

## 2.1 INTRODUCTION

Fatty acids have to be removed from oils for different purposes. In refining procedures of edible oils, the free fatty acids (FFA) have to be removed as a contaminant [1,2], since too high levels of FFA will result in rancidity of the oil [3]. In the enzymatic production of fatty acids from triglycerides, the reaction rate strongly decreases with an increasing fraction of fatty acids in the oil phase [4]. To maintain a sufficiently high reaction rate, the fatty acids should be removed continuously.

The classical method for the removal of fatty acids from an oil is the so called caustic refining. Soaps are formed by adding alkali to the oil, and the formed soapstock is consequently separated from the oil by high speed separators [5]. The most important problem occurring in this procedure is the inclusion of triglycerides into the soapstock. Usually, this amount will equal the amount of fatty acids that is saponified [6]. This included oil is difficult to recover and is therefore considered to be a loss. Evidently, caustic refining of oils with high fatty acid contents will introduce considerable losses of triglycerides. In the enzymatic oil splitting, the soapstock phase contains the fatty acids, which are the products. As a recovery process for these fatty acids in the enzymatic oil splitting [4], caustic refining will result in a very poor product, containing about 50% fatty acids.

The crude oil losses inherent to the caustic refining can be avoided by the use of other refining procedures such as distillation or steam distillation [7]. The high temperatures needed for these processes may especially affect highly unsaturated fatty acids, either present as free fatty acids or in triglycerides. A membrane separation process might be a mild alternative for these processes. For the application of membranes for a fat/fatty acid separation three configurations can be envisaged. Firstly, a direct filtration with a retention based on molecular size differences can be used. This will be difficult because of the small differences in molecular weights. Secondly, an extraction mode can be applied. However, the extractants found in literature (mostly alcohols) are not very specific [8,9], and will also introduce losses of crude oil.

The third mode to apply membranes is the formation of a dispersion that can be separated in the two phases by a hydrophilic and a hydrophobic membrane in series. The two-membrane system for the separation of such a dispersion is shown schematically in figure 1 [10]. In order to separate a particular phase from a two phase mixture, the membrane used has to fulfill the requirement that it is preferentially wetted by this phase. The phase that does not wet the membrane (exhibits a contact angle on the surface larger than  $90^\circ$ ) can be retained, provided the system's Laplace

pressure is higher than the applied trans-membrane pressure.

The separation of a dispersion into its two phases will largely depend on the type of dispersion to be separated. The most simple types of dispersions are emulsions of a dispersed aqueous phase in a continuous organic phase (a w/o emulsion), and of a dispersed organic phase in a continuous aqueous phase (an o/w emulsion). In the absence of a stabilizing agent (surfactant) or in the presence of sufficiently large droplets (in the order of 1 mm) these dispersions are not very stable and their separation into the two phases is relatively easy. Other, more complicated, types of dispersions may also occur. Examples are dual emulsions and microemulsions. In dual emulsions the continuous phase is also present as small droplets in the dispersed phase [11,12]. Microemulsions can be formed in the presence of a surfactant and a cosurfactant (usually an alcohol). They are thermodynamically stable water-in-oil dispersions with very small droplet sizes (in the order of 20 nm [13]). Upon increasing the fraction of the dispersed phase in such a microemulsion system, a transition into a bicontinuous system can be observed [14]. Several types of bilayer and liquid crystal structures have been found in this type of dispersed systems [15]. However, no literature is available on the filtration characteristics of those, more complicated, types of dispersions.

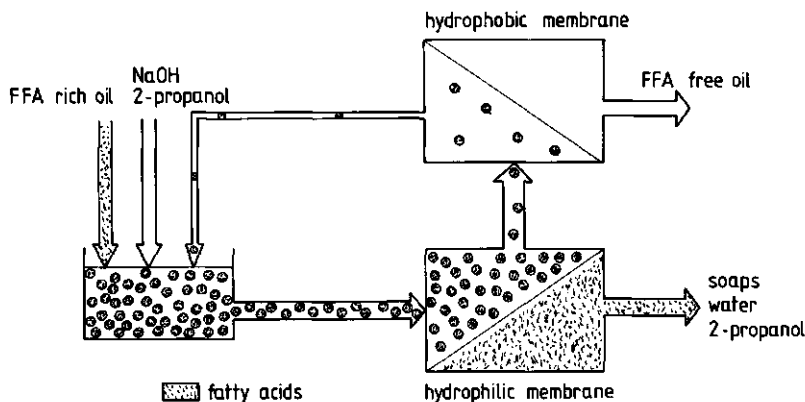


Figure 1. Two-membrane system for the removal of fatty acids from an oil

In this study the soapstock obtained by the addition of alkali to the fatty acid rich oil is solubilized by an alcohol under the formation of a dispersion. A suitable membrane for the removal of the dispersed water phase from this dispersion will be selected and the mechanisms underlying the permeation characteristics of the water phase will be investigated.

## 2.2 MATERIALS

Dispersions were prepared by adding alkali to oleic acid containing soy bean oil in order to saponify the oleic acid. Subsequently, isopropanol was added to solubilize the soaps, and water was added to lower the viscosity of the water/soap/alcohol phase. The soy bean oil used was of edible quality (obtained from Rhenus Inc., The Netherlands). In this two phase system the solubility of isopropanol in the oil phase was determined to be below 0.5%. In order to avoid the formation of insoluble calcium and manganese soaps, demineralized water was used. All chemicals used were purchased from Merck (FRG) and were reagent grade. The dispersion was stored in a stoppered bottle to avoid the evaporation of isopropanol and was continuously stirred by means of a magnetic stirrer.

A qualitative analysis for fatty acids, its soaps and triglycerides was made by means of TLC. The stationary phase was 0.2 mm Silicagel 60 F 254 purchased from Merck (FRG) and the mobile phase petroleum ether 40-60, diethylether and acetic acid (80:20:1(v/v/v)). After developing, the sheets were colored with iodine vapour.

Several hydrophilic membranes were tested for their capability to separate this dispersion and are summarized in table 1. Flux measurements of the flat sheet membrane were carried out in a New Brunswick Scientific Megaflow TM 100 test module. The membrane surface in this module is 64.5 cm<sup>2</sup> and the channel height is 0.4 mm. All membranes were rinsed thoroughly with demineralized water before use to remove preservative liquids.

Table 1. *Hydrophilic membranes tested; HF=hollow fiber, FS=flat sheet*

| Membrane                | Type | Pore Size/Cut Off | Manufacturer  |
|-------------------------|------|-------------------|---------------|
| Cellulose               | HF   | 6,000             | ENKA          |
| Celluloseacetate        | HF   | 200,000           | ENKA          |
| Polyacrylonitrile (PAN) | FS   | 30,000            | Rhone-Poulenc |
| Polyamide               | HF   | 0.2 $\mu$ m       | ENKA          |

The viscosity of the water phase was determined using an Ostwald viscosimeter. After phase separation, the interfacial tension between the two phases was measured using a spinning drop tensiometer [16,17]. A small drop of the low density phase is brought into a rotating tube containing the high density phase. The drop will deform along the axis of the tube. In case the length of the droplet is more than 4 times its height, the Vonnegut approach gives the following

relation:

$$\gamma = \frac{\Delta\rho.\omega^2.r_d^3}{4} \quad (1)$$

in which is  $\gamma$  the interfacial tension between the two phases,  $\Delta\rho$  the density difference between the two phases,  $\omega$  the angular velocity and  $r_d$  the half height of the droplet.

In order to establish the transition from a continuous into a discrete oil phase, a thin layer of pure oil containing the dissolved dye Sudan III making it intensely red was brought on top of a non-stirred dispersion. In the case of a continuous oil phase, the red colored oil moves from the top downwards by diffusion and convection, whereas in the case of a discrete oil phase, no downward movement of the colored oil occurs.

The transition from a continuous into a discrete water phase was established by conductivity measurements. Conductivity measurements were performed using a 400 Hz AC current in order to avoid electrophoresis. All measurements have been carried out at 20 °C, unless stated otherwise.

## 2.3 RESULTS AND DISCUSSION

### Membrane selection

The membrane selection experiments have been carried out with a dispersion containing 54% soy bean oil, 10% sodium oleate, 14% water and 22% isopropanol (v/v). The water phase contains the soaps, water and 2-propanol, while the organic phase contains oil and only traces of 2-propanol. It is not possible to detect any soaps in the organic phase. The membranes given in table 1 have been tested for their capability to separate this dispersion. The results are summarized in table 2.

Table 2. Fluxes determined with the standard dispersion

| membrane         | flux (l/(m <sup>2</sup> .h.bar)) |
|------------------|----------------------------------|
| Cellulose        | 1                                |
| Celluloseacetate | —*)                              |
| PAN              | 30                               |
| Polyamide        | —*)                              |

\*) both phases permeate



For all membranes, the permeate is examined for the presence of soaps and triglycerides by means of TLC. In the case of a cellulose and PAN membrane, no triglycerides could be detected in the permeate, thus indicating that the separation of the fatty acids from the triglycerides is complete. From table 2 it can also be concluded, that the pore size of the membrane influences the separation characteristics: the membranes with the large pore sizes could not retain the oil phase. However, the celluloseacetate and polyamide are expected to be slightly more hydrophobic compared to cellulose and PAN [18]. This also might be part of the reason for the permeation of both phases. It is evident from table 2, that the PAN membrane gives the best flux and a complete separation. Therefore, the PAN membrane is used for the flux optimization experiments.

#### Flux optimization in the PAN membrane

The clean water flux of the PAN membrane is found to vary from 300 to 700 l/(m<sup>2</sup>.h.bar), depending on the sheet of material used. To allow a comparison of the results obtained with different sheets of the membrane material, the flux is standardised to a virtual clean water flux of 500 l/(m<sup>2</sup>.h.bar), the average of the measured clean water flux of the sheets used. This correction is allowed, since in our system permeation of the water phase is determined entirely by the resistance of the membrane.

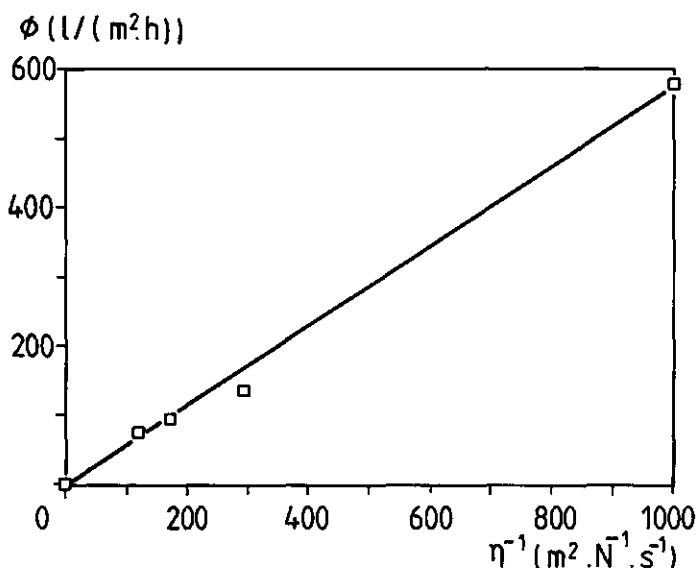


Figure 2. Permeation flux through the PAN membrane versus the inverse of the viscosity of the water phase at 1 bar trans-membrane pressure

This is shown in figure 2, in which the measured (non-corrected) flux is plotted versus the inverse of the viscosity of the water phase with different compositions. This appears to be a straight line through the origin. The clean water flux of this particular sheet is  $580 \text{ l}/(\text{m}^2 \cdot \text{h} \cdot \text{bar})$ , which falls within the range of clean water fluxes measured. This means that although a dispersion is present at the retentate side of the membrane, the membrane is completely wetted by the water phase and the resistance against permeation is completely determined by only the hydrodynamic resistance of the membrane: there is no additional resistance at the retentate side.

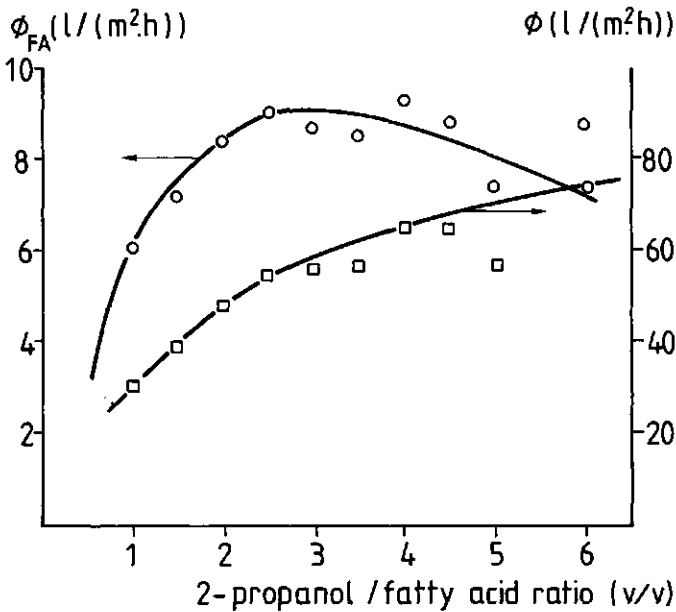


Figure 3. Permeation flux and fatty acid flux through a PAN membrane at different isopropanol/fatty acid ratios ( $P=1 \text{ bar}$ )

To optimize the flux of the PAN membrane, the fatty acid to water and 2-propanol ratio is varied. The experiments are carried out at 1 bar trans-membrane pressure. Varying the isopropanol content of the dispersion at a fixed water content results in a permeation flux and fatty acid flux as shown in figure 3. It can be seen, that although the permeation flux increases with an increase in isopropanol content (due to a decrease in viscosity of the water phase), the fatty acid flux (this

is the permeation flux times the fatty acid concentration) has an optimum value at an isopropanol to fatty acid ratio of 3:1. At this optimum isopropanol content the water content is varied and the same type of curves are obtained (figure 4). The optimum composition of the water phase with respect to the fatty acid flux appears to be a fatty acid, water, isopropanol ratio of 1:6.5:3. At this optimum composition of the water phase a permeation flux of  $95 \text{ l}/(\text{m}^2 \cdot \text{h} \cdot \text{bar})$  can be achieved, resulting in a fatty acid flux of  $15 \text{ l}/(\text{m}^2 \cdot \text{h} \cdot \text{bar})$ . All experiments described further are carried out with this composition of the water phase.

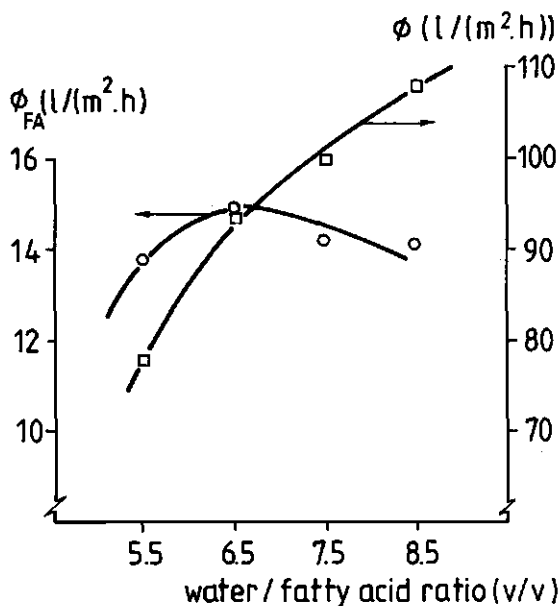


Figure 4. Permeation flux and fatty acid flux through a PAN membrane at different water / fatty acid ratios at the optimum isopropanol content ( $P=1 \text{ bar}$ )

Although not performed here because it is not relevant for our purposes, the relation between flux and viscosity and therewith with the composition can easily be brought in an optimization model with the fatty acid flux as the parameter to be optimized.

#### Long term performance of the PAN membrane

In a series of consecutive batch experiments the performance of the PAN membrane has been investigated. Every new batch is started without cleaning the membrane. In these experiments the permeate is recirculated to the feed vessel. From figure 5 it can be seen, that the flux gradually

decreases from an initial flux of  $105 \text{ l}/(\text{m}^2 \cdot \text{h} \cdot \text{bar})$  to around  $30 \text{ l}/(\text{m}^2 \cdot \text{h} \cdot \text{bar})$  after 560 hours. Every new batch initially gives a higher flux, however, after one day the flux decrease continues according to the pattern of the batch before. Rinsing the membrane with isopropanol for 3 hours restores the flux to  $53 \text{ l}/(\text{m}^2 \cdot \text{h} \cdot \text{bar})$ , a value comparable with the value after 60 hours. Rinsing with nitric acid (0.1%), however, has no effect, indicating that the flux decay is probably due to a clogging of the membrane with non dissolved soap molecules.

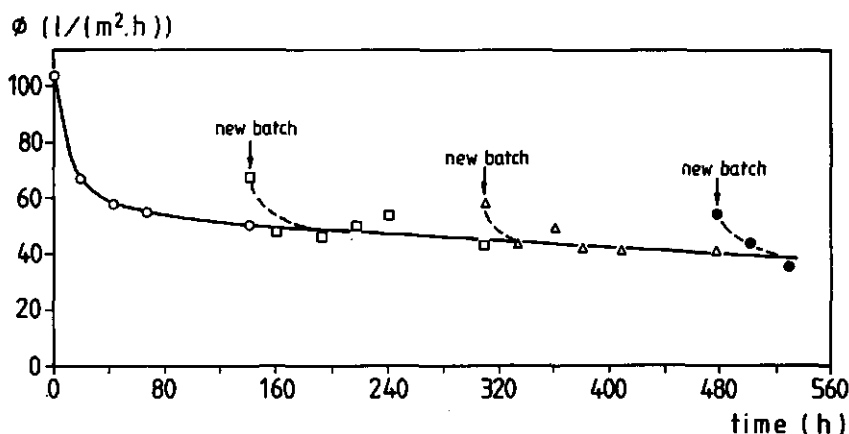


Figure 5. Long term performance of a PAN membrane in the separation of a two-phase system ( $P=1 \text{ bar}$ )

#### Characterization of the dispersion

To reveal the nature of the dispersion, several experiments have been performed. It appeared to be impossible to estimate the particle size by microscopy. This indicates, that a more complicated system than a water in oil dispersion is formed. This might be due to a low interfacial tension. From spinning drop measurements at different angular velocities it follows, that  $\gamma$  equals  $0.27 \pm 0.01 \text{ mN/m}$ . This value is sufficiently low to form a microemulsion. However, laser light scattering experiments indicate, that in the water phase as well as the oil phase no microemulsion is formed.

Performing conductivity measurements it can be seen (Figure 6), that the conductivity of the system increases almost stepwise by two decades at a water phase content of around 20%. It also shows, that no other stepwise increase in conductivity takes place, which indicates that water is present as a continuous phase above 20% water phase in the dispersion. The experiments with colored oil show a similar abrupt change around 35% oil phase. It can therefore be concluded that

the oil phase is present as a continuous phase above 35% oil phase.

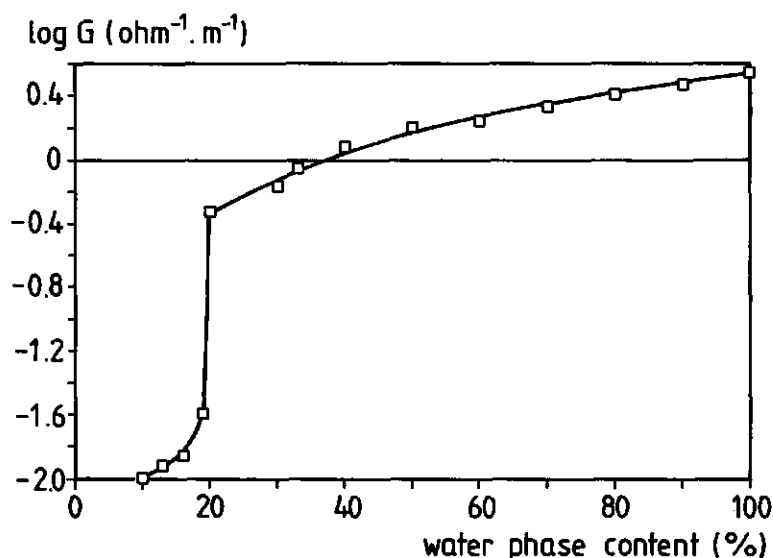


Figure 6. Conductivity of the dispersion at different water phase contents

From these experiments it can be concluded that the system behaves similar to the concentrated microemulsions used by Lagües [19], and forms a bicontinuous system at a water phase content between 20% and 65%. However, it has to be noted, that bicontinuous in this context is not the same as the expression bicontinuous in the classical way: the dispersion is not transparent, and it definitely is not the result of a highly concentrated microemulsion [20,21]. Lowering the fraction of the water phase below 20% will result in a transition from bicontinuous into a discrete emulsion containing water spheres in oil. According to Kirkpatrick [22] this transition is expected to take place between 15 and 29% dispersed phase in the system, based on a percolation theory approach. Above this threshold value, the conductivity is expected to increase according to a power law with an exponent of around 1.6 [22]. However, from a log-log plot of the results given in figure 6 follows a maximum exponent of 0.8, showing that the conductivity of the system increases less with an increase of the water phase content than expected from the percolation theory.

It can be concluded, that for our system three regions can be distinguished: between 0% and 20% water phase a dispersion of water droplets in oil is formed, between 20% and 65% water phase the water phase as well as the oil phase is present as a continuous phase, although it is not yet clear which type of bicontinuous system is present. Above 65% water phase a dispersion of oil droplets

in water is formed.

### **Effect of composition on the flux**

In a batch experiment the water phase content will decrease upon filtration. For a dispersion containing 45% water phase, the flux can be plotted versus the water phase content, giving figure 7 as a typical result. The maximum flux found in this plot equals the flux in case the water phase only is applied as feed solution on the same sheet of membrane, which is in agreement with the fact that the water phase is present as a continuous phase and is wetting the membrane completely. It is also found, that the same curves are obtained in the case of sodium, potassium and lithium soaps, and an increase in the temperature only influences the maximum flux, which is merely due to a decrease in viscosity of the water phase. In figure 7 a steep decrease of the flux can be observed below 20% water phase in the system, and the flux finally becomes zero at 18%. The same phenomenon has been observed in the case of the cellulose membrane, thus indicating, that this stepwise flux decrease is a property of the dispersion rather than an effect caused by the membrane.

This transition point coincides with the transition from a continuous water phase into a water phase consisting of discrete spheres in oil. Apparently, the dispersed droplets cannot coalesce with the same phase present in the membrane. The size of the droplets is many times smaller than the height of the flow channel, and dispersed droplets will be lifted away from the surface because of the tubular pinch effect [23,24]. This will result in an extremely low flux.

By removing the oil phase from this poor emulsion it is possible to obtain again a dispersion with more than 20% water phase. Consequently, the flux then can be restored to the value it has above 20% water phase. This can be done in the two membrane system as proposed for the separation of this dispersion [10].

### **The effect of pressure and flow conditions on filtration**

For a filtration in which no concentration polarization occurs, the flux will be entirely determined by the hydrodynamic membrane resistance. It has been found above, that the flux increases proportionally to the inverse of the viscosity. This implies that for a fixed feed flow velocity the flux will also increase linearly with the trans-membrane pressure:

$$\phi = \frac{\phi_{cw} \cdot A \cdot P \cdot \eta_w}{\eta} \quad (2a)$$

with  $\phi$  the permeation flux and  $\phi_{cw}$  the clean water permeation flux at  $10^5 \text{ Nm}^{-2}$  trans-membrane pressure and  $1 \text{ m}^2$  membrane area, respectively,  $P$  the trans-membrane pressure,  $A$  the membrane surface,  $\eta$  the viscosity of the permeate and  $\eta_w$  the viscosity of water. A mass balance then yields

$$\phi = \frac{Q(f_{in} - f_{out})}{A} \quad (2b)$$

in which is  $Q$  the feed flow and  $f_{in}$  and  $f_{out}$  the dispersed fraction in the feed flow and the flow leaving the system, respectively. From the experiments mentioned above it follows, that  $f_{out}$  can not be smaller than 0.2. This implies, that the flux can not increase above the value calculated from equation 2b with  $f_{out}=0.2$ :

$$\phi_{max} = \frac{Q(f_{in} - 0.2)}{A} \quad (2c)$$

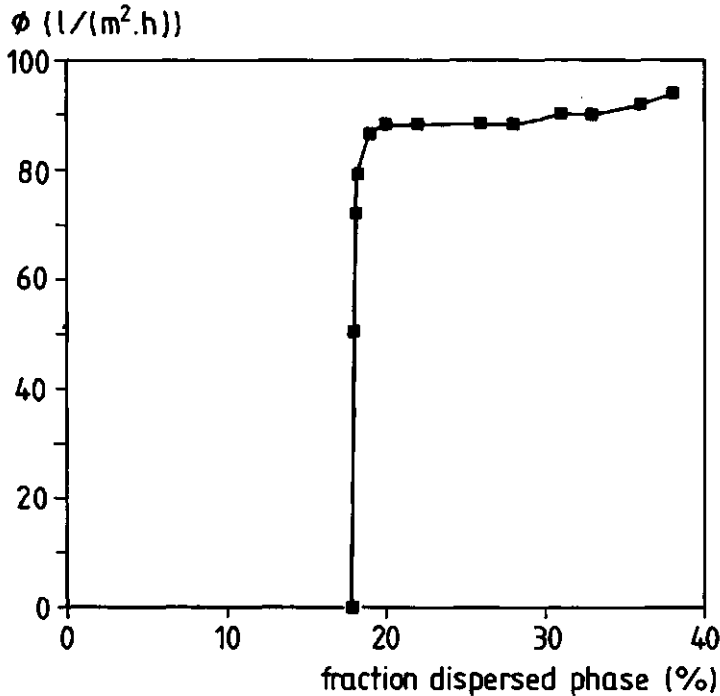


Figure 7. The permeation flux through a PAN membrane varying with the fraction dispersed phase in the system

In figure 8 it is shown that the predicted and measured permeation flux at conditions for which  $f_{out} > 0.2$  (equation 2b) show a good agreement at the condition of pressure dependent permeation. From figure 9 it can be concluded, that the maximum permeation flux, i.e. for  $f_{out} = 0.2$  (equation 2c), in this system is well described by the amount of water phase that is present in the inflow. Both figures 8 and 9 confirm that the pressure limited permeation at low trans-membrane pressures (determined by the membrane resistance), and the inflow limited permeation at high trans-membrane pressures determine the flux/pressure curve.

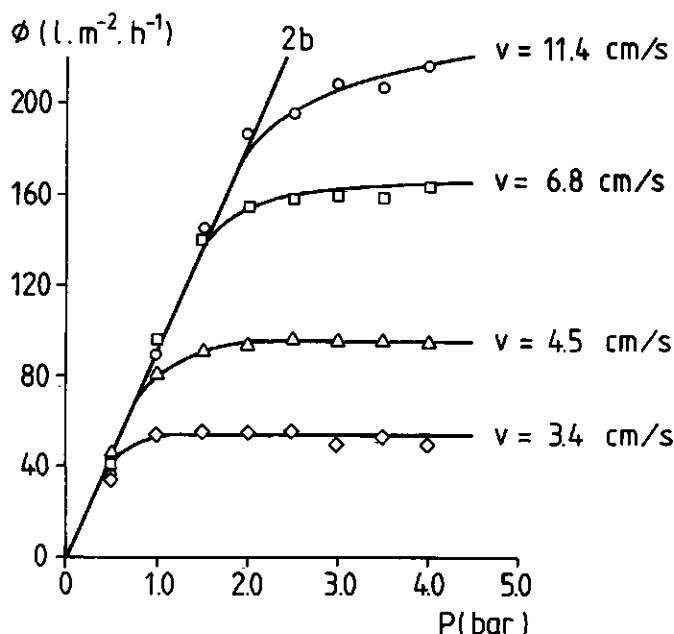


Figure 8. Permeation flux through a PAN membrane at different feed flow velocities and trans-membrane pressures

#### Prediction of the membrane performance

With the thus obtained experimental data it is possible to predict the performance of a membrane used in this separation. Firstly, it has to be established whether a membrane is capable to retain the oil phase or not. Subsequently, the performance can be determined as shown schematically in figure 10. A change in the composition of the water phase will result in a change in viscosity. Using the ratio of the viscosity of the water phase over the viscosity of pure water together with the clean water flux, the permeation rate can be calculated. A mass balance over the system gives



the maximum product flux that can be attained. Combining the concentration of the product in the water phase with the maximum flux finally results in the product flux.

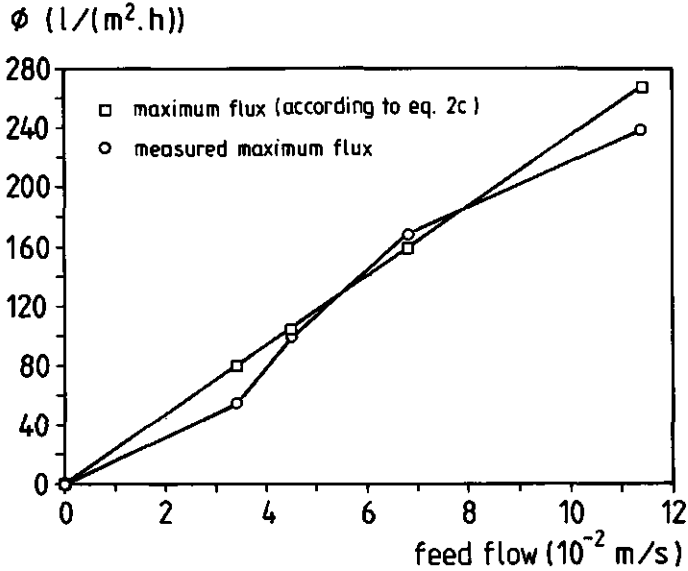


Figure 9. Permeation flux through a PAN membrane at different feed flow velocities. The calculated maximum flux is calculated according to eq. 2c

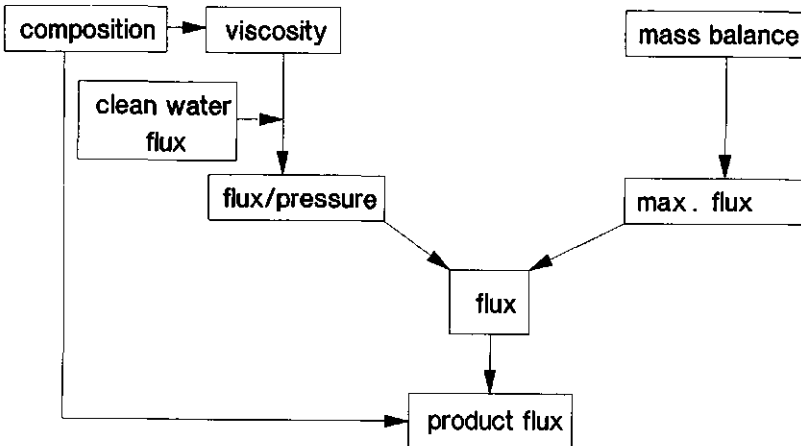


Figure 10. Route for the prediction of the performance of a membrane for the removal of the water phase from the dispersion

## 2.4 CONCLUSIONS

From this work it can be concluded, that it is very well possible to separate the fatty acids from an oil by forming a dispersion of saponified fatty acids/water/isopropanol in oil. It follows from conductivity and diffusion measurements, that a bicontinuous system is formed between 20% and 65% water phase in the system. The filtration characteristics at a hydrophilic membrane have been investigated. The permeation flux through a PAN ultrafiltration membrane is optimized with respect to the fatty acid/water/isopropanol ratio. It follows, that a 1:6.5:3 (v/v) ratio gives the highest flux ( $95 \text{ l}/(\text{m}^2 \cdot \text{h} \cdot \text{bar})$ ). In these experiments the flux is limited by the amount of dispersion that is led across the membrane. It appears, that it is not possible to go below 20% water phase in the dispersion, which can be explained by a transition from a bicontinuous system into a discrete dispersion. This 20% value falls within the range predicted by percolation theory for the transition between spheres and a bicontinuous system. However, by removing the oil phase by a hydrophobic membrane in series, it will be possible to restore the water phase content to a value above 20%.

## ACKNOWLEDGMENT

The authors wish to thank the Dutch Program Committee for Industrial Biotechnology (PCIB) for their financial support.

## LIST OF SYMBOLS

|                     |                                       |  |
|---------------------|---------------------------------------|--|
| A                   | membrane surface area                 | $[\text{m}^2]$   |
| $f_{\text{in}}$     | dispersed fraction in feed            | $[-]$  |
| $f_{\text{out}}$    | dispersed fraction leaving the system | $[-]$  |
| G                   | conductivity                          | $[\text{ohm}^{-1} \cdot \text{m}^{-1}]$                |
| $r_d$               | half droplet height                   | $[\text{m}]$   |
| P                   | trans-membrane pressure               | $[\text{N} \cdot \text{m}^{-2}]$                       |
| Q                   | feed flux                             | $[\text{m}^3 \cdot \text{h}^{-1}]$                     |
| $\gamma$            | interfacial tension                   | $[\text{N} \cdot \text{m}^{-1}]$                       |
| $\phi$              | permeation flux                       | $[\text{m}^3 \cdot \text{m}^{-2} \cdot \text{h}^{-1}]$ |
| $\phi_{\text{cw}}$  | clean water flux                      | $[\text{m}^3 \cdot \text{m}^{-2} \cdot \text{h}^{-1}]$ |
| $\phi_{\text{max}}$ | maximum attainable permeation flux    | $[\text{m}^3 \cdot \text{m}^{-2} \cdot \text{h}^{-1}]$ |
| $\eta$              | viscosity                             | $[\text{Ns} \cdot \text{m}^{-2}]$                      |
| $\eta_w$            | viscosity of water                    | $[\text{Ns}/\text{m}^2]$                               |

## chapter 2

|              |                    |                       |
|--------------|--------------------|-----------------------|
| $\Delta\rho$ | density difference | $[\text{kg.m}^{-3}]$  |
| $\omega$     | angular velocity   | $[\text{rad.s}^{-1}]$ |

## REFERENCES

- 1) Sullivan, F.E., Steam refining, *J. Am. Oil Chem. Soc.* 53 (1976) 358-360
- 2) Cavanagh, G.C., Miscella refining, *J. Am. Oil Chem. Soc.* 53 (1976) 361
- 3) Allen, R.R. et al., *Bailey's industrial oil and fats products*, J. Wiley and Sons, New York, 1982
- 4) Pronk, W., P.J.A.M. Kerkhof, C. van Helden and K. van 't Riet, The hydrolysis of triglycerides by immobilized lipase in a hydrophilic membrane reactor, *Biotech. Bioeng.* 32 (1988) 512-518
- 5) Carr, R.A., Degumming and refining practices in the U.S., *J. Am. Oil Chem. Soc.* 53 (1976) 347-352
- 6) Braae, B., Degumming and refining practices in Europe, *J. Am. Oil Chem. Soc.* 53 (1976) 353-357
- 7) List, G.R., T.L. Mounts, K. Warner and A.J. Heakin, Steam refined soy bean oil: 1. Effect of refining and degumming methods on oil quality, *J. Am. Oil Chem. Soc.* 55 (1978) 277-279
- 8) Gloyer, S.W., Furans in vegetable oil refining, *Ind. Eng. Chem.* 40 (1948) 228-236
- 9) Shah, K.J. and T.K. Venkatesan, Aqueous isopropyl alcohol for extraction of free fatty acids from oils, *J. Am. Oil Chem. Soc.* 66 (1989) 783-787
- 10) Keurentjes, J.T.F., W.Pronk, G.I. Doornbusch and K. van 't Riet, Downstream processing of fatty acid/lipid mixtures using membranes, *Proc. Second Annual National Meeting of the North American Membrane Society*, Syracuse, New York, June 1-3, 1988
- 11) Matsumoto, S., Y. Ueda, Y. Kita and D. Yonezawa, Preparation of water-in -olive oil-in-water multiple phase emulsions in an eatable form, *Agric. Biol. Chem.* 42 (1978) 739-743
- 12) Matsumoto, S. and P. Sherman, A preliminary study of w/o/w emulsions with a view to possible food applications, *J. Texture Studies* 12 (1981) 243-257
- 13) Müller, B.W. and R.H. Müller, Particle size distributions and particle size alterations in microemulsions, *J. Pharm. Sci.* 73 (1984) 919-922
- 14) Kahlweit, M. et al., How to study microemulsions, *J. Colloid Interface Sci.* 118 (1987) 436-453
- 15) Tiddy, G.J.T., Surfactant-water liquid crystal phases, *Phys. Rep.* 57 (1980) 1-46
- 16) Vonnegut, B., Rotating bubble method for the determination of surface and interfacial tensions, *Rev. Sci. Instruments* 13 (1942) 6-9
- 17) Princen, H.M., I.Y.Z. Zia and M.S. Mason, Measurement of interfacial tension from the shape of a rotating drop, *J. Coll. Int. Sci.* 23 (1967) 99-107
- 18) Shafirin, E.G. in *Polymer Handbook*, 2<sup>nd</sup> ed., J. Brandrup and E.H. Immergut (eds.) Wiley and Sons, New York, 1975, p.III-221
- 19) Lagûes, M., R. Ober and C. Taupin, Study of structure and electrical conductivity in microemulsions: evidence for percolation mechanism and phase inversion, *J. Phys. Lettres* 39 (1978) L487-L491
- 20) Baker, R.C., A.T. Florence, R.H. Ottewill and Th.F. Tadros, Investigations into the formation and characterization of microemulsions II. Light scattering, conductivity and viscosity studies of microemulsions, *J. Colloid Interface Sci.* 100 (1984) 332-349
- 21) Lundström, I. and K. Fontell, Lateral electrical conductivity in aerosol-OT water systems, *J. Colloid Interface Sci.* 59 (1977) 360-370
- 22) Kirkpatrick, S., Percolation and conduction, *Rev. Mod. Phys.* 45 (1973) 574-588
- 23) Altena, F.W., G. Belfort, J. Otis, F. Fiessinger, J.M. Rowel and J. Nicoletti, Particle motion in a laminar slit flow:

*chapter 2*

a fundamental fouling study, *Desalination*, 47 (1983) 221-232

- 24) Altena, F.W. and G. Belfort, Lateral motion of spherical particles in porous flow channels: application to membrane filtration, *Chem. Eng. Sci.* 39 (1984) 343-355

## MULTICOMPONENT DIFFUSION IN DIALYSIS MEMBRANES

---

### SUMMARY

Multicomponent diffusion through porous media is usually described by an effective diffusivity for each component. In such a diffusivity many different effects are lumped together, which makes its behaviour very difficult to understand. In this study we use a different approach in which each species has a driving force which is counteracted by friction due to its motion relative to the surroundings. The resulting equation is a difference form of what is known as the Generalized Maxwell Stefan equation (GMS). We apply this to describe transport through cellulose dialysis membranes.

Friction between water and the membrane matrix is determined by isobaric dialysis experiments in mixtures with methanol, ethanol and 2-propanol. The water/membrane friction strongly depends on the water content. The friction of methanol or ethanol with the membrane is almost constant, while that of 2-propanol decreases with an increase in the 2-propanol concentration. The resulting friction coefficients give a quantitative description of transport of a ternary liquid mixture through the membrane. Using similar mixtures with a hollow fiber device shows that only the external area of the fiber bundle is effectively used. Apparently there is insufficient flow of the external phase between the fibers.

In a second set of experiments a multicomponent system is studied. At the feed side of the membrane a solution of water, 2-propanol and sodium oleate is applied; on the permeate side an NaCl solution. A small pressure gradient from feed to permeate is applied. Initially a mass flux against the pressure gradient is observed. After some time the flux changes direction and becomes 2 to 10 times larger than the permeation rate would be for the feed solution alone with the same applied pressure. These effects can not be explained using effective diffusivities, but they can be understood qualitatively from the GMS equations.

---

J.T.F. Keurentjes, A.E.M. Janssen, A.P. Broek, A. van der Padt, J.A. Wesselingh\* and K. van 't Riet

\*Dept. of Chemical Engineering, University of Groningen, The Netherlands

This chapter is submitted for publication

### 3.1 INTRODUCTION

Membrane processes can be applied to a wide range of separation processes. They can be driven by different forces. A pressure gradient over the membrane is used in processes such as reverse osmosis, ultrafiltration and microfiltration [1]. Essentially, these three processes are the same: the membrane acts as a sieve. In electrodialysis it is an electrical field over the membrane that causes transport of charged molecules [2]. In dialysis [3], pervaporation [4] and pertraction [5,6] a chemical potential gradient (concentration gradient) causes transport.

In almost all membrane processes, there are more than two components [7]. Therefore, an analysis of multicomponent transport phenomena is important. Also, it is desirable to describe transport in terms that have a simple physical interpretation. Only then is it possible to use the coefficients obtained for a given system, to predict the behaviour of other systems. Several approaches can be followed to describe transport in multicomponent systems [8,9]. Traditionally, diffusion phenomena in membranes are described by an effective diffusion coefficient ( $D_{eff}$ ). This effective diffusion coefficient can be related to the free (Fickian) diffusion coefficient by the characteristics of the membrane material [10,11]. The most widely used equation in this respect is the equation of Mackie and Meares [11], which relates the accessible volume (the non-polymer volume  $\epsilon$ ) to the diffusivity in free solution  $D_0$ :

$$\frac{D_{eff}}{D_0} = \left( \frac{\epsilon}{2-\epsilon} \right)^2 \quad (1)$$

However, the description of transport phenomena in terms of these phenomenological effective diffusivities does not result in quantities with an unambiguous physical interpretation.

In the Maxwell-Stefan equations, transport is described in terms of intermolecular friction [12]. The Generalized Maxwell Stefan equation (GMS) relates driving forces and intermolecular friction to net diffusion velocities, and hence to fluxes [12,13]. The equations contain frictional interactions between each set of species (including the membrane).

The GMS equation is a first order differential equation. For the sake of convenience, we use in this study the GMS equation in the form of an (approximate) difference equation [14] in order to determine membrane-solute friction coefficients and to describe the diffusion of multicomponent mixtures through a dialysis membrane. It will be shown that effects that cannot be accounted for using Fickian diffusion theory can be explained using the GMS equation.

### 3.2 THEORY

#### The Generalized Maxwell-Stefan equation

The starting point for the derivation of an equation for transport velocities in a mixture is the expression for the rate of entropy production ( $\sigma$ ). For an isothermal system [15,16]:

$$\sigma = -c_t R \sum_{i=1}^n d_i (u_i - u) \geq 0 \quad (2)$$

Here  $d_i$  is the driving force on a species  $i$  (per unit of volume of the mixture),  $u_i - u$  is the relative velocity of species  $i$  with respect to the mixture,  $c_t$  is the total molar concentration of the mixture and  $R$  is the gas constant. At thermodynamic equilibrium  $d_i = 0$  and  $\sigma = 0$ .

The driving force  $d_i$  may have various constituents. For example a chemical potential gradient due to composition gradients, a pressure gradient and an electrical potential gradient. Of course the driving force may, if necessary, be extended by adding gravitational, centrifugal or other terms. For our example it can be written as follows [15]:

$$d_i = \frac{x_i}{RT} \nabla_{T,P} \mu_i + \frac{(\phi_i - \omega_i)}{c_t RT} \nabla P + x_i z_i \frac{F}{RT} \nabla \varphi \quad (+ \text{ other terms}) \quad (3)$$

|      |            |   |
|------|------------|---|
| with | $x_i$      | = mole fraction component $i$ [-]                             |
|      | $\phi_i$   | = volume fraction component $i$ [-]                           |
|      | $\mu_i$    | = chemical potential due to composition component $i$ [J/mol] |
|      | $\omega_i$ | = mass fraction component $i$ [-]                             |
|      | $P$        | = pressure [Pa]   |
|      | $T$        | = absolute temperature [K]                                    |
|      | $\varphi$  | = electrical potential [V]                                    |
|      | $z_i$      | = charge number of component $i$ [-]                          |
|      | $F$        | = Faraday constant [C/mol]                                    |

The driving force on a species is counteracted by friction with the other species. The friction between two species is taken proportional to their relative amounts and to the differences in velocities [15,16]:

$$d_i = \sum_{j=1}^n \frac{x_i x_j (u_j - u_i)}{D_{ij}} \quad i=1, 2, \dots, n \quad (4)$$

This is the Generalized Maxwell-Stefan equation. The  $D_{ij}$ 's are interaction coefficients between the species  $i$  and  $j$ . They have the dimensions of a diffusivity and are known as Maxwell-Stefan (MS) diffusivities. From the Onsager reciprocal relation it is known that  $D_{ij} = D_{ji}$  [17,18,19].

The MS-diffusivities are only identical to the better known Fick diffusivities in two cases:

- for ideal binary mixtures and
- for solutes at infinite dilution in a solvent.

The behaviour of MS-diffusivities as a function of concentration is thought to be much simpler than that of Fick diffusivities [14,20].

#### Transport through a porous medium

If the spatial variations of  $\mu_i$ ,  $P$  and  $\varphi$  are low enough, one can always rewrite equations (3) and (4) in terms of differences over a distance  $\delta$ . This is a second order approximation of the differential equation [14]:

$$\frac{\Delta(\gamma_i x_i)}{(\gamma_i x_i)^*} + \frac{\Delta P}{P_i} + \frac{\Delta \varphi}{\varphi_i} = \sum_{j=1}^n x_j \frac{(u_j - u_i)}{k_{ij}} \quad (5)$$

Here  $\gamma_i$  is the activity coefficient of component  $i$  and  $(\gamma_i x_i)^*$  is taken at the average composition in the membrane,  $\varphi_i = RT/(Fz_i)$  and  $P_i = RT/V_i$  where  $V_i$  is the partial molar volume of  $i$ . For one-dimensional problems equation (5) is usually a good approximation [14]. In equation (5) the diffusion coefficients  $D_{ij}$  of equation (4) have been replaced by a transfer coefficient  $k_{ij}$ , which is defined as:

$$k_{ij} = \frac{D_{ij}}{\delta} \quad (6)$$

here  $\delta$  is the layer thickness over which diffusion takes place. In a porous body the layer thickness  $\delta$  has to be corrected for porosity ( $\epsilon$ ) and tortuosity ( $\tau$ ), yielding [21]

$$k_{ij} = \frac{D_{ij} \epsilon}{\delta \tau} \quad (7a)$$



### chapter 3

In this paper we are dealing with a membrane which we will regard as a single phase. Since it is difficult to define a mole fraction for the membrane we will replace the factor  $x_m/k_{im}$  by  $1/k'_{im}$ . The mole fraction membrane is taken equal to zero, so those of the permeants sum up to unity. This effectively removes the porosity correction  $\epsilon$  from equation 7a, so that:

$$k_{ij} = \frac{D_{ij}}{\delta\tau} \quad (7b)$$

The coefficients in solution can be estimated from literature data. However, since almost no data are available from the literature for the membrane coefficients, these values must be determined experimentally.

In addition to the diffusive mechanism described above, transport in porous media can involve a second mechanism [22,23,24]. This is viscous or convective flow and it is caused by a pressure difference. We will assume that the viscous flow is non-separative, so that each species has the same viscous velocity  $v^v$ . The total mass transfer velocity is the sum of the diffusive and viscous velocities:

$$v_i = v^v + u_i \quad (8)$$

### 3.3 MATERIALS

The membrane material used in this study is cellulose (Cuprophane), supplied by ENKA AG, FRG, both as flat sheets or hollow fibers with a dry membrane thickness of  $8 \mu\text{m}$ . The flat sheet membrane is used in a New Brunswick Scientific Megaflow TM-100 filtration module. This module has an effective membrane area of  $6.45 \cdot 10^{-3} \text{ m}^2$ . Liquid can be circulated at both sides of the membrane. The hollow fiber membrane device (artificial kidney) contained fibers of the same cellulose as used in the flat sheet module. The membrane area of the hollow fiber device is  $0.77 \text{ m}^2$ . Before use the membranes are rinsed with demineralized water to remove preservatives.

The water used in this study is demineralized. Methanol, ethanol and 2-propanol have been purchased from Merck, FRG, and are reagent grade. The temperature used throughout the study is  $20^\circ\text{C}$ .

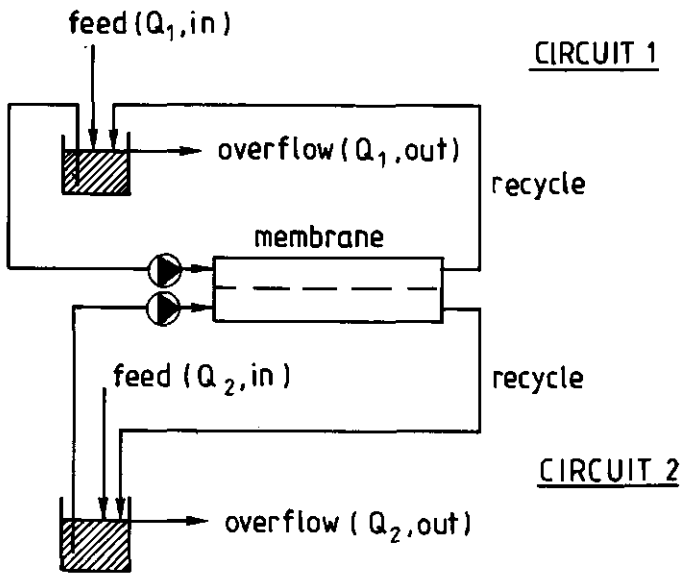


Figure 1. *Experimental set-up for steady state experiments*

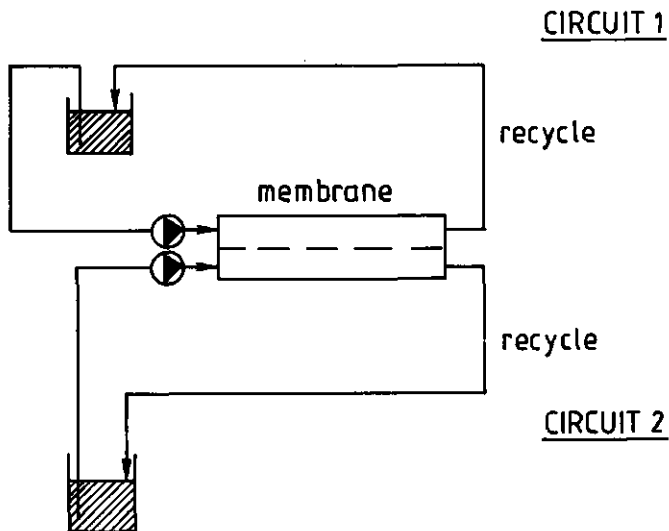


Figure 2. *Experimental set-up for batch experiments*

### chapter 3

The set-up for the experiments is shown in figures 1 and 2. It consists of two flow circuits on each side of the membrane. It can be operated in two different ways:

(1) Both compartments with a continuous feed and an overflow (figure 1). The system then eventually reaches a steady state.

(2) The batch mode, without feed to the compartments and without overflow (figure 2). In this mode a pressure difference can be applied across the membrane.

In case (1) the composition in both compartments is measured. In case (2) the mass of one of the compartments is measured.

Diffusion experiments with binary and ternary mixtures are performed with both a flat sheet and a hollow fiber membrane module. In these experiments there is no pressure difference across the membrane.

Table 1. *Initial circuit composition (in moles) in filtration experiments. On circuit 1 an excess pressure of 1 bar is applied*

|               | circuit 1 | circuit 2 |
|---------------|-----------|-----------|
| 1) oleate     | 0.032     | 0         |
| 2) sodium     | 0.032     | 0.3       |
| 3) water      | 3.65      | 7.5       |
| 4) 2-propanol | 1.51      | 0         |
| 5) chloride   | 0         | 0.3       |

With the same equipment "filtration" experiments have also been performed. Here a pressure gradient is applied, so there is not only diffusive, but also viscous transport through the membrane. The mixtures used here are complex. One circuit contains a two phase system with soy bean oil as the organic phase and a sodium oleate solution in water/2-propanol as the water phase. In this dispersion the water phase is continuous between 20% and 65% water phase [25]. Since the membrane is hydrophilic, it will be entirely wetted by the water phase and the oil phase does not enter the membrane. A typical set of initial compositions is given in table 1.

### 3.4 MEASUREMENT OF MEMBRANE FRICTION COEFFICIENTS

The membrane friction coefficients  $k'_{im}$  and  $k'_{jm}$  are measured by steady state dialysis measurements. Two streams of a binary mixture (with different compositions) are circulated through the two compartments. Both compartments have a steady feed and the volumes are kept

constant. In the following it is assumed that there are no volume changes in the mixing process. The flow rates in the two circuits are such that they may be regarded as well mixed.

The two circuits are fed at a constant rate ( $Q_{1in}$  and  $Q_{2in}$ ) and the volume of both circuits is kept constant (figure 1). For compartment 1 the following volume balance can be written in case two components  $i$  and  $j$  are present:

$$\frac{dV_1}{dt} = Q_{1in} \left[ \frac{X_{i1in}}{\rho_i} + \frac{1 - X_{i1in}}{\rho_j} \right] - Q_{1out} \left[ \frac{X_{i1}}{\rho_i} + \frac{1 - X_{i1}}{\rho_j} \right] + J_i + J_j \quad (9)$$

Here  $V_1$  is the volume of compartment 1,  $\rho_i$  and  $\rho_j$  are the densities of the two components,  $X_{i1in}$  and  $X_{i1}$  the mass fraction of component  $i$  in the inflow of compartment 1 and in the compartment, respectively.  $J_i$  and  $J_j$  are the diffusion fluxes through the membrane and  $t$  represents time. With a constant composition of  $i$  and  $j$  in the feed, and a constant volume of the two compartments, the system will reach steady state after some time. Since  $V_1$  is kept constant ( $dV_1/dt=0$ ), equation (9) results in the following expression for  $Q_{1out}$ :

$$Q_{1out} = \left[ \frac{\rho_i + (\rho_j - \rho_i) * X_{i1in}}{\rho_i + (\rho_j - \rho_i) * X_{i1}} \right] * Q_{1in} + (J_j + J_i) * \left[ \frac{\rho_i \rho_j}{\rho_i + (\rho_j - \rho_i) * X_{i1}} \right] \quad (10)$$

A mass balance over compartment 1 gives

$$\frac{d[V_1((\rho_j - \rho_i)X_{i1} - \rho_j)]}{dt} = Q_{1in} - Q_{1out} + \rho_i J_i + \rho_j J_j \quad (11)$$

For the steady state this yields:

$$-\rho_j J_j = Q_{1in} - Q_{1out} + \rho_i J_i \quad (12)$$

Similar equations can be derived for compartment 2. From equation (12) and (10) (and their analogs for compartment 2) the outflows can be eliminated, finally resulting in

$$-\rho_j J_j = \left[ \frac{X_{i1} - X_{i1in}}{X_{i1}} \right] * Q_{1in} + \frac{\rho_i J_i (X_{i1} - 1)}{X_{i1}} \quad (13)$$

$$\rho_i J_i = \left[ \frac{X_{i2} - X_{i2in}}{X_{i2} - 1} \right] * Q_{2in} - \frac{\rho_j J_j X_{i2}}{X_{i2} - 1} \quad (14)$$

From equation (13) and (14) the diffusion fluxes  $J_i$  and  $J_j$  can be calculated when the inflow and steady state concentrations are known. The diffusion velocities are related to these fluxes by

$$u_i = \frac{J_i}{\epsilon A} \quad (15a)$$

$$u_j = \frac{J_j}{\epsilon A} \quad (15b)$$

in which  $A$  is the membrane area over which transport occurs and  $\epsilon$  the porosity of the membrane material.

The pressure and electrical terms in equation (5) are zero in these experiments. The activity coefficients are obtained from existing data [26,27]. The binary diffusivities  $D_{ij}$  (and therefrom  $k_{ij}$ ) are calculated from known values at infinite dilution  $D_{ij}(x_i=0)$  and  $D_{ij}(x_i=1)$ . This is done by linear interpolation [20]:

$$D_{ij} = D_{ij}(x_i=0)^{x_j} * D_{ij}(x_i=1)^{x_i} \quad (16)$$

Both the partial densities and diffusivities are weak functions of composition. The accuracy of the experiments, however, does not make it necessary to take this into account. When  $k_{ij}$  is estimated using equations (7b) and (16) the calculation of  $k'_{im}$  and  $k'_{jm}$  is straightforward.

### 3.5 RESULTS AND DISCUSSION

#### Membrane friction coefficients

Membrane friction coefficients have been determined for the systems ethanol–water–cellulose, methanol–water–cellulose and 2–propanol–water–cellulose. Parameters used in the calculations are given in table 2.

Steady state concentrations are reached within about one hour in the two compartment module. The results of the measured membrane–solute transfer coefficients are given in figures 3 and 4.

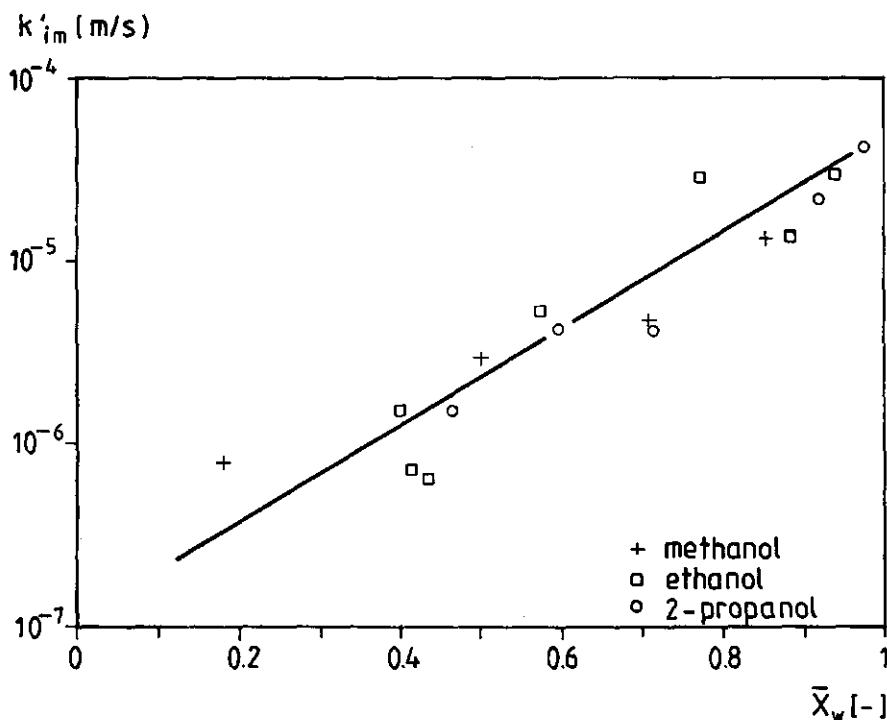


Figure 3. Membrane-water friction coefficients for water-methanol, water-ethanol and water-2-propanol mixtures versus water content in solution

In figure 3 the water-membrane friction is given for all three liquid mixtures as a function of the water fraction in the liquid. It appears, that the friction between water and the cellulose membrane strongly depends on the water fraction, but is virtually independent of the nature of the second liquid component. This strong dependence of the water-membrane friction with composition may be due to binding of part of the water to the cellulose matrix. From figure 4 it appears that the methanol and ethanol membrane coefficients vary little with composition. The 2-propanol-membrane coefficient shows the opposite trend as compared to water. From these results it can be concluded, that water diffuses more rapidly through the cellulose matrix than the alcohols at relatively high water contents in the system ( $x_w > 0.5$ ), whereas at low water contents the alcohols diffuse more rapidly through the membrane.

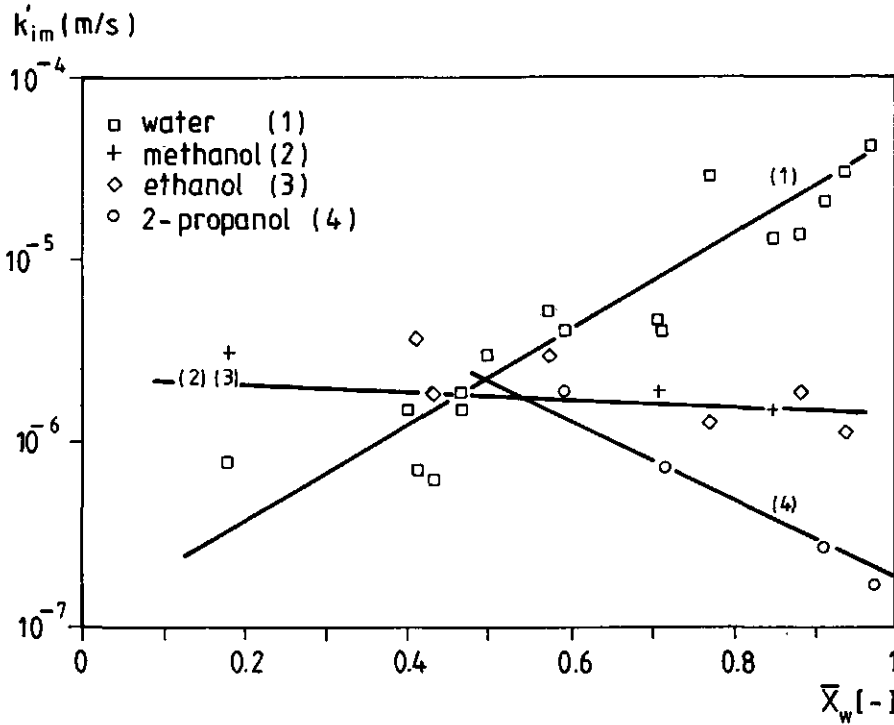


Figure 4. Membrane-solute friction coefficients for water, methanol, ethanol and 2-propanol versus water content in solution

#### Mass transport in a four component system

We have also done batch experiments with ternary mixtures and zero pressure gradient. In these experiments only the mass of the two compartments was measured as a function of time. The initial compositions in the three experiments are listed in table 3. The results are shown in figure 5 (flat membrane) and figure 6 (hollow fiber module).

For the description of mass transfer with time, we proceeded as follows. With known values of the transfer coefficients and the compositions on both sides of the membrane the velocities through the membrane can be calculated (equation (5)). Each component is assumed to be transported with its average concentration inside the membrane. This transport will cause a change

in composition at both sides of the membrane. These changed compositions are used for the calculation of the new transport velocities and so on. In this manner the mass of each component in either compartment can be calculated as a function of time.

Table 2. *Parameters used for the calculation of  $k'_{im}$*

| membrane parameters  |                     |                  |      |
|--|---------------------|------------------|------|
|  | porosity            | 0.65             | [28] |
|  | tortuosity          | 1.9              | [11] |
|  | thickness (dry)     | 8 $\mu\text{m}$  | [28] |
|  | thickness (swollen) | 15 $\mu\text{m}$ | [29] |
| densities ( $\text{kg/m}^3$ )  |                     |                  |      |
|  | water               | 1000             |      |
|  | methanol            | 790              |      |
|  | ethanol             | 790              |      |
|  | 2-propanol          | 785              |      |
| MS-diffusivities in free solution ( $10^{-9} \text{ m}^2/\text{s}$ ) |                     |                  |      |
|  | water/methanol      | 1.7              | [31] |
|  | water/ethanol       | 1.0              | [30] |
|  | water/2-propanol    | 1.3              | [32] |
|  | methanol/ethanol    | 2.15             | [32] |

We have done these calculations using the transfer coefficients given in table 4, which were all taken from the previous experiments. The coefficients are related to the average composition in the membrane. In these batch experiments the average values do not change significantly with time, and the coefficients may be taken as constant.

Table 3. *Initial circuit compositions (in moles) for ternary diffusion experiments*

|       | flat sheet module |       |       |       | hollow fiber |       |
|-------|-------------------|-------|-------|-------|--------------|-------|
|       | exp.1             |       | exp.2 |       |              |       |
|       | left              | right | left  | right | left         | right |
| water | 10                | 0     | 5     | 0     | 11           | 0     |
| MeOH  | 0                 | 2     | 1     | 2     | 0            | 2     |
| EtOH  | 0                 | 2     | 0     | 2     | 0            | 2     |



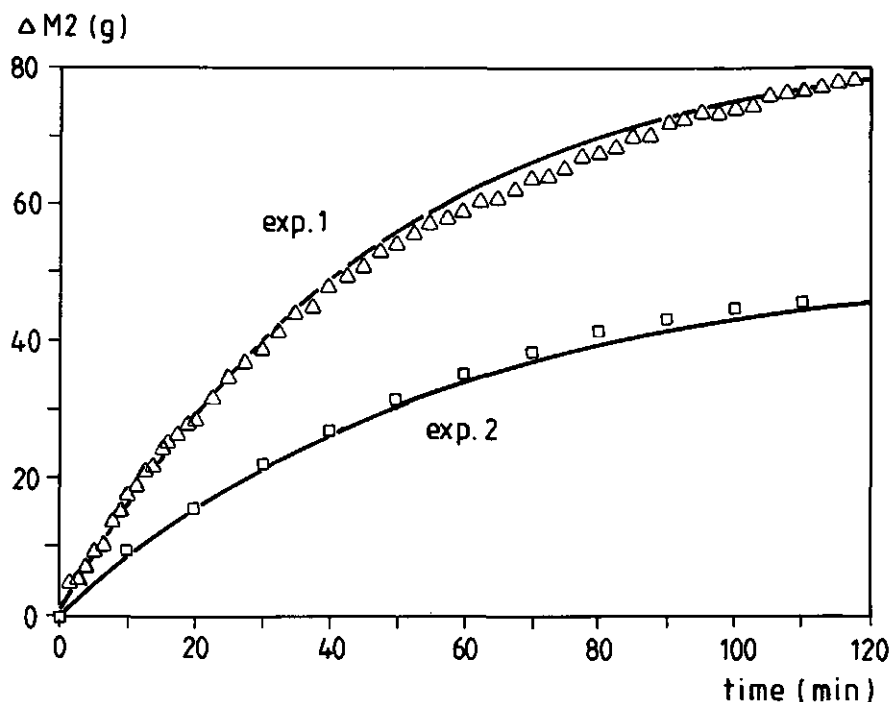


Figure 5. Mass of circuit 2 in flat sheet diffusion experiments.  $\Delta$  and  $\square$  are measured values, the lines are simulations

The measured and simulated changes agree well for the two experiments with a flat membrane (solid lines in figure 5). However, the fluxes calculated for the hollow fiber module are much too high. Correct results are predicted with an effective membrane area of  $0.045 \text{ m}^2$ , instead of the actual fiber area of  $0.77 \text{ m}^2$ . It was shown by residence time distribution measurements in the same dialysis modules [33], that these modules can be considered as a plug flow vessel with a "dead volume" corresponding to the fiber bundle volume. The outer area of the bundle of fibers is  $0.032 \text{ m}^2$ . All this indicates that within the time scale of the process studied here only the outer surface of the bundle of fibers is effective for mass transfer.

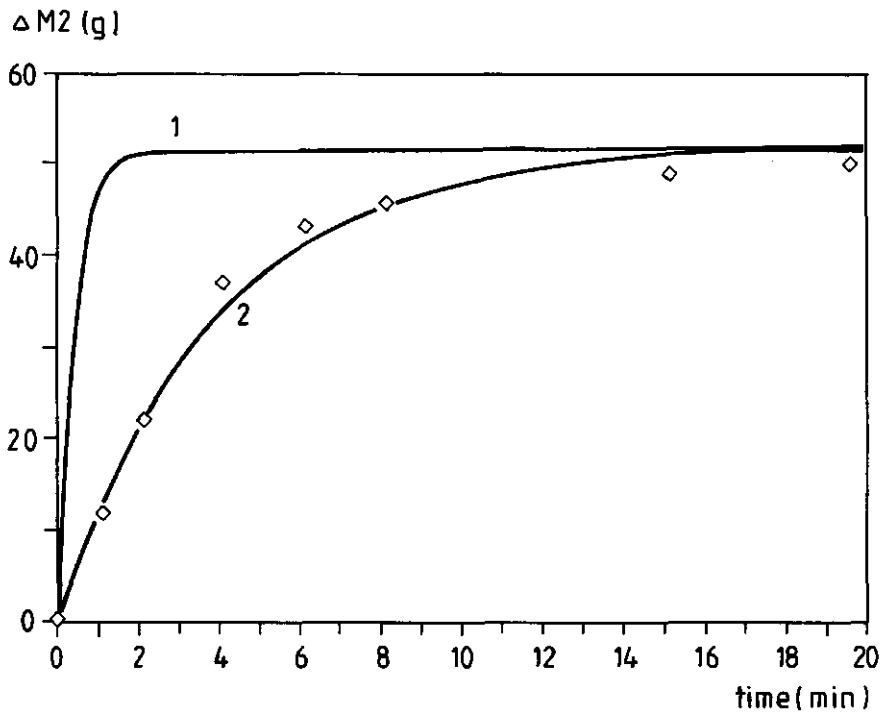


Figure 6. Mass of circuit 2 in a hollow fiber diffusion experiment.  $\diamond$  are measured values, line 1 is a simulation with  $A=0.77 \text{ m}^2$  and line 2 is a simulation with  $A=0.045 \text{ m}^2$

Table 4. Transport coefficients (m/s) used for the simulation of mass transport in four component diffusion experiments. (1)=water, (2)=methanol, (3)=ethanol and (m)=membrane.  $k_{12}=5.9 \cdot 10^{-5}$ ,  $k_{13}=3.4 \cdot 10^{-5}$  and  $k_{23}=6.7 \cdot 10^{-5} \text{ m/s}$

|           | exp.1               | exp.2             | hollow fiber        |
|-----------|---------------------|-------------------|---------------------|
| $k'_{1m}$ | $1.1 \cdot 10^{-5}$ | $6 \cdot 10^{-6}$ | $7.8 \cdot 10^{-6}$ |
| $k'_{2m}$ | $1.6 \cdot 10^{-6}$ | $8 \cdot 10^{-7}$ | $2 \cdot 10^{-7}$   |
| $k'_{3m}$ | $1.6 \cdot 10^{-6}$ | $8 \cdot 10^{-7}$ | $2 \cdot 10^{-7}$   |

## Mass transport in a complex system

The origin of this study lies in effects observed in an even more complicated system. Initially we did not understand these effects; even with our current knowledge we can only explain them qualitatively. In these experiments, a solution of sodium oleate in a 2-propanol/water mixture is to be pumped through a membrane into a solution of sodium chloride in water. To attain this, a pressure difference of 1 bar is applied across the membrane. With both compartments filled with the sodium oleate/2-propanol/water solution this gives a trans-membrane velocity of  $1.4 \cdot 10^{-6}$  m/s. We shall assume that this is the viscous flow velocity.

In experiments with the sodium chloride solution at the permeate side, fluxes were obtained 2 to 10 times larger than the flux based on viscous flow. Not only that, but they were initially directed against the pressure gradient (figures 7 and 8). This reverse flux could be increased by either reducing the NaCl concentration or increasing the 2-propanol concentration.

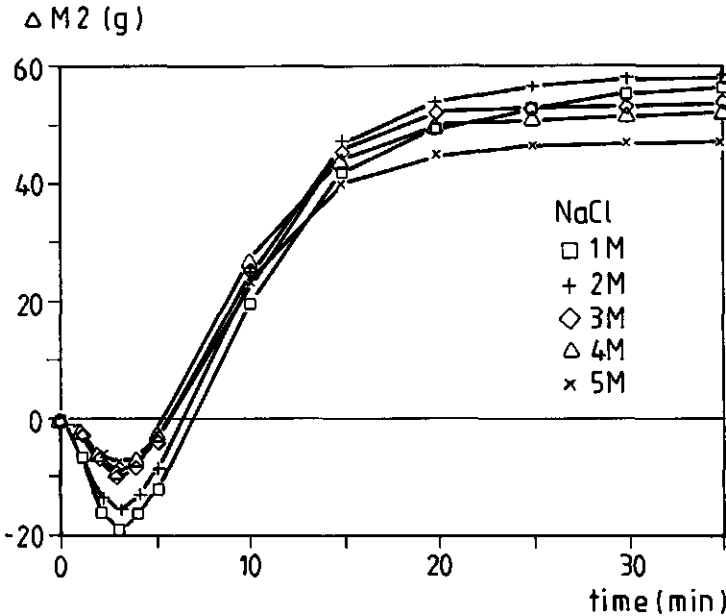


Figure 7. Measurements of the effect of NaCl concentration at the permeate side of the membrane on permeation behaviour

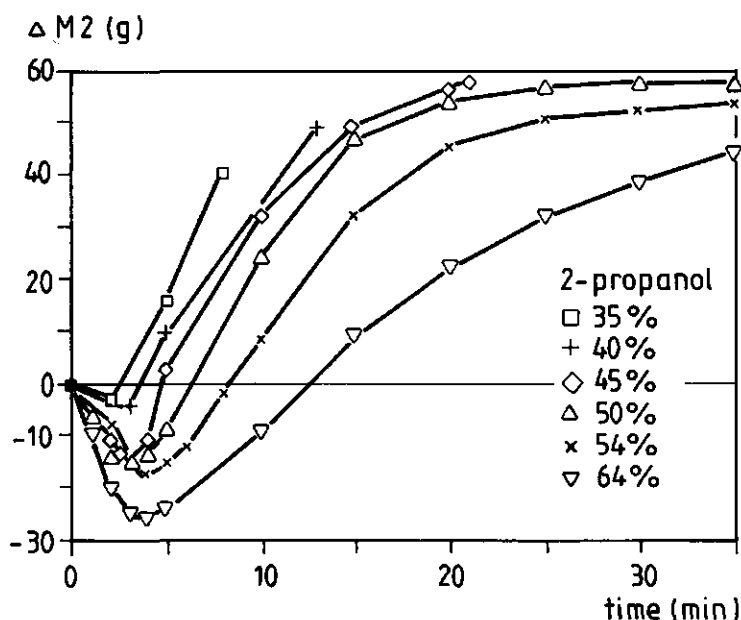


Figure 8. Measurement of the effect of 2-propanol concentration at the feed side of the membrane on permeation behaviour

This very complex system can be analyzed using the same techniques as in the previous paragraph. However, now there are 5 permeating species in addition to the membrane (table 5). Also, we apply a pressure gradient. Because ionic species are involved, an electrical potential difference may be generated. So we have 5 unknown species velocities and an unknown electrical potential difference. There are 5 transport equations, and the sixth is due to the constraint that there is no net charge transfer across the membrane.

Again we have made simulations of the batch experiments using the same technique as in the former paragraph. A large set of transport coefficients is required (table 5). The greater part of these coefficients are only known within an order of magnitude. However, only the coefficients belonging to water, 2-propanol and the membrane are important for the final result. They can be estimated from figure 4. As thermodynamic data for such a system are non-existent we have

chosen to ignore variations of the activity coefficients. Although it was shown in the former paragraph that for diffusive transport in a fiber bundle only the outer fibers are important, we used an effective surface area of  $0.77 \text{ m}^2$  here. Since viscous flow occurs, the bundle of fibers will be more open, and flow will occur in between.

Table 5. *Estimated transfer coefficients for a multicomponent mixture. (1)=oleate, (2)=sodium, (3)=water, (4)=2-propanol, (5)=chloride and (m)=membrane*

|                      |                       |                       |                     |                     |
|----------------------|-----------------------|-----------------------|---------------------|---------------------|
| $k_{12}=5*10^{-6}$   | $k_{13}=2*10^{-5}$    | $k_{14}=3*10^{-5}$    | $k_{15}=5*10^{-6}$  | $k'_{1m}=5*10^{-8}$ |
| $k_{23}=5*10^{-5}$   | $k_{24}=3*10^{-5}$    | $k_{25}=5*10^{-6}$    | $k'_{2m}=1*10^{-6}$ |                     |
| $k_{34}=4.5*10^{-5}$ | $k_{35}=7*10^{-5}$    | $k'_{3m}=1.5*10^{-5}$ |                     |                     |
| $k_{45}=3*10^{-5}$   | $k'_{4m}=1.5*10^{-6}$ |                       |                     |                     |
| $k'_{5m}=1*10^{-6}$  |                       |                       |                     |                     |

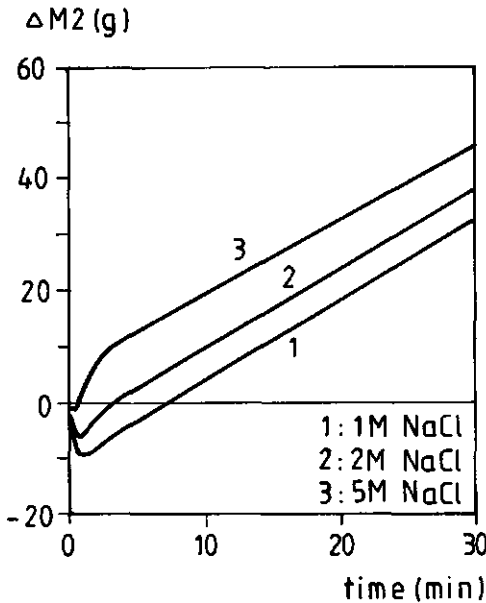


Figure 9a. *Simulations of the effect of NaCl concentration on the mass of the permeate circuit*

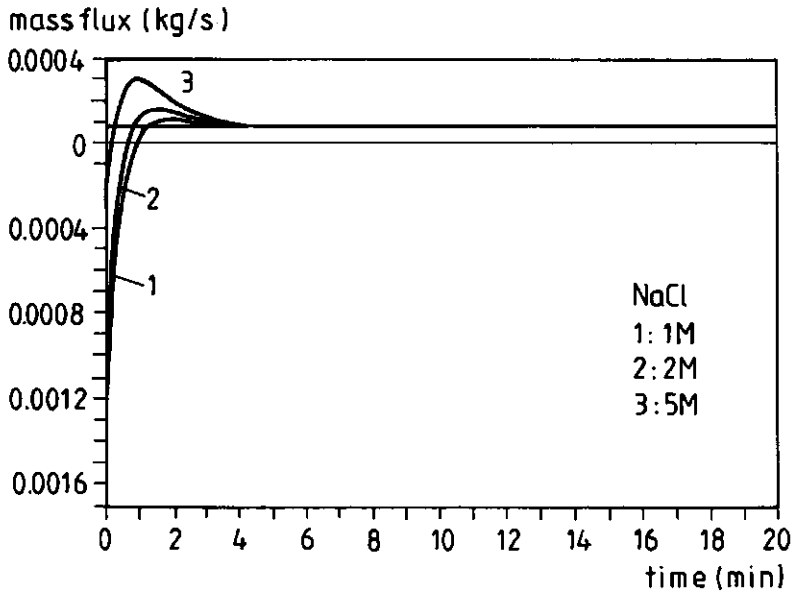


Figure 9b. Simulations of the effect of NaCl concentration on flux

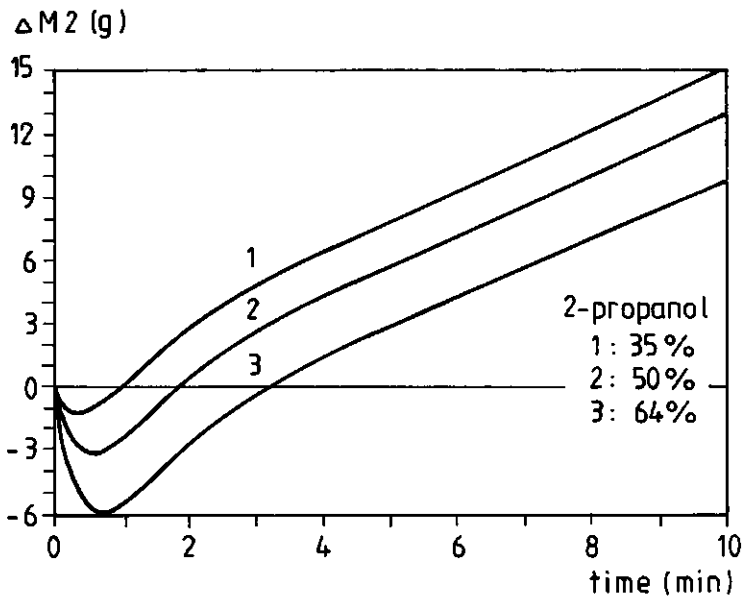


Figure 10a. The effect of 2-propanol concentration on the mass of the permeate circuit (simulations)

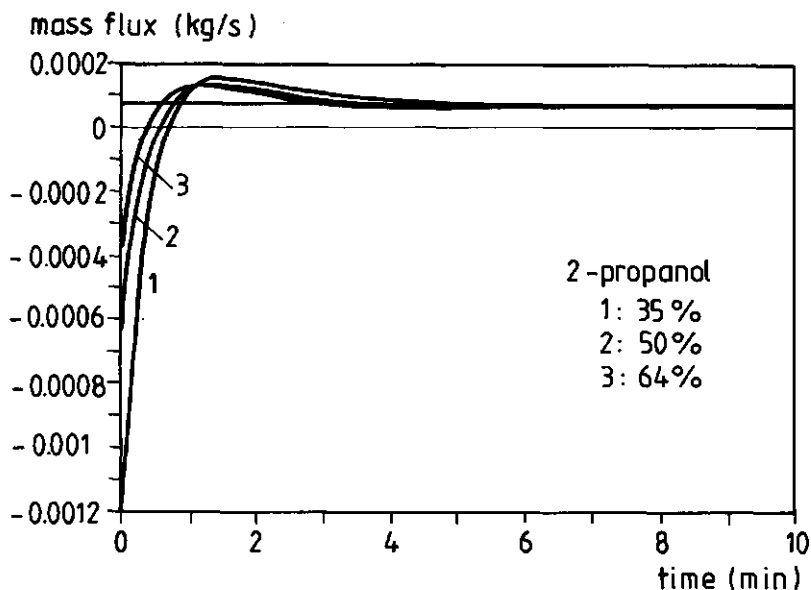


Figure 10b. *The effect of 2-propanol concentration on flux (simulations)*

Results of such simulations are shown in figures 9 and 10. They indeed show the reverse fluxes found experimentally and also the effects of the NaCl and 2-propanol concentration are predicted. However, the fluxes thus predicted are roughly 3 times higher than those measured. With the assumptions made, this deviation can indeed occur. Another possible explanation is precipitation of sodium oleate onto or inside the membrane at high NaCl concentrations. This precipitation was observed in separate experiments, and will result in a reduced membrane area over which transport can take place.

The simulations yield transport velocities of all components separately (figure 11). From these we see that there are three main contributions to the overall flow:

- (1) the viscous flow, which dominates for long times
- (2) the transport of 2-propanol, which is in the direction expected (going both down the pressure and the concentration gradient)
- (3) the transport of water.

Water is initially transported with a high velocity against the pressure gradient into the 2-propanol solution. The reversed mass flow is explained by this phenomenon. When sufficiently 2-propanol has been transferred its direction also reverses. The electrical and pressure terms in the diffusion

equation were found not to be important.

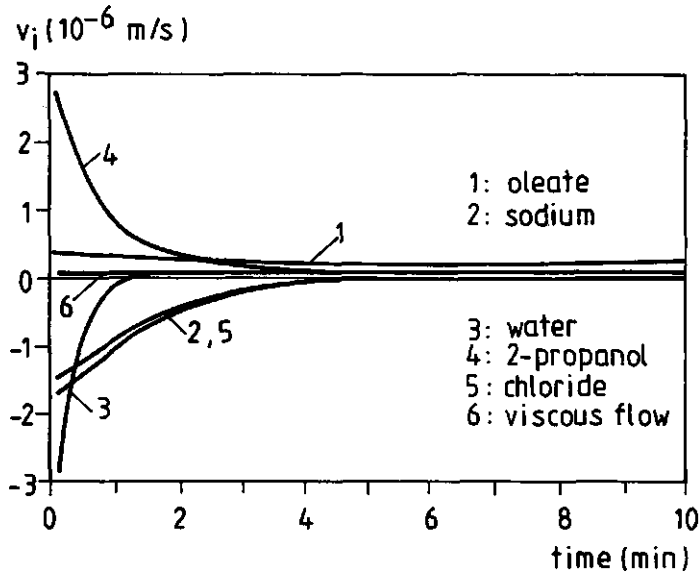


Figure 11a. Transport velocities of all components

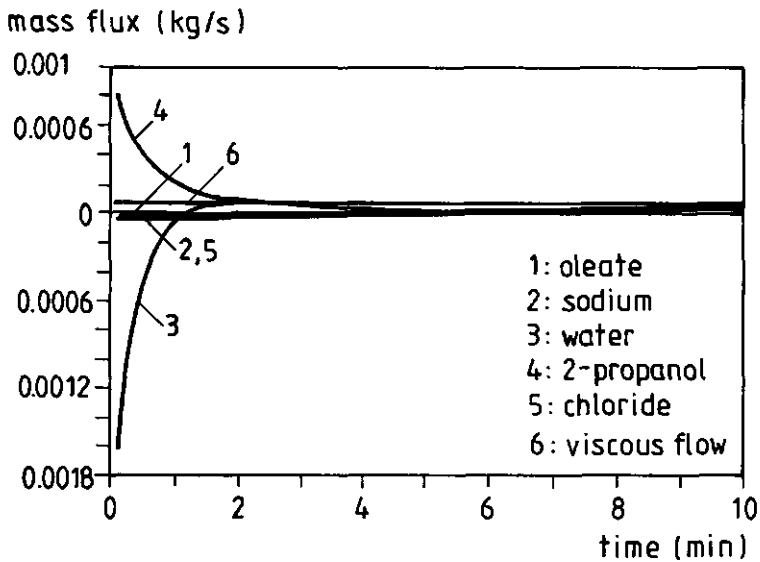


Figure 11b. Transport fluxes of all components



### 3.6 CONCLUSIONS

In this study a difference approximation of the generalized Maxwell-Stefan (GMS) equation is used to describe transport through homogeneous cellulose dialysis membranes. Solute-membrane friction is determined for water, methanol, ethanol and 2-propanol. It appears, that the friction between water and the cellulose matrix strongly depends on the water concentration. At low water contents water is strongly retarded, probably by binding of water to the membrane matrix. At higher water contents the transfer coefficients for water are two decades larger. Using these measured friction coefficients it is possible to describe transport of a ternary liquid mixture through a flat sheet membrane quantitatively. However, for a hollow fiber device containing fibers of the same material the calculated mass flux through the membrane is much faster than the observed transport. It appears that the surface area over which diffusion occurs is almost identical to the outer surface of the fiber bundle. In a complex system containing water, 2-propanol and sodium oleate at the feed side and a NaCl solution at the permeate side of the membrane, initially a flux against the pressure gradient is observed (i.e. from permeate to feed). After some time the flux changes direction and becomes 2 to 10 times larger than the permeation rate would be at the same pressure. These effects can be explained qualitatively by the difference approximation of the GMS equations.

### ACKNOWLEDGEMENTS

The authors wish to thank the Dutch Program Committee for Industrial Biotechnology (PCIB) for their financial support and B.K. Kumbhar (G.B. Pant Univ. of Agric. and Technol., Pantnagar, India) and B. Hasenack for performing experiments.

### LIST OF SYMBOLS

|                  |  |                       |
|------------------|--|-----------------------|
| A                | membrane surface area                      | [m <sup>2</sup> ]     |
| c <sub>t</sub>   | mixture molar density                      | [mol/m <sup>3</sup> ] |
| d <sub>i</sub>   | driving force for diffusion of component i | [m <sup>-1</sup> ]    |
| D <sub>eff</sub> | effective diffusion coefficient            | [m <sup>2</sup> /s]   |
| D <sub>ij</sub>  | Maxwell Stefan diffusivity                 | [m <sup>2</sup> /s]   |
| D <sub>o</sub>   | diffusivity in free solution               | [m <sup>2</sup> /s]   |
| F                | Faraday constant                           | [C/mol]               |
| J                | volumetric diffusion flux                  | [m <sup>3</sup> /s]   |

### chapter 3

|            |  |                           |
|------------|--|---------------------------|
| $k_{ij}$   | binary mass transfer coefficient             | [m/s]                     |
| $k'_{im}$  | reduced membrane-solute transfer coefficient | [m/s]                     |
| $n$        | number of components                         | [-]                       |
| $P$        | pressure                                     | [Pa]                      |
| $R$        | gas constant                                 | [J/(mol.K)]               |
| $Q$        | mass flow                                    | [kg/s]                    |
| $T$        | temperature                                  | [K]                       |
| $t$        | time   | [s]                       |
| $u$        | reference velocity                           | [m/s]                     |
| $u_i$      | velocity of species i                        | [m/s]                     |
| $V$        | volume                                       | [m <sup>3</sup> ]         |
| $V_i$      | partial molar volume of component i          | [m <sup>3</sup> /mol]     |
| $v_i$      | diffusion velocity of component i            | [m/s]                     |
| $v^v$      | viscous flow velocity                        | [m/s]                     |
| $X_i$      | mass fraction component i                    | [-]                       |
| $x_i$      | mole fraction component i                    | [-]                       |
| $z_i$      | charge number on component i                 | [-]                       |
| $\gamma_i$ | activity coefficient component i             | [-]                       |
| $\delta$   | diffusion layer thickness                    | [m]                       |
| $\epsilon$ | membrane porosity                            | [-]                       |
| $\mu_i$    | chemical potential component i               | [J/mol]                   |
| $\sigma$   | rate of entropy production                   | [J/(m <sup>3</sup> .s.K)] |
| $\tau$     | membrane tortuosity                          | [-]                       |
| $\rho_i$   | density component i                          | [kg/m <sup>3</sup> ]      |
| $\phi_i$   | volume fraction component i                  | [-]                       |
| $\varphi$  | electrical potential                         | [V]                       |
| $\omega_i$ | mass fraction component i                    | [-]                       |

### REFERENCES

- 1) Sourirajan, S. and T. Matsuura, Reverse Osmosis/Ultrafiltration, Process Principles, National Research Council Canada, Ottawa, 1985
- 2) Cheryan, M., Ultrafiltration Handbook, Technomic Publishing Co. Inc., Lancaster, 1986
- 3) Klein, E., F.F. Holland and K. Eberle, Comparison of experimental and calculated permeability and rejection coefficients for hemodialysis membranes, J. Membrane Sci. 5 (1979) 173-188
- 4) Brun, J.P., C. Larchet, R. Melet and G. Bulvestre, Modelling of the pervaporation of binary mixtures through

### chapter 3

- moderately swelling, non-reacting membranes, *J. Membrane Sci.* 23 (1985) 257-283
- 5) Dahuron, L. and E.L. Cussler, Protein extractions with hollow fibers, *Am. Inst. Chem. Eng. J.* 34 (1988) 130-136
  - 6) Keurentjes, J.T.F., Th. G.J. Bosklopper, L.J. van Dorp and K. van 't Riet, The removal of metals from edible oil by a membrane extraction procedure, *J. Am. Oil Chem. Soc.* 67 (1990) 28-32
  - 7) Thiel, S.W. and D.R. Lloyd, Multicomponent diffusion in the pressure-driven membrane separation of dilute solutions of nonelectrolytes, *J. Membrane Sci.* 42 (1989) 285-302
  - 8) Cussler, E.L., *Multicomponent Diffusion*, Elsevier, Amsterdam, 1976
  - 9) Peppas, N.A. and D.L. Meadows, Macromolecular structure and solute diffusion in membranes: an overview of recent theories, *J. Membr. Sci.* 16 (1983) 361-377
  - 10) Mackie, J.S. and P. Meares, The diffusion of electrolytes in a cation exchange resin membrane, *Proc. Roy. Soc. (London)*, A232 (1955) 498-509
  - 11) Peppas, N.A. and C.T. Reinhart, Solute diffusion in swollen membranes: Part I. A new theory, *J. Membrane Sci.* 15 (1983) 275-287
  - 12) Krishna, R., A unified theory of separation processes based on irreversible thermodynamics, *Chem. Eng. Comm.* 59 (1987) 33-64
  - 13) Thiel S.W. and D.R. Lloyd, Application of the Stefan-Maxwell equations to the pressure-driven membrane separation of dilute multicomponent solutions of nonelectrolytes, *J. Membrane Sci.* 37 (1988) 233-249
  - 14) Wesselingh, J.A. and R. Krishna, *Mass Transfer*, To be published by Ellis Horwood Ltd., october 1990
  - 15) Lightfoot, E.N., *Transport Phenomena and Living Systems*, John Wiley, New York, 1974
  - 16) Standart, G.L., R. Taylor and R. Krishna, The Maxwell-Stefan formulation of irreversible thermodynamics for simultaneous heat and mass transfer, *Chem. Eng. Comm.* 3 (1979) 277-289
  - 17) Onsager, L., Reciprocal relations in irreversible processes, *Phys. Rev.* 37 (1931) 405-426
  - 18) Dunlop, P.J., Diffusion and frictional coefficients for two concentrated compositions of the system water-mannitol-sodium chloride at 25°C; tests of the Onsager reciprocal relation, *J. Phys. Chem.* 69 (1965) 4276-4283
  - 19) Chu, R., D. Gisser, M. Kupferschmid and A. Zelman, An automated data collection system for membrane transport experiments. Part I. Test of Onsager reciprocity, *J. Membrane Sci.* 22 (1985) 77-109
  - 20) Vignes, A., Diffusion in binary solutions, *Ind. Eng. Chem. Fundam.*, 5 (1966) 189-199
  - 21) D'Elia, N.A., L. Dahuron and E.L. Cussler, Liquid-liquid extractions with microporous hollow fibers, *J. Membrane Sci.* 29 (1986) 309-319
  - 22) Jackson, R., *Transport in porous catalysts*, Elsevier, Amsterdam, 1977
  - 23) Mason, E.A. and L.F. del Castillo, The role of viscous flow in theories of membrane transport, *J. Membrane Sci.* 23 (1985) 199-220
  - 24) Mason, E.A. and L.A. Viehland, Statistical mechanical theory of membrane transport for multicomponent systems: passive transport through open membranes, *J. Chem. Phys.* 68 (1978) 3562-3575
  - 25) Keurentjes, J.T.F., G.I. Doornbusch and K. van 't Riet, The removal of fatty acids from edible oil; removal of the dispersed phase of a water in oil dispersion by a hydrophilic membrane, to be published in *Sep. Sci. Technol.*
  - 26) Prausnitz, J.M., *Molecular Thermodynamics of Fluid-Phase Equilibria*, Prentice-Hall, Inc., 1969
  - 27) Gmehling, J. and U. Onken, Vapour-liquid equilibrium data collection. Aqueous-organic systems. *Chemistry Data Series vol. 1, part 1*, Dechema, Frankfurt a.M., FRG, 1977
  - 28) ENKA AG, FRG, data sheet Cuprophon
  - 29) Sakai, K., S. Takesawa, R. Mimura and H. Ohashi, Structural analysis of hollow fiber dialysis membranes for clinical use, *J. Chem. Eng. Japan* 20 (1987) 351-356
  - 30) Pratt, K.C. and W.A. Wakeham, The mutual diffusion coefficient of ethanol-water mixtures: determination by a rapid, new method, *Proc. R. Soc. Lond. A* 336 (1974) 393-406
  - 31) Derlacki, Z.J., A.J. Easteal, A.V.J. Edge, L.A. Woolf and Z. Roksandic, Diffusion coefficients of methanol and

### *chapter 3*

water and the mutual diffusion coefficient in methanol-water solutions at 278 and 298 K, J. Phys. Chem. 89 (1985) 5318-5322

- 32) Wilke, C.R. and P. Chang, Correlation of diffusion coefficients in dilute solutions, Am. Inst. Chem. Eng. J. 1 (1955) 264-270
- 33) Padt, A. van der and K. van 't Riet, Membrane bioreactors, in: NATO ASI Series, Chromatographic and Membrane Processes in Biotechnology, C.A. Costa and J. Cabral (Eds.), 1990

## HYDROPHOBICITY MEASUREMENTS OF MF AND UF MEMBRANES

---

### SUMMARY

A method for the determination of the hydrophobicity of membrane materials is developed. The advantage of this method over existing methods is that it is not influenced by the presence of the pores. A piece of the membrane material is submerged horizontally in a liquid with surface tension  $\gamma_L$ . Hydrophobicity is expressed in terms of  $\gamma_d$ , the surface tension at which an air bubble brought into contact with the top surface of the membrane has a 50% chance of detaching from the surface. Values of  $\gamma_d$  are expected to be 2-4 mN/m higher than critical surface tension ( $\gamma_c$ ) values found in the literature. For PP, PTFE and PDMS membranes, a good agreement was found between  $\gamma_d$  and  $\gamma_c$  values. PVDF, PSf and PES membranes appeared to be more hydrophilic than was expected on the basis of the literature  $\gamma_c$  values for the polymers. Using XPS, constituents that are not present in the pure polymer have been found in the surface of some membranes. These constituents and the production techniques are shown to influence the hydrophobicity of the membranes investigated.

---

J.T.F. Keurentjes, J.G. Harbrecht, D. Brinkman, J.H. Hanemaaijer\*, M.A. Cohen Stuart\*\* and K. van 't Riet

\*NIZO, P.O. Box 20, 6710 BA Ede, The Netherlands (present address: MT-TNO, P.O. Box 108, 3700 AC Zeist, The Netherlands)

\*\*Agricultural University Wageningen, Dept. of Physical and Colloid Chemistry, De Dreijen 6, 6703 BC Wageningen, The Netherlands

This chapter has been published in J. Membrane Sci. 47 (1989) 333-344

## 4.1 INTRODUCTION

In many membrane processes, the choice of the membrane is based on the pore size of the material. However, for the separation of organic molecules from aqueous solutions in membrane distillation processes [1,2], for the separation of dispersions [3,4] or for explaining fouling phenomena [5,6], this property does not suffice. Interactions of the solvent and solutes with the membrane material will be an important parameter in these processes; therefore, in addition to the pore size, the hydrophobicity of the membrane material needs to be known.

Hydrophobicity of a solid material is usually expressed in terms of a contact angle ( $\theta$ ) or a critical surface tension. The most widely used method for the determination of the contact angle of a liquid (with surface tension  $\gamma_L$ ) on a surface, is a direct measurement of  $\theta$  using a sessile drop of the liquid on the surface. Because of surface inhomogeneity, either an advancing, receding or equilibrium contact angle can be determined [7]. The critical surface tension of a solid ( $\gamma_c$ ) is defined as the surface tension at which the contact angle of a liquid just vanishes on that solid [8,9], or:

$$\gamma_c = \lim(\theta \rightarrow 0) \gamma_L \quad (1)$$

Usually,  $\theta$  is measured using different liquids or mixtures of two liquids having different surface tensions. If  $\cos\theta$  is plotted versus the surface tension of the liquid (Zisman plot), extrapolation to  $\cos\theta=1$  gives the critical surface tension  $\gamma_c$  [9].

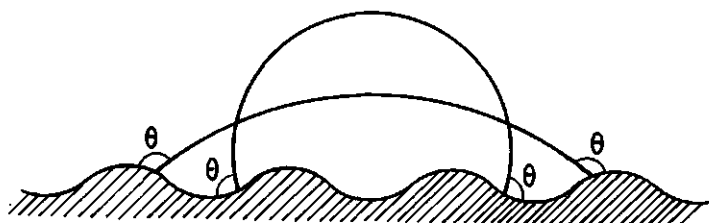


Figure 1. *Two different metastable configurations of a liquid drop having the same contact angle  $\theta$  on a rough surface*

Conditions for correct measurements of  $\theta$  are a homogeneous and ideally smooth surface. Because of surface roughness, the observed contact angle may differ significantly from the real contact

angle. This is shown schematically in figure 1. The only general method to predict the effect of surface roughness on contact angle measurements is based on Wenzel's theory [10]. This theory gives a relationship between the advancing contact angle on the smooth surface ( $\theta_E$ ) and the advancing contact angle on a rough surface ( $\theta_A$ ):

$$\cos \theta_A = r_s \cos \theta_E \quad (2)$$

in which the surface roughness is quantified by  $r_s$ , the roughness factor, defined as the ratio of the actual to the apparent area of the surface. Several other models have been proposed, however, their use is restricted to special types of surface roughness [11,12,13]. The surface roughness of membrane materials is caused by the presence of pores and the roughness of the polymer material, the latter often being in the order of several microns [2].

Beside surface roughness, capillary forces also play an important role for the determination of the hydrophobicity of a membrane material. Due to capillary forces, a droplet of liquid with  $\gamma_L > \gamma_c$  can penetrate into a hydrophobic membrane, even though it does not spread on a non-porous sheet of the same material. Using the Laplace equation, a correction for these forces in cylindrical pores can be made. Franken et al. [1] introduced a pore geometry coefficient to correct for non-cylindrical pores.

A method for the determination of the hydrophobicity of membrane materials should preferably be independent of the presence of pores. For this purpose, several existing methods can be taken into consideration. As mentioned before, methods for the direct determination of contact angles are sensitive to surface roughness. Therefore, these methods are of limited interest for the determination of the hydrophobicity of membrane materials. Two methods have been developed specifically to determine the hydrophobicity of porous or inhomogeneous materials. Of practical interest is the penetrating drop method [1], although this method is restricted to microporous membranes. Distribution of material over two aqueous polymer phases has proven to be very useful for the determination of hydrophobicity of bacterial material [14,15]. An advantage of this method is that pore effects can be avoided. This method could perhaps be used for homogeneous membranes, but must obviously be excluded for non-woven supported and composite membranes, unless a complete separation of the skin layer from the backing material can be achieved.

In this study, a method is developed for the determination of the hydrophobicity of membrane materials. This method is not influenced by the presence of pores, and applies to homogeneous as well as to composite membranes and over a broad range of pore sizes.

## 4.2 METHODS

### 1. Sticking bubble technique

Bubble adhesion measurements are carried out as follows. A piece of membrane material (about  $1 \text{ cm}^2$ ) is placed horizontally at the bottom of a beaker containing a liquid with surface tension  $\gamma_L$ . In order to vary  $\gamma_L$ , water-methanol mixtures are used, giving a range in  $\gamma_L$  from 23 to 72 mN/m. Using a  $10 \mu\text{l}$  syringe (Hamilton Co.) with a flat ended needle (horizontal), air bubbles are brought into contact with the surface. The smallest distance between the open end of the needle and the membrane surface is about 0.5 times the bubble diameter. At high values of  $\gamma_L$ , air bubbles will stick easily to the surface. When the surface tension of the liquid decreases, the adhesion of the air bubbles becomes weaker. Below a certain value of  $\gamma_L$ , bubbles will not adhere at all because the liquid wets the surface completely (figure 2). The surface tension at detachment ( $\gamma_d$ ) is determined by plotting the percentage of bubbles which sticks versus  $\gamma_L$ ; a sudden transition is observed at  $\gamma_d$ .

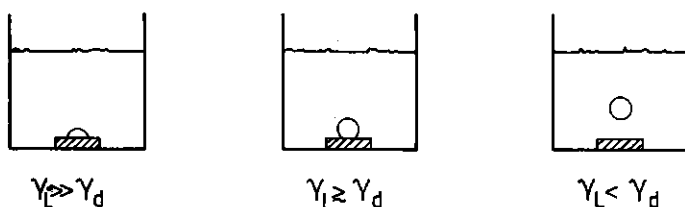


Figure 2. Three situations of an air bubble brought into contact with a surface

### 2. X-ray photoelectron spectroscopic measurements

Surface analysis on membranes by X-ray photoelectron spectroscopy was performed at AKZO (Arnhem, The Netherlands) using a Vacuum Generators Scientific MA 500 instrument. The excitation X-ray source was  $\text{MgK}\alpha$  (excitation energy 1253.6 eV). Sample orientation was chosen normal to the electron energy analyzer, resulting in an "analysis depth" of approximately 5 nm, and also in a skimming position, decreasing the depth of analysis to approximately 1 nm.



## 4.3 MATERIALS

In this study the hydrophobicity of several hydrophobic membrane materials has been measured. All membranes used are summarized in table 1. Data are according to the suppliers; most of the membranes are commercially available.

Table 1. *Membranes used for the determination of  $\gamma_d$*

| Material               | Code      | Manufacturer  | Pore size/cut off  |
|------------------------|-----------|---------------|--------------------|
| PTFE                   |           | Gore          | 0.2 $\mu\text{m}$  |
| PVDF                   |           | Millipore     | 0.14 $\mu\text{m}$ |
| PVDF                   |           | Millipore     | 0.2 $\mu\text{m}$  |
| PVDF                   | IRIS 3065 | Rhone-Poulenc | 10,000 D           |
| Polypropylene (PP)     | Accurel   | ENKA          | 0.2 $\mu\text{m}$  |
| Polysulfone (PSf)      | GR 81 PP  | DDS           | 6,000 D            |
| Polysulfone (PSf)      | GR 61 PP  | DDS           | 25,000 D           |
| Polysulfone (PSf)      | GR 51 PP  | DDS           | 50,000 D           |
| Polysulfone (PSf)      | GR 60 PP  | DDS           | 25,000 D           |
| Polysulfone (PSf)      | S-30      | Dorr Oliver   | 30,000 D           |
| Polyethersulfone (PES) | Omega     | Filtron       | 100,000 D          |
| PDMS                   | *)        | -             |                    |

\*) Dense film made of PDMS obtained from Dow Chemical

Some of the membranes mentioned in table 1 are microporous homogeneous membranes. These membranes are stored as dry sheets and do not have to be cleaned before use. However, most of the ultrafiltration membranes are impregnated with a preservative liquid (usually containing glycol) that has to be removed before use. The cleaning procedure used in this study is as follows. First, a sheet of the membrane material (65 cm<sup>2</sup>) is washed with a detergent solution (1% SDS). Next, 20 l doubly distilled water is filtered through the membrane. Then the material is dried at 40 °C, and is ready for use.

All experiments are carried out at 20 °C. The water used is doubly distilled, and the methanol (analytical grade) was obtained from Merck (F.R.G.). Before each experiment the water-methanol mixtures are freshly prepared. Udel polysulfone is obtained from Union Carbide Corp. (CU 4750) and polyethersulfone from ICI (4800 G).

## 4.4 THEORY

We consider the simple case of a bubble with spherical contour attached to the surface with contact angle  $\theta_2$ , as shown in figure 3. At the point of detachment, the vertical component of the adhesion forces exactly compensates the gravitational forces:

$$V \Delta \rho g = 2 \pi r \gamma_d \sin \theta_2 \quad (3)$$

where  $V$  is the air bubble volume,  $g$  the acceleration due to gravity,  $\Delta \rho$  the difference between liquid and air density,  $r$  the radius of the contact plane and  $\gamma_d$  the surface tension of the liquid at the point of detachment. The radius of the contact plane ( $r$ ) is given by:

$$r = R \sin \theta_2 \quad (4)$$

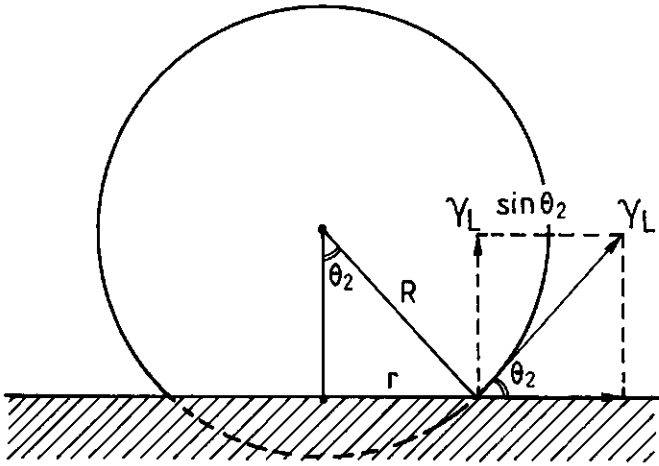


Figure 3. The air bubble-liquid-membrane system in the case of an air bubble with spherical contour

Since part of the sphere is only virtually present, the volume of the bubble ( $V$ ) is:

$$V = \pi R^3 \left( \frac{2}{3} + \cos \theta_2 - \frac{1}{3} \cos^3 \theta_2 \right) \quad (5)$$

Combining equations (3), (4) and (5) gives the surface tension ( $\gamma_d$ ) of the liquid at which the bubble will just detach:

$$\gamma_d = \frac{\Delta \rho g R^2 \left( \frac{2}{3} + \cos \theta_2 - \frac{1}{3} \cos^3 \theta_2 \right)}{2 \sin^2 \theta_2} \quad (6)$$

From equation (6)  $\theta_2$  can be calculated.

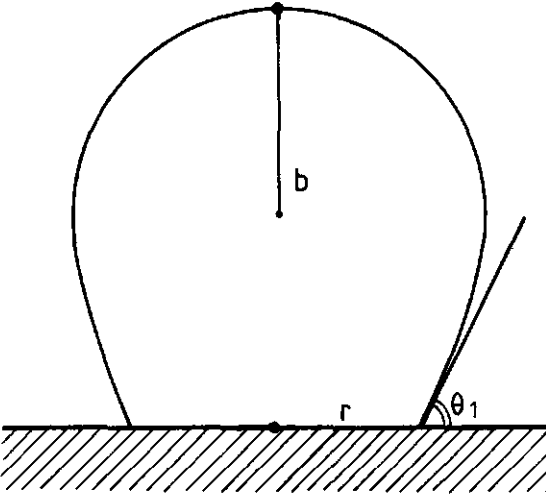


Figure 4. The air bubble-liquid-membrane system in the case of a deformed air bubble

Since air bubbles attached to a surface tend to deform (to an extent depending on their size), the approximation of a spherical bubble is not entirely correct. The curvature at the bottom of the bubble is less than for the spherical case, and the contact angle with the surface changes from  $\theta_2$  to  $\theta_1$  while  $r$  remains the same. For this case (fig. 4) one can write [16]:

$$V \Delta \rho g = 2 \pi r \gamma_d (\sin \theta_1 - (\frac{R}{b}) \sin \theta_2) \quad (7)$$

where  $b$  is the radius of curvature at the top of the bubble. In the case where  $R \approx b$ , equation (7) simplifies to:

$$V \Delta \rho g = 2 \pi r \gamma_d (\sin \theta_1 - \sin \theta_2) \quad (8)$$

It should be noted, that  $R \approx b$  does not imply that the bubble is spherical. The deformation at the top of the bubble can be small with respect to the deformation at the bottom. It was also shown in ref. [16], that this approximation gives a good accordance between experimental and theoretical results for  $\theta_2$  smaller than  $30^\circ$ . Combining equations (5) and (8) gives the following expression for the calculation of  $\theta_1$ :

$$\sin \theta_1 = \frac{\Delta \rho g R^2 (\frac{2}{3} + \cos \theta_2 - \frac{1}{3} \cos^3 \theta_2)}{2 \gamma_d \sin \theta_2} + \sin \theta_2 \quad (9)$$

## 4.5 RESULTS AND DISCUSSION

Exact determination of the surface tension at which there are just no bubbles that stick to the surface proved to be difficult. This might be caused by inhomogenities of the surface. Therefore,  $\gamma_d$  is (arbitrarily) chosen as the surface tension at which 50% of the bubbles brought into contact with the surface adheres. Graphically, this point can be determined as shown for the  $0.2\ \mu\text{m}$  polypropylene membrane in figure 5. Each point of this curve is determined by bringing 20 air bubbles into contact with the membrane surface. The standard deviation in the points around the 50% value is 4%, resulting in an accuracy of  $0.2\ \text{mN/m}$  in the 50% value.

As the air bubble size detaching from the needle end decreases with decreasing surface tension of the liquid, calculations have to be carried out with a different bubble radius  $R$  (and density  $\rho_L$ ) for each liquid mixture. In table 2 the results are summarized. The values of  $\theta_2$  and  $\theta_1$  are calculated from equations (6) and (9), respectively. Values for  $\gamma_c$  are obtained from ref. [17] and were measured on a flat non-porous sheet of the pure polymer.

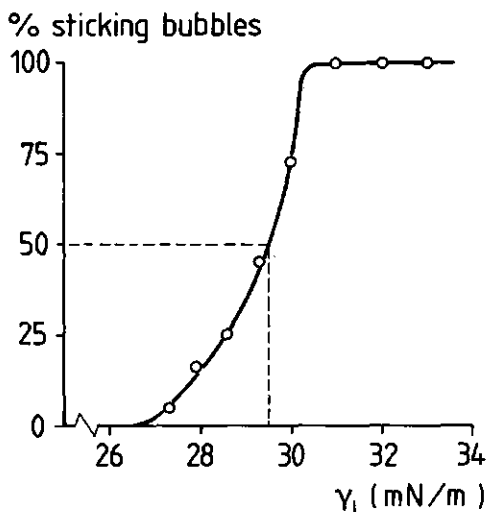


Figure 5. Percentage of air bubbles brought into contact with the surface of a  $0.2\ \mu\text{m}$  PP membrane that becomes attached, versus the surface tension of the liquid

Plotting a number of contact angle data given by Fowkes [18] for water–butanol droplets on graphite (figure 6) reveals that the difference in  $\gamma_L$  between  $\theta=25^\circ$  and  $\theta=0^\circ$  is of the order of  $1\text{--}2\ \text{mN/m}$ . Since  $\gamma_c$  is defined at  $\theta=0^\circ$  it is clear that values of  $\gamma_d$  should be  $1\text{--}2\ \text{mN/m}$  higher than  $\gamma_c$  values. Together with the systematic error introduced by taking the 50% adhesion value instead

of 0% (which is also of the order of 1–2 mN/m), it can be concluded that  $\gamma_d$  values obtained with this method are expected to be 2–4 mN/m higher than  $\gamma_c$  values found in literature.

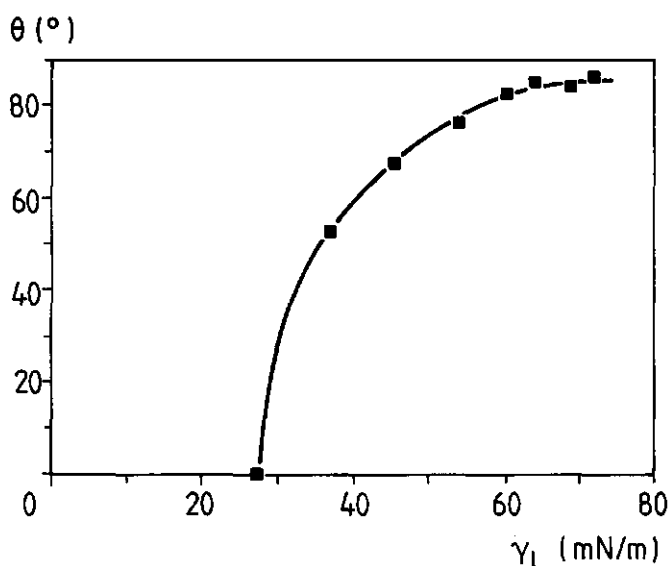


Figure 6. Contact angle of droplets of water-butanol mixtures on graphite. Data are from ref. [18]

Table 2. Results from hydrophobicity measurements for different hydrophobic membranes

| membrane          | $\rho_L$<br>kg/m <sup>3</sup> | R<br>10 <sup>-4</sup> m | $\gamma_d$<br>mN/m | $\gamma_c$<br>mN/m | $\theta_2$<br>° | $\theta_1$<br>° |
|-------------------|-------------------------------|-------------------------|--------------------|--------------------|-----------------|-----------------|
| PP                | 853                           | 4.7                     | 29.5               | 29–34              | 11.9            | 24.3            |
| PVDF 0.2 $\mu$ m  | 924                           | 5.2                     | 42.4               | 25                 | 11.2            | 22.9            |
| PVDF 0.14 $\mu$ m | 922                           | 5.1                     | 41.3               | 25                 | 11.3            | 23.0            |
| PVDF IRIS 3065    | 941                           | 5.3                     | 47.0               | 25                 | 11.1            | 22.6            |
| PTFE              | 805                           | 4.6                     | 24.2               | 16–22              | 12.3            | 25.2            |
| PSf GR 51 PP      | 990                           | 5.9                     | 65.0               | 41                 | 10.7            | 21.9            |
| PSf GR 61 PP      | 1000                          | –                       | >72                | 41                 | –               | –               |
| PSf GR 81 PP      | 973                           | 5.6                     | 56.3               | 41                 | 10.9            | 22.2            |
| PSf GR 60 PP      | 1000                          | –                       | >72                | 41                 | –               | –               |
| PSf S-30          | 992                           | 6.0                     | 66.8               | 41                 | 10.7            | 21.8            |
| PES               | 1000                          | –                       | >72                | *                  | –               | –               |
| PDMS              | 807                           | 4.6                     | 24.5               | 24.2               | 12.2            | 25.1            |

\* no value found in literature;  $\gamma_d$  on bulk material 56.3 mN/m

Table 2 shows that the results obtained for PP, PDMS and PTFE membranes show a fairly good agreement between  $\gamma_d$  and  $\gamma_c$  values. However, the other membrane materials show measured  $\gamma_d$  values more than 2–4 mN/m above the  $\gamma_c$  values reported in the literature. We now discuss possible reasons for these discrepancies.

#### PVDF membranes

XPS measurements performed on the PVDF IRIS 3065 ultrafiltration membrane clearly show the presence of oxygen and nitrogen in the top layer of the membrane (table 3). From these results it may be concluded that, at least, the IRIS 3065 PVDF membrane surface has some constituents that may make the membrane more hydrophilic than the pure polymer.

Table 3. *Atomic ratios found by XPS measurements on the PVDF IRIS 3065 ultrafiltration membrane*

| atom | theor. | depth of analysis |      |
|------|--------|-------------------|------|
|      |        | 5 nm              | 1 nm |
| C    | 50     | 57.6              | 60.6 |
| F    | 50     | 29.1              | 26.1 |
| O    | 0      | 7.7               | 7.9  |
| N    | 0      | 5.6               | 5.3  |

Microporous PVDF membranes (obtained from ENKA AG) have been investigated by Franken [1] using the penetrating drop method. He found a value for  $\gamma^p$  of about 38 mN/m, i.e. 13 mN/m above the  $\gamma_c$  value and in agreement with our results. The same method applied to polypropylene membranes gives  $\gamma^p \approx 29$  mN/m, in good agreement with the  $\gamma_c$  value (29–34 mN/m) and our results. It might therefore be concluded from these results that the high values found for PVDF membranes, as compared to bulk PVDF, are an inherent property of the membrane surface, rather than an artifact introduced by the method.

#### Polysulfone membranes

Measurements were carried out on pure bulk PSf and PES (grains and sheets). Values for  $\gamma_d$  of 48.8 and 56.3 mN/m, respectively, were obtained. The  $\gamma_c$  value reported for PSf is 41 mN/m. This value indicates that, on somewhat more hydrophilic materials, the deviation between  $\gamma_d$  and  $\gamma_c$  might be larger (although only one reference for  $\gamma_c$  data was found). The value found for the polysulfone membranes is more than 15 mN/m above the  $\gamma_c$  value found in the literature. For both PSf and PES we found  $\gamma_d$  on membranes more than 7 mN/m higher than the value obtained by

us on the pure polymer. Possible explanations for this phenomenon are i) constituents that are present in the membrane material but not in the pure polymer and ii) conformational changes induced by the production method.

i) From XPS measurements carried out on the DDS PSf membranes (table 4), it can be concluded that the GR 51, 61 and 81 membranes seem to be made of the same material (Udel polysulfone), which was shown before and confirmed by the manufacturer [19]. Oxygen and nitrogen are obviously more abundant than would be expected on the basis of atomic ratios in the pure polymer. It therefore seems plausible that the membrane surface is more hydrophilic, although it is impossible to quantify this effect. The nitrogen and oxygen may come from dimethylformamide (DMF) used as a solvent in the production [20].

Table 4. Atomic ratios as determined by XPS (1 nm) for the DDS GR 51, 61 and 81 PSf membrane; the theoretical ratio is given for Udel Polysulfone and Victrex Polyethersulfone

| atom | theor. |         | GR 51 | GR 61 | GR 81 |
|------|--------|---------|-------|-------|-------|
|      | Udel   | Victrex |       |       |       |
| C    | 84.5   | 75.0    | 82.5  | 81.6  | 82.6  |
| O    | 12.5   | 18.75   | 13.8  | 14.9  | 13.2  |
| S    | 3.0    | 6.25    | 3.0   | 2.3   | 2.2   |
| N    | 0      | 0       | 0.7   | 1.1   | 2.0   |

ii) Conditions during production used for polysulfone membranes (made by phase inversion techniques) may also influence the value of  $\gamma_d$ . We checked this as follows. Membranes of the pure Udel polysulfone or polyethersulfone were made by spreading a viscous solution of PSf in DMF on a polypropylene sheet. This sheet was submerged in water and rinsed with water. It was found, that, by varying polymer concentrations and the time of exposure to air before immersion, values for  $\gamma_d$  varied between 49 and 72 mN/m for PSf and between 56 and 72 mN/m for PES. This is probably due to surface-induced conformational changes of the polymer, which are "frozen in" at a particular stage of the phase inversion process. This kind of induced orientation of polymers has been reported by Ray et al. [21] and Lee [22]. It can therefore be concluded that, even though membranes are made of the same polymeric material, hydrophobicity may vary significantly with conditions during production.

The effect of surface roughness can be estimated using equation (6) and (9). The effect of a rough surface will be expressed in a longer contact line than the same bubble will have on a flat surface.

Therefore  $\theta_2$  and  $\theta_1$  have been calculated for a flat surface for which the contact line is doubled. The results for the two extremes (PTFE and PSf) are given in table 5.

Table 5. *Calculated effect of surface roughnesses on  $\theta_2$  and  $\theta_1$ ; the effect of roughness is introduced by multiplying the length of the contact line on the flat surface by an (arbitrary) factor of 2*

| membrane     | $\gamma_d$ | rough      |            | smooth     |            |
|--------------|------------|------------|------------|------------|------------|
|              |            | $\theta_2$ | $\theta_1$ | $\theta_2$ | $\theta_1$ |
| PTFE         | 24.2       | 8.6        | 17.5       | 12.3       | 25.2       |
| PSf GR 51 PP | 65.0       | 7.6        | 15.3       | 10.7       | 21.9       |

Obviously, on a rough surface, the values for the contact angles are smaller than those on a smooth surface. However, the lower the contact angle at the point of detachment, the closer the value of  $\gamma_d$  will approach the value of  $\gamma_c$ , as can be seen in figure 6. From this it may be concluded that values of  $\gamma_d$  obtained on a rough surface are even closer to the values of  $\gamma_c$  than values obtained on a smooth surface. Therefore,  $\gamma_d$  measured on membranes will differ less than 2–4 mN/m from  $\gamma_c$  values measured on smooth surfaces.

#### 4.6 CONCLUSIONS

In this study a method has been developed to measure hydrophobicity of porous materials, such as membranes, which is not influenced by the presence of the pores. Hydrophobicity is expressed in terms of  $\gamma_d$ , the surface tension at which an air bubble has a 50% chance of detaching from the surface. Values of  $\gamma_d$  may be compared with  $\gamma_c$  values found in literature, although the present method gives values that are expected to be 2–4 mN/m higher. By means of XPS it has been found that some membrane surfaces are representative of the pure polymer, whereas others have surface atomic compositions which differ from those of the pure polymer, perhaps due to trace contaminants. This may be the reason why some membranes are more hydrophilic than might be expected on the basis of the chemistry of the pure polymer. It was also found that, for PSf membranes, the conditions during production have a large effect on the hydrophobicity of the membrane surface.

#### ACKNOWLEDGEMENT

The authors wish to thank the Dutch Program Committee for Industrial Biotechnology (PCIB) for



their financial support.

## LIST OF SYMBOLS

|              |   |                      |
|--------------|---|----------------------|
| $\gamma_L$   | liquid surface tension                      | $[\text{N.m}^{-1}]$  |
| $\gamma_c$   | critical surface tension                    | $[\text{N.m}^{-1}]$  |
| $\gamma_d$   | surface tension at detachment               | $[\text{N.m}^{-1}]$  |
| $\gamma^p$   | surface tension at penetration              | $[\text{N.m}^{-1}]$  |
| $\theta$     | contact angle                               | $[\circ]$            |
| $\theta_2$   | contact angle of a spherical air bubble     | $[\circ]$            |
| $\theta_1$   | contact angle of a deformed air bubble      | $[\circ]$            |
| $\theta_A$   | advancing contact angle on a rough surface  | $[\circ]$            |
| $\theta_E$   | advancing contact angle on a smooth surface | $[\circ]$            |
| $\Delta\rho$ | density difference between liquid and gas   | $[\text{kg.m}^{-3}]$ |
| $\rho_L$     | liquid density                              | $[\text{kg.m}^{-3}]$ |
| $b$          | radius at the top of a deformed air bubble  | $[\text{m}]$         |
| $g$          | acceleration of gravity                     | $[\text{m.s}^{-2}]$  |
| $r$          | contact plane radius                        | $[\text{m}]$         |
| $R$          | air bubble radius                           | $[\text{m}]$         |
| $r_s$        | surface roughness factor                    | $[-]$                |
| $V$          | air bubble volume                           | $[\text{m}^3]$       |

## REFERENCES

- 1) Franken, A.C.M., J.A.M. Nolten, M.H.V. Mulder, D. Bargeman and C.A. Smolders, Wetting criteria for the applicability of membrane distillation, *J. Membrane Sci.* 33 (1987) 315-328
- 2) Schneider, K. and T.J. van Gassel, Membrane distillation, *Chem.-Ing.-Tech.* 56 (1984) 514-521
- 3) Vigo, F., C. Uliana and P. Lupino, The performance of a rotating module in oily emulsions ultrafiltration, *Sep. Sci. Technol.* 20 (1985) 213-230
- 4) Keurentjes, J.T.F., W.Pronk, G.I. Doornbusch and K. van 't Riet, Downstream processing of fatty acid/lipid mixtures using membranes, *Proc. Second Annual National Meeting of the North American Membrane Society*, Syracuse, New York, June 1-3, 1988
- 5) Baier, R.E., Modification of surfaces to reduce fouling and/or improve cleaning, *Proc. of the Workshop Fundamentals and Applications of Surface Phenomena associated with Fouling and Cleaning in Food Processing*, Tylösand, Halmstad, Sweden, April 6-9, 1981
- 6) Fontyn, M., B.H. Bijsterbosch and K. van 't Riet, Chemical characterization of ultrafiltration membranes by spectroscopic techniques, *J. Membrane Sci.* 36 (1988) 141-145
- 7) Furrmidge, C.G.L., Studies at phase interphases. I. The sliding of liquid drops on solid surfaces and a theory for spray retention, *J. Colloid Sci.* 17 (1962) 309-324

#### chapter 4

- 8) Fox, H.W. and W.A. Zisman, The spreading of liquids on low- energy surfaces. I. Polytetrafluoroethylene, *J. Colloid Sci.* 5 (1950) 514-531
- 9) Zisman, W.A., Relation of the equilibrium contact angle to liquid and solid constitution, *Adv. Chem. Ser.* 43 (1964) 1-51
- 10) Wenzel, R.N., Resistance of solid surfaces to wetting by water, *Ind. Eng. Chem.* 28 (1936) 988-994
- 11) Busscher, H.J., A.W.J. van Pelt, P. de Boer, H.P. de Jong and J. Arends, The effect of surface roughening of polymers on measured contact angles of liquids, *Colloids and Surfaces* 9 (1984) 319-331
- 12) Johnson, R.E. and R.H. Dettre, Contact angle hysteresis. I. Idealized rough surface, *Adv. Chem. Ser.* 43 (1964) 112-135
- 13) Oliver, J.F., C. Huh and S.G. Mason, An experimental study of some effects of solid surface roughness on wetting, *Colloids and Surfaces* 1 (1980) 79-104
- 14) Van Loosdrecht, M.C.M., J. Lyklema, W. Norde, G. Schraa and A.J.B. Zehnder, The role of bacterial cell wall hydrophobicity in adhesion, *Applied and Environmental Microbiol.* 53 (1987) 1893-1897
- 15) Gerson D.F. and J. Akit, Cell surface energy, contact angles and phase partition. II. Bacterial cells in biphasic aqueous mixtures, *Biochim. Biophys. Acta* 602 (1980) 281-284
- 16) Janczuk, B., Detachment force of air bubble from the solid surface (sulfur or graphite) in water, *J. Colloid Interface Sci.* 93 (1983) 411-418
- 17) Shafirin, E.G., in *Polymer Handbook*, 2<sup>nd</sup> ed., J. Brandrup and E.H. Immergut (eds.) Wiley and Sons, New York, 1975, p.III-221
- 18) Fowkes F.M. and W.D. Harkins, The state of monolayers adsorbed at the interface solid-aqueous solution, *J. Am. Chem. Soc.* 62 (1940) 3377-3386
- 19) Hanemaaijer, J.H., T. Robbertsen, T.H. van de Boomgaard and J.W. Gunnink, Fouling of ultrafiltration membranes. The role of protein adsorption and salt precipitation, *J. Membrane Sci.* 40 (1989) 199-217
- 20) Fontyn, M., K. van 't Riet and B.H. Bijsterbosch, to be published
- 21) Ray, B.R., J.R. Anderson and J.J. Scholz, Wetting of polymer surfaces. I. Contact angles of liquids on starch, amylose, amylopectin, cellulose and polyvinylalcohol, *J. Phys. Chem.* 62 (1958) 1220-1230
- 22) Lee, L.H., Adhesion of high polymers. II. Wettability of elastomers, *J. Polymer Sci. A-2* 5 (1967) 1103-1118

## SURFACTANT-INDUCED WETTING TRANSITIONS: ROLE OF SURFACE HYDROPHOBICITY AND EFFECT ON OIL PERMEABILITY OF ULTRAFILTRATION MEMBRANES

---

### SUMMARY

In this study the effect of surface hydrophobicity on adsorption of sodium oleate from a mixture of water and 2-propanol is investigated as well as consequences of this adsorption for wettability by oil or water/2-propanol, respectively. The surface hydrophobicity is varied by the use of compatible mixtures of a hydrophobic (polystyrene) and a more hydrophilic polymer (polyamide or poly(methylmethacrylate)). It appears that for the adsorption onto these surfaces three regions can be distinguished. In the case of a hydrophobic surface adsorption of the surfactant is due to van der Waals and/or hydrophobic interactions between the apolar tails of the surfactant and the surface. Upon an increase of the surface hydrophilicity a large region in which adsorption takes place is followed by a very narrow region of 0.5 mN/m in which no adsorption is found. A further increase in surface hydrophilicity results in an almost stepwise increase of the amount adsorbed, now due to polar interactions between the polar head groups of the surfactant and the surface, possibly followed by the adsorption of a second layer. The adsorption behavior in the three regions can be explained in a semi-quantitative way, considering interfacial free energies between different components present in the system.

This result can be used in order to design an oil-selective ultrafiltration membrane for the separation of a system of two immiscible liquids (i.e., o/w or w/o emulsions). It was found that only in the region where no surfactant is adsorbed the surface is preferentially wetted by oil and that only then is an UF membrane is entirely permeable to oil and not to the aqueous phase.

---

J.T.F. Keurentjes, M.A. Cohen Stuart\*, D. Brinkman, C.G.P.H. Schroën and K. van 't Riet

\*Wageningen Agricultural University, Dept. of Physical and Colloid Chemistry, Dreijenplein 6, 6703 HB Wageningen, The Netherlands

This chapter has been published in *Colloids and Surfaces* 51 (1990) 189-205

## 5.1 INTRODUCTION

The presence of amphiphilic molecules in a solution usually affects the hydrophobicity (or wettability) of a surface in contact with this solution [1-3]. In flotation and detergency this effect is used to improve the efficiency of the process. In flotation a surfactant that adsorbs preferentially onto one of the minerals to be separated is added which makes the surface of this mineral more hydrophobic. Air bubbles will preferentially adhere to the more hydrophobic mineral grains, and a separation can be achieved [4-6]. In detergency (washing) adsorption of surfactants with their hydrophobic part onto a fibrous substrate will increase the wettability for water. Subsequently water can penetrate into the pores, thus removing oily materials from the pores by a combined displacement and solubilisation mechanism [7].

Usually, the effect of surfactant concentration on the wetting of a solid substrate is studied [8,9], and little attention is paid to the surface energy of the solid as a parameter in adsorption and wettability of solids. Polymer surfaces may consist of materials with a broad range of surface energies varying from low energy solids like PTFE to rather high energy solids like cellulose, and both dispersive (apolar) and polar or electrostatic interactions may play a role in adsorption and wetting phenomena on those surfaces.

Adsorption and wetting phenomena will play an important role in membrane separation processes. The permeability of hydrophobic membranes for water can be improved by the presence of a surfactant [10] or an alcohol [11]. Two-phase systems can be separated using two membranes of opposite polarity (of which an example is given in figure 1). In these systems the polar phase (usually containing water) is allowed to permeate through the hydrophilic membrane, whereas the apolar part (usually containing an organic liquid) permeates through the hydrophobic membrane. In this way, either water-in-oil or oil-in-water emulsions can be separated [12,13].

To alter the membrane surface so as to obtain specified wettability characteristics several modification methods exist. Firstly, surfaces can be treated by radiation induced grafting [14]. However, heavily grafted membranes often exhibit poor mechanical properties compared to ungrafted membranes [15]. Surfaces can also be treated with plasmas, resulting in a coupling of functional groups to the polymer substrate. In addition, several deposition methods have been proposed. Dip-coating [16,17], deposition by plasma polymerization [18,19] and interfacial polymerization [20] are frequently used methods. A particularly practical deposition method was proposed by Franken [21], who simply modified (hydrophobic) membranes by passing a suitable (water soluble) polymer solution over them. After drying, the membrane has the wettability

characteristics of the deposited polymer.

In this study the effect of the surface hydrophobicity on the adsorption of a surfactant (sodium oleate) from solution is investigated. Also, the effect of hydrophobicity on wettability by a two-phase system, namely, an emulsion consisting of soy bean oil and an aqueous solution of sodium oleate and 2-propanol is investigated. In order to vary the hydrophobicity we used a modification of Franken's method: mixtures of two polymers are deposited on the membranes by passing suitable solutions through them [22]. Finally, we studied the oil selectivity of the modified membranes in the two-phase system described below.

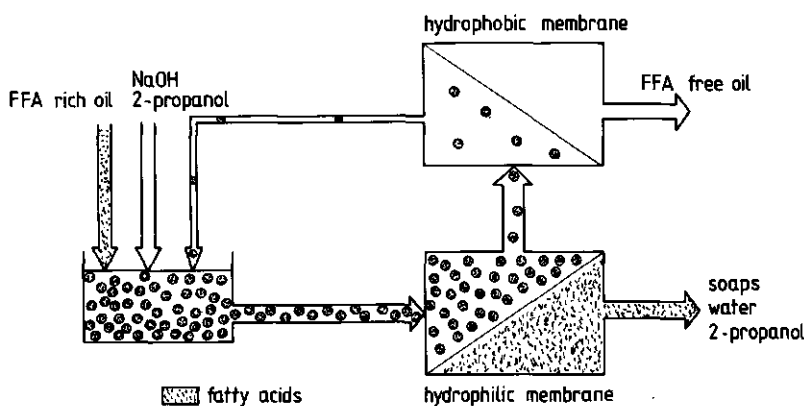


Figure 1. Two-membrane system for the removal of fatty acids from oil [13]

## 5.2 MATERIALS

For hydrophobicity measurements, as well as wetting experiments, films consisting of mixtures of two compatible polymers have been prepared. The polymers used are summarized in table 1. Soy bean oil (triesters of glycerol and fatty acids (of which more than 95% are C16 and C18)) of edible quality was supplied by Rhenus Inc. (The Netherlands). All other chemicals are purchased from Merck (F.R.G.) and were reagent grade. The water used was doubly distilled, and the temperature used throughout the study is 20°C. The balance used for surface tension measurements was a Mettler AE 50-S analytical balance.

Wetting behavior and separation characteristics of the different membranes used in this study were tested with an emulsion containing soy bean oil as the oil phase, and water containing 2-

propanol and sodium oleate (the sodium salt of cis-9-octadecenoic acid) as the water phase. The water/2-propanol/sodium oleate ratio in the water phase was 6.5:3:1 (v/v/v). The ratio between the oil and the water phase in the dispersion was 4:3 (v/v). In a previous paper [13] it was shown, that in this dispersion the oil phase as well as the water phase are present as a continuous phase at water phase contents between 20% and 65%. The transition into a discrete water-in-oil dispersion occurs at 20% water phase. The interfacial tension between the two phases was measured by the spinning drop technique and was found to be 0.27 mN/m. This is a relatively low value but it did not result in the formation of a microemulsion [13].

Table 1. *Polymers used to produce surfaces with a range in hydrophobicity*

| Polymer                        | MW      | Manufacturer             |
|--------------------------------|---------|--------------------------|
| Polyamide (PA)                 | 42,000  | Aldrich Chem. Corp. Inc. |
| Polystyrene (PS)               | 150,000 | Aldrich Chem. Corp. Inc. |
| Poly(methylmethacrylate)(PMMA) | unknown | Aldrich Chem. Corp. Inc. |

Several commercially available membranes have been tested for their capability to separate the emulsion. Of those membranes, the 0.1  $\mu\text{m}$  polypropylene has also been used as support material for applied coatings. The membranes used in this study are summarized in table 2.

Table 2. *Membranes used; all membranes are commercially available*

| Material           | Code      | Pore size/cut off | Manufacturer  |
|--------------------|-----------|-------------------|---------------|
| Polypropylene (PP) | Accurel   | 0.2 $\mu\text{m}$ | ENKA          |
| Polypropylene (PP) | Accurel   | 0.1 $\mu\text{m}$ | ENKA          |
| PVDF               |           | 0.2 $\mu\text{m}$ | Millipore     |
| PVDF               | IRIS 3065 | 10,000 D          | Rhone Poulenc |
| PTFE               |           | 0.2 $\mu\text{m}$ | Gore          |
| Polysulfone (PSf)  |           | 30,000 D          | Amicon        |

### 5.3 METHODS

#### Hydrophobicity

A useful measure of the wettability of a surface is the critical surface tension  $\gamma_c$ , i.e. the surface tension of a liquid that is just capable of giving complete wetting [23]. A good approximation of  $\gamma_c$  is the surface tension  $\gamma_a$  at which air bubble detachment takes place [24]. Since surfaces of low

$\gamma_d$  are hydrophobic, whereas a high value of  $\gamma_d$  indicates a hydrophilic surface, we can use  $\gamma_d$  as a quantitative measure of hydrophobicity.

Measurements of  $\gamma_d$  were carried out using the sticking bubble technique [24]. A piece of membrane material or polymer film (about  $1 \text{ cm}^2$ ) is placed horizontally at the bottom of a beaker containing a liquid with surface tension  $\gamma_L$ . Water/methanol mixtures used gave a range in  $\gamma_L$  of 23 to 72 mN/m. Using a 10  $\mu\text{l}$  syringe with a flat ended needle (horizontal), air bubbles were brought into contact with the membrane surface. The surface tension at which the transition from adhesion to detachment takes place ( $\gamma_d$ ) has been shown to be a measure for the surface hydrophobicity comparable to the Zisman critical surface tension ( $\gamma_c$ ) [23].

#### Adsorption measurements

Adsorption of surfactant on a ground polymer material was measured from pure water as well as from water/isopropanol mixtures. Films of the different polymer mixtures were prepared by evaporation of the solvent from a 40 g/l solution in chloroform. The polymer films were then frozen in liquid nitrogen and ground in a Retsch mill with a slit size of 0.5 mm. The specific surface area of each sample was determined by methylene blue adsorption. Adsorption of sodium oleate onto the surface was measured by the usual depletion method starting from a  $3.15 \cdot 10^{-2}$  mol/l solution in water or water/2-propanol solution (6.5:3 v/v). Oleate concentrations were determined by adding 9 ml of 2.5 M HCl to a 1 ml sample, extracting the oleic acid thus formed into hexane, and the concentrations were determined on a Carlo Erba gas chromatograph with a 5 m CP-Sil 5 CB (Chrompack, The Netherlands) capillary column with a cold on-column injection system using caproic acid as an internal standard.

#### Contact angle measurements

Advancing contact angles of both the oil and water phase on different polymer surfaces were determined. For this purpose the emulsion was separated into its two bulk phases by centrifugation. Glass Wilhelmy plates were dip-coated in 40 g/l polymer solutions in chloroform and air-dried. The surface tension of both the water and the oil phase is determined using these plates (figure 2a). Next, the plates were pretreated in one phase, resulting in a thin liquid film on the polymer surface. Thereafter, the force acting on the Wilhelmy plate was measured when the plate was brought into contact with the surface of the other phase. This is shown schematically in figure 2b. By measuring the forces  $F_1$  and  $F_2$  for a particular phase (1) on a Wilhelmy plate pretreated with the same phase (1) and with the other phase (2), respectively, one finds the

advancing contact angle  $\theta_2$  for phase 2 from  $\cos\theta_2 = F_2/F_1$ . The surface tension  $\gamma_1$  of phase 1 was obtained as usual from  $F_1 = L\gamma_1$ , where  $L$  is the length of the contact line. By measuring both the contact angle of the oil phase on water prewetted plates ( $\theta_o$ ) and of the water phase on oil prewetted plates ( $\theta_w$ ) and taking the difference between the two, one has a measure for the capability of one phase to remove the other phase from the surface.

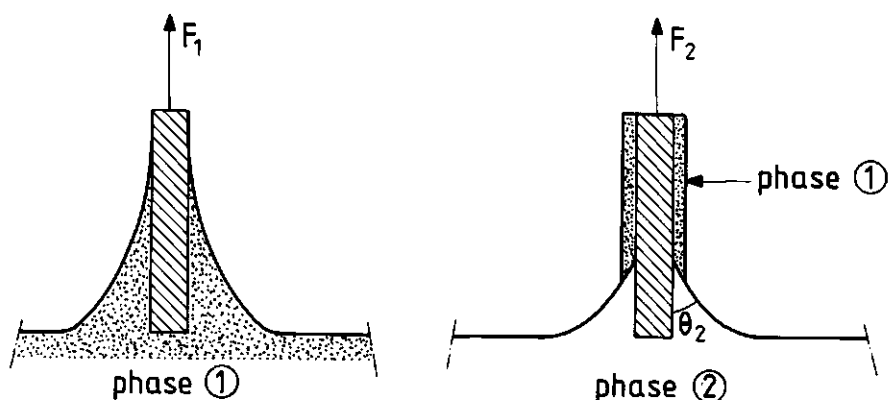


Figure 2. Measurement of the surface tension of a liquid and the three phase advancing contact angle

### Coating experiments

Membranes were coated using a flat sheet membrane test module (Megaflow TM 100, New Brunswick Scientific Co. Inc., USA). A polymer solution (40 g/l) in chloroform was applied as a feed solution at 100 ml/min, at a starting static pressure of  $0.3 \cdot 10^5$  N/m<sup>2</sup>. Under these conditions only a part of the polymer solution permeated and the pores and the surface were gradually filled with polymer, which resulted in an increase of the pressure as a result of an increase in the membrane resistance. At a pressure of  $1.0 \cdot 10^5$  N/m<sup>2</sup> circulation of the chloroform solution was stopped and the flow circuit was rinsed with oil to remove the chloroform [22].

### Membrane selectivity



To investigate the selectivity of commercially available membranes and coated membranes, the emulsion described above was led over the membrane applying a trans-membrane pressure of  $10^5$  N/m<sup>2</sup>. The permeate was analysed for the presence of glycerides and oleate by TLC using silicagel 60 F254 TLC sheets purchased from Merck (F.R.G.).

## 5.4 RESULTS

### Adsorption of sodium oleate

Mixtures of polystyrene (PS) with polyamide (PA) or with poly(methylmethacrylate) (PMMA), were used to create surfaces varying in hydrophobicity. The results are presented as  $\gamma_d$  (determined by bubble detachment) versus mixture composition in figure 3 and 4 for PS/PA and PS/PMMA mixtures, respectively. These curves show that  $\gamma_d$  does not depend linearly on the polymer composition of the mixture.

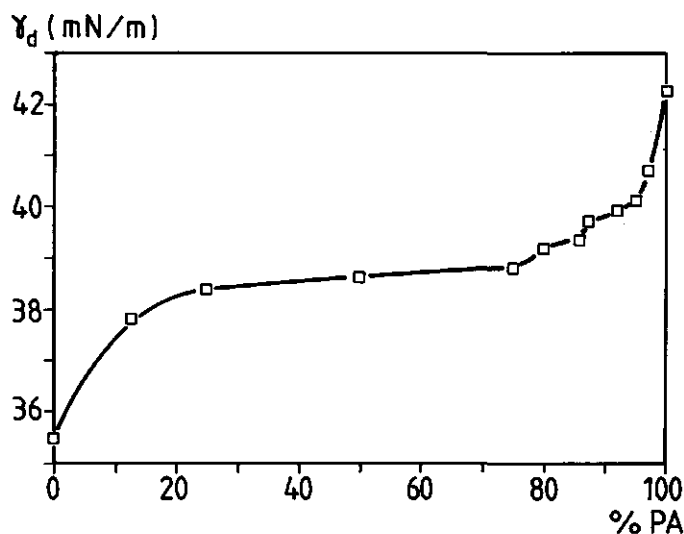


Figure 3.  $\gamma_d$  of PS/PA mixtures versus composition

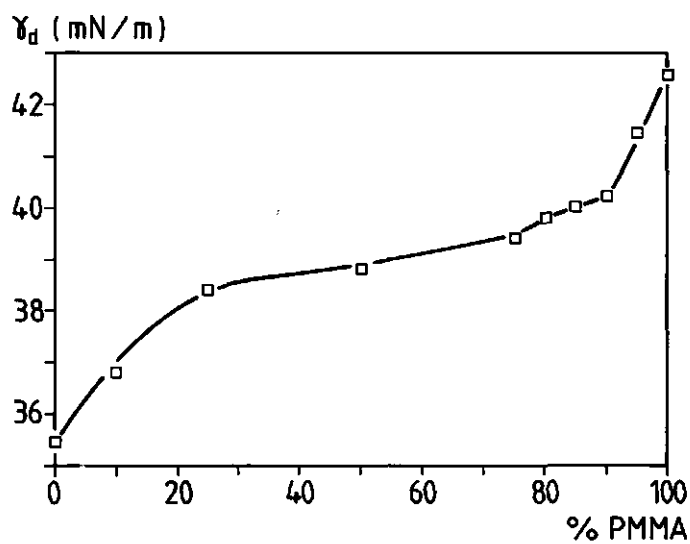


Figure 4.  $\gamma_d$  of PS/PMMA mixtures versus composition

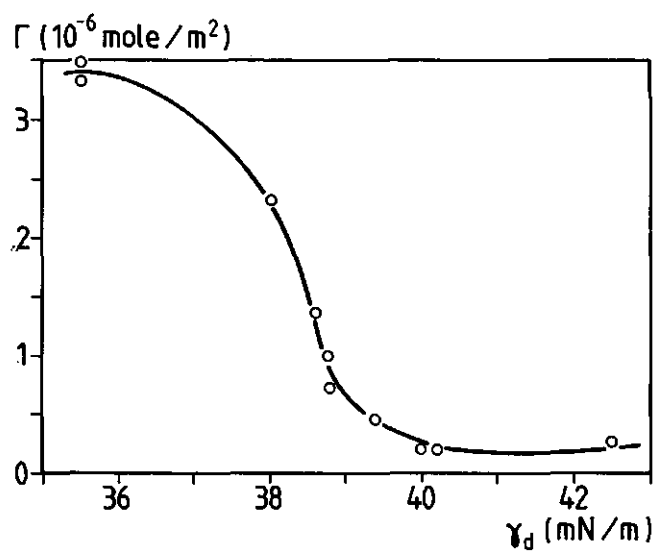


Figure 5. Adsorption of sodium oleate onto PS/PMMA particles from water

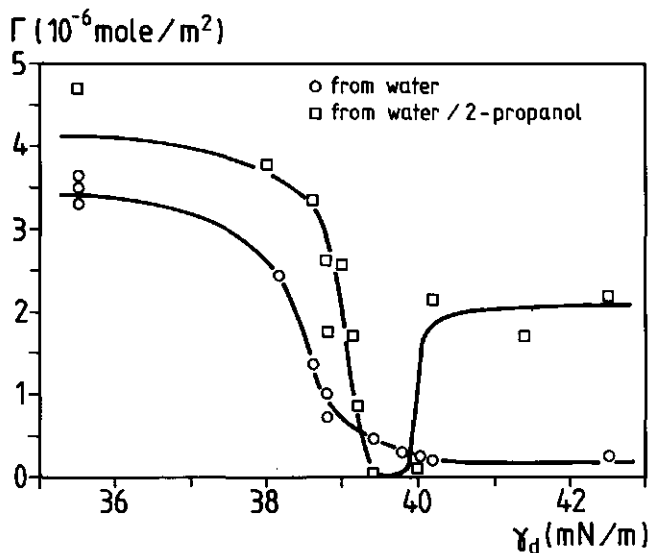


Figure 6. Adsorption of sodium oleate onto PS/PMMA particles from water/2-propanol (6.5:3 v/v) and water

In figures 5 and 6 the adsorbed amounts of sodium oleate onto PS/PMMA surfaces as a function of hydrophobicity ( $\gamma_d$ ) are shown, from water and from water/isopropanol solutions, respectively. The adsorption from water (fig. 5) decreases with increasing  $\gamma_d$  to almost zero above a  $\gamma_d$  value of 39.5 mN/m. This result is in agreement with that obtained by Piirma and Chen [25] for the adsorption of sodium dodecyl sulfate (SDS) on PS/PMMA copolymer latex particles. In the case of adsorption from water/isopropanol mixtures (figure 6) it can be seen, that the adsorbed amounts at  $\gamma_d$  values below 39 mN/m are comparable to those from water. In the region  $38.5 < \gamma_d < 39.5$  mN/m the adsorbed amount drops sharply to zero. However, in contrast to the adsorption from water, a further increase of the surface hydrophilicity results in an almost stepwise increase of the amount adsorbed. Hence, three regions can be distinguished: both at low and at high  $\gamma_d$  we find adsorption, but in between there is a very narrow region where no significant adsorption is detected.

#### Wetting of the surface

Wettability by each of the liquid phases (oil and water phase, respectively) as a function of  $\gamma_d$  was studied by measuring the advancing contact angle. The surface tension of the water phase and the

oil phase against air is determined using dip-coated Wilhelmy plates and appears to be  $28.5 \pm 0.1$  and  $32.5 \pm 0.3$  mN/m, respectively. In figure 7a and 7b the difference in advancing contact angle ( $\Delta\theta = \theta_o - \theta_w$ ) is plotted against  $\gamma_d$  for PS/PMMA and PS/PA surfaces, respectively.

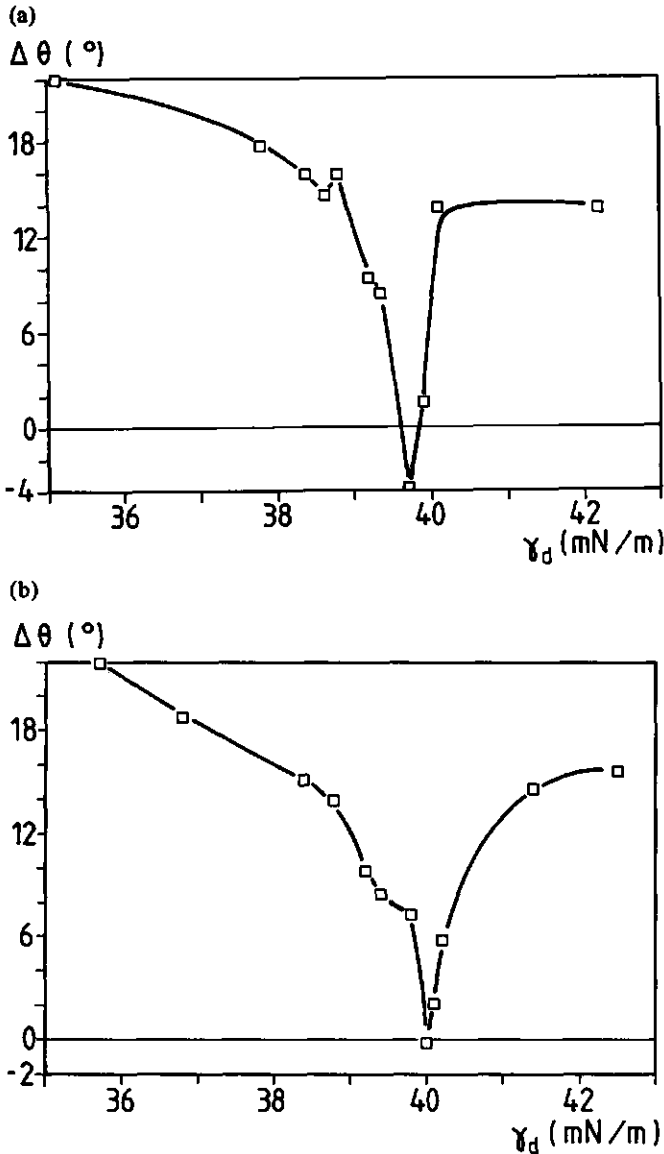


Figure 7. The difference in advancing three phase contact angles of the water and the oil phase versus surface hydrophobicity: (a) on PS/PA and (b) on PS/PMMA

It turns out, that only in a very small region of  $\gamma_d$  did the oil phase exhibit a smaller contact angle than the water phase. This region is almost the same for both polymer mixtures. (The slight discrepancy between the two curves is presumably due to the fact that PS/PA mixtures result in somewhat rougher coatings than PS/PMMA mixtures. From contact angle calculations it was shown [24], that a rougher surface will result in a  $\gamma_d$  value that is slightly lower than that obtained on a smooth surface with the same hydrophobicity.) These results imply, that only in this small region of  $\gamma_d$  is the surface better wetted by oil than by water/2-propanol. A simple analysis shows that the difference in interfacial tension ( $\Delta\gamma$ ) between the water-wet and the oil-wet polymer surface can be related to the contact angles  $\theta_o$  and  $\theta_w$  and the surface tensions  $\gamma_o$  and  $\gamma_w$ :

$$\gamma_o \cos \theta_o - \gamma_w \cos \theta_w = \Delta\gamma + (\gamma_w - \gamma_o) \quad (1)$$

Since  $\gamma_o \approx \gamma_w$  it follows that  $\cos \theta_o - \cos \theta_w \approx \Delta\gamma / \gamma_o$  (provided  $\gamma_w - \gamma_o$  is negligible as compared to  $\Delta\gamma$ ). When  $\theta_o - \theta_w$  changes sign, this must imply that  $\Delta\gamma$  (which is nearly equal to the spreading coefficient since  $\gamma_{o/w}$  is very small) changes sign also and the oil/water contact angle will change abruptly when this happens.

Comparing figures 6 and 7, it can be seen that the region in which no adsorption of sodium oleate takes place coincides with the region of preferential wettability for the oil phase. We conclude that the change in wettability is caused by the fact that no adsorption takes place, and that adsorption of the surfactant improves the wettability for the water phase.

Table 3.  $\gamma_d$  of several hydrophobic membranes; the range given for polysulfone follows from ref. [24]

| Membrane                           | $\gamma_d$ (mN/m) |
|------------------------------------|-------------------|
| Polypropylene (0.2 $\mu\text{m}$ ) | 29.5              |
| Polypropylene (0.1 $\mu\text{m}$ ) | 29.5              |
| PVDF (0.2 $\mu\text{m}$ )          | 42.4              |
| PVDF (10,000D)                     | 47.0              |
| PTFE (0.2 $\mu\text{m}$ )          | 24.2              |
| Polysulfone (30,000D)              | 49-72             |

### Membrane selectivity

Hydrophobicity measurements were carried out on different commercially available membrane materials. For the polysulfone membrane (which is a hollow fibre device) it is not possible to measure the hydrophobicity without damaging the module severely. Therefore, a range is given

for the hydrophobicity of polysulfone as it appears from earlier measurements [24]. The results are given in table 3.

It appears that none of the membranes listed in table 3 is selective for one of the two phases. However, from the experiments described above, it may be expected that membranes possessing a hydrophobicity (expressed in  $\gamma_d$ ) in the narrow range between 39.5 and 40.0 mN/m should be capable to separate the oil phase from the surfactant and isopropanol containing dispersion, since on these materials no adsorption of the surfactant occurs, resulting in a good wettability for the oil phase. In order to test this hypothesis a microporous polypropylene support was coated with different PS/PA and PS/PMMA mixtures, making membranes with hydrophobicities corresponding with the hydrophobicity of the applied coating. Subsequent permeation experiments clearly showed that indeed only those coatings on which no surfactant adsorption takes place (i.e.  $39.5 < \gamma_d < 40.0$  mN/m) are capable of separating the oil phase from the dispersion. Polymer compositions very close to, but not in this composition range are not capable of accomplishing the separation. The measured fluxes for one phase (oil) permeation are between 5 and 50 l/(m<sup>2</sup>.h.bar). These are common fluxes for ultrafiltration of solutions with comparable viscosities. No significant change in flux or selectivity was observed when experiments were run for several days.

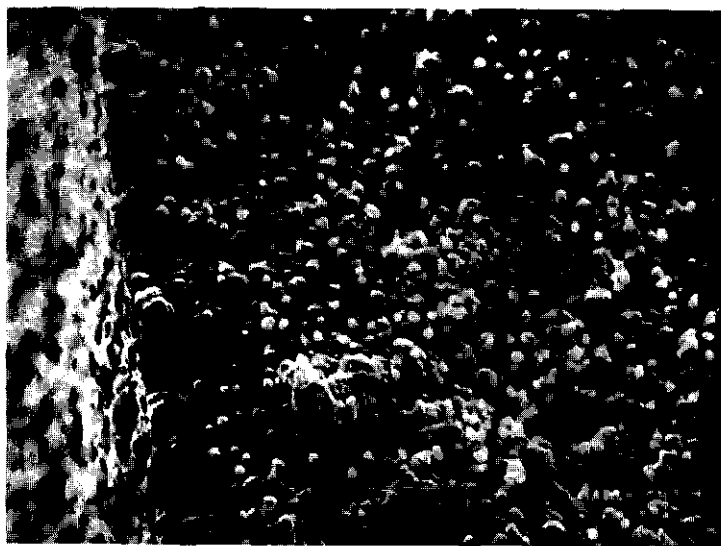


Figure 8a. SEM micrograph of the polypropylene support

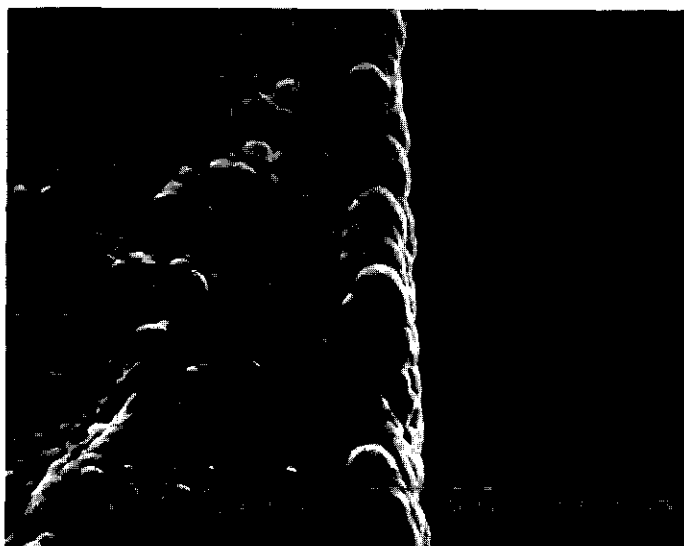


Figure 8b. *SEM micrograph of the coated side of the microporous support*

In order to investigate the structure of the coated layer on top of the polypropylene support material, SEM micrographs were taken. From figure 8 it can be seen, that the nodular structure of the polypropylene (figure 8a) was still present at the coated side of the membrane (figure 8b). A layer of the applied coating onto each of the polypropylene nodules was observed, revealing that the polymer was not present as a separate film on top of the microporous support, but as a coating on the nodules of the polypropylene support. Polymer was, therefore, present in the pores, down to about  $20\text{ }\mu\text{m}$  from the top surface. For this reason the adhesion between the microporous support and the coated layer was good: it is not possible to peel off the coated layer. An additional factor is the strong interaction between the hydrophobic polymer in the blend (PS) and the polypropylene support. It has been shown by Franken [21], that strong interactions are a prerequisite for a good adhesion.

## 5.5 DISCUSSION

As shown in figure 6, three regions can be distinguished for the adsorption of sodium oleate from the water/2-propanol mixture onto surfaces with different hydrophobicities. Firstly, in the hydrophobic region the surfactant is expected to adsorb with the apolar tails towards the surface.

Upon increasing the hydrophilicity of the surface, there is an almost stepwise transition into a region in which no adsorption takes place, followed by another almost stepwise increase in the amount adsorbed. In the latter region the surfactant will presumably adsorb with its polar head group towards the surface, probably followed by the adsorption of a second layer (surfactant or alcohol) on top of this first layer. From the fact that this third region is absent in pure water, it is tempting to conclude that coadsorption of 2-propanol plays also a role here.

The double adsorption transition observed gives rise to two questions. Firstly, one might wonder why the two transitions are so sharp. Secondly, it is important to know what determines their positions and why they are so close. With respect to the first question, it can be said in general that the adsorption of surfactants is a cooperative process because of the tendency of these molecules to associate. Both theoretical [26,27] and experimental [28,29] studies have provided ample evidence of this in the form of sudden jumps in the adsorption isotherm. A change in adsorption energy (at fixed surfactant concentration) may also give rise to sharp adsorption/desorption transitions. Theoretical models predict this [30] and some evidence comes from neutron scattering studies on nonionic surfactants adsorbed onto  $\text{SiO}_2$  where the adsorption energy was varied via pH [31]. Since adsorption/desorption transitions are so sharp it is justified, for a crude description, to consider only either entirely covered or entirely bare surfaces. It is then relatively easy to estimate surface free energies for each of these two cases and finding the transition(s) by balancing them.

In order to simplify the matter, the alcohol/water mixture is considered as one component, the solvent (o). On very hydrophobic surfaces the interfacial energy between surfactant molecules adsorbed onto the surface (s) with their tails (t) will be very low, and increasing the surface hydrophilicity, the interfacial free energy will increase also. For adsorption with the head groups (h) the pattern will be reversed compared to adsorption with the tails: the more hydrophilic the surface, the smaller the interfacial free energy will be.

For adsorption with the tails onto the surface, the following requirement has to be fulfilled:

$$\gamma_{ts} < \gamma_{so} + \gamma_{to} \quad (2)$$



in which  $\gamma_{ij}$  is the interfacial tension between components  $i$  and  $j$ ;  $t$ ,  $s$  and  $o$  refer to components as listed above. The term  $\gamma_{to}$  is a constant since it does not depend on the nature of  $s$ , but the other two vary with surface hydrophobicity. It is not necessary to incorporate a term for the head groups of the surfactant, since they remain in the solvent after adsorption. For adsorption of the head groups of the surfactant molecules an equivalent equation can be written:

$$\gamma_{hs} < \gamma_{so} + \gamma_{ho} \quad (3)$$

where  $\gamma_{ho}$  is, again, a constant, and the other two vary with  $\gamma_d$ . Each of the conditions (2) and (3) may give rise to a transition; in between, one might even find a region where  $\gamma_d$  of the solid is such that none of them are met, so that the free energy will not decrease by exchanging solvent by heads or tails of the surfactant on the surface, and a negligible adsorption results.

In order to obtain estimates of  $\gamma_{ij}$  we proceed as follows. Surface tensions can be divided into a dispersive and a polar contribution. Following Fowkes [32,33], we write:

$$\gamma = \gamma^d + \gamma^p \quad (4)$$

where  $\gamma$  is the surface tension of the liquid, and  $\gamma^d$  and  $\gamma^p$  are the dispersive and polar components of the surface tension of the liquid, respectively. Interfacial tensions between two phases ( $\gamma_{12}$ ) can be determined from the geometric mean of the polar and the dispersive intermolecular interactions [34,35]:

$$\gamma_{12} = \gamma_1 + \gamma_2 - 2(\gamma_1^d \gamma_2^d)^{\frac{1}{2}} - 2(\gamma_1^p \gamma_2^p)^{\frac{1}{2}} \quad (5)$$

in which the subscripts 1 and 2 denote the two different liquid phases. For an estimate of interfacial tensions, surface tensions of each of the different species have to be divided into a dispersive and a polar part. For our system, tentative estimates are given in table 4.

Table 4. *Estimates of surface tension components of the different components in the system*

|                | $\gamma$ | $\gamma^d$ | $\gamma^p$ | ref  |
|----------------|----------|------------|------------|------|
| solvent (o)    | 29       | 21         | 8          | [35] |
| tails (t)      | 25       | 21         | 4          |      |
| heads (h)      | 40       | 20         | 20         |      |
| surface (s) PS | 38       | 33         | 5          | [34] |
| PMMA           | 41       | 30         | 11         | [34] |

Surface tension components for water/alcohol mixtures have been reported by Janczuk et al. [35].

Although 2-propanol has not been investigated, it can be seen from the data for ethanol and n-propanol that the dispersive component for these two substances is almost the same: namely 20 and 21 mN/m for a 30% solution of ethanol and n-propanol in water, respectively. Therefore, a dispersive component of 21 mN/m for 30% 2-propanol in water is a reasonable estimate. The tails of the surfactant will be rather apolar. However, they contain a double bond, which gives rise to a small polar part in the surface tension. The estimate for the head group is more difficult, and although head groups usually are considered as hydrophilic, a significant part will still be due to dispersive intermolecular interactions. For the polymer surfaces we used the values reported by Wu [34], although the  $\gamma$  values used by this author differ slightly from  $\gamma_d$  as determined by us.

Using equations 4 and 5 and the values of table 4, we find interfacial tensions between the different components as plotted in figure 9. We can locate the intersection points and determine regions of 'tail down' and 'head down' adsorption as defined by equations 2 and 3. It is gratifying to note that the region in which adsorption with the tails towards the surface occurs does not overlap with that in which adsorption with the head groups towards the surface occurs. As a consequence, a region of surface hydrophobicity occurs in which no adsorption takes place. Moreover, our analysis predicts transitions nearly there where they are found experimentally. We should note, however, that the calculation of the interfacial tensions is rather sensitive for differences in the chosen values for  $\gamma$ ,  $\gamma^d$  and  $\gamma^p$ . Most values in table 4 are reasonably reliable, but the value for the head groups is perhaps less certain.

With help of figure 9 it is now possible to estimate the effect of changes in one or more of the components. The effect of a change in the solvent can be predicted: reducing the amount of alcohol will result in an increase of the polar part of the surface tension of the solvent, while the dispersive part will remain the same. In this region of  $\gamma_d$  this causes an increase in  $\gamma_{os}$  and  $\gamma_{to}$  and a decrease in  $\gamma_{ho}$ . This will narrow down the range in which no adsorption takes place. Eventually, the non-adsorption region may even completely disappear. The ultimate case, in which the solvent merely consists of water, clearly does not obey this rule, as is shown in figure 5. This can perhaps be explained by the uptake of surfactant molecules in micelles which occurs in pure water, but not in the water/2-propanol mixture. According to our simple model, cooperative adsorption from water onto a not too hydrophobic surface is possible due to polar interactions. If the molecules already associate in the bulk solution as micelles, the tendency to adsorb will be much reduced.

For a surfactant with a saturated hydrocarbon tail, the polar part of its surface tension will almost vanish, which results in an increase in  $\gamma_{to}$ . Similarly, in this region of  $\gamma_d$ ,  $\gamma_{ts}$  will increase, and it will be the ratio of the two terms that determines whether the range in which no adsorption takes

place will be broadened or reduced. The fact that a change in one component affects two or three curves at the same time makes it difficult to give precise predictions of the effects, and it will therefore be necessary that values for  $\gamma$ ,  $\gamma^d$  and  $\gamma^p$  are known exactly to give real quantitative predictions.

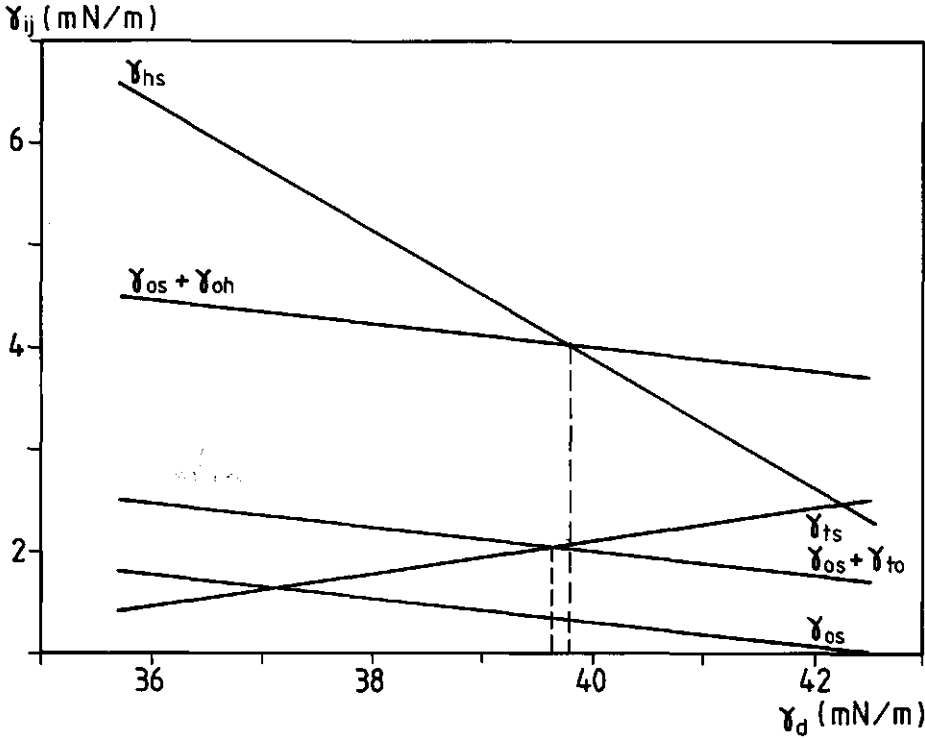


Figure 9. *Calculated interfacial tensions between the different constituents of the system versus the surface hydrophobicity*

## 5.6 CONCLUSIONS

In this study the effect of surface hydrophobicity on adsorption of sodium oleate from a water/2-propanol solution is investigated. It appears that adsorption of the surfactant takes place in three regions. On a more hydrophobic surface the surfactant will adsorb with the hydrophobic tails onto the surface; increasing the surface hydrophilicity leads to a narrow region in which virtually no

adsorption occurs, followed by a region in which adsorption occurs again, presumably by interactions between the head groups of the surfactant and the surface. From wetting studies it follows that in the regions where adsorption takes place the surface appears to be rather hydrophilic. Surfactant adsorbed onto the hydrophobic solid will expose its polar headgroups to the solution, whereas in the case of the more polar solid a second surfactant or alcohol layer will adsorb on top of the first layer, also rendering the surface more hydrophilic. These adsorption phenomena can be explained in a semi-quantitative way by taking the cooperative nature of surfactant adsorption into account and making estimates of free energies for various conceivable interfaces in the system.

It appeared that surfaces in the region where no adsorption of sodium oleate occurs are preferentially wetted by the oil phase of a two-phase system consisting of soy bean oil as the oil phase and a sodium oleate solution in water/2-propanol as the water phase. These results have been used to develop a membrane material with the required wetting properties for the separation of such a mixture. Since the range in hydrophobicity in which no adsorption occurs is only 0.5 mN/m wide, it is not surprising that no commercially available membrane is capable of separating the oil phase from this two-phase system. However, it should be realized that a change in the composition of the mixture to be separated can induce significant changes in the adsorption and wetting behavior. In order to obtain guidelines, it is necessary to have estimates of the different contributions to the surface tension of each of the components of the mixture to be separated and to use these to predict adsorption/desorption transitions of the system.

#### ACKNOWLEDGEMENTS

The authors wish to thank the Dutch Program Committee for Industrial Biotechnology (PCIB) for their financial support, and F.P. Cuperus of the Twente University for his help with the SEM micrographs.

#### LIST OF SYMBOLS

|       |  |     |
|-------|--|-----|
| $F_1$ | : force acting on Wilhelmy plate wetted by phase 1 | [N] |
| $F_2$ | : force acting on Wilhelmy plate wetted by phase 2 | [N] |
| $h$   | : head groups of surfactant                        |     |
| $o$   | : solvent  |     |
| $s$   | : surface  |     |
| $t$   | : tails of surfactant                              |     |

## chapter 5

|                |   |        |
|----------------|---|--------|
| $\gamma$       | : surface tension   | [mN/m] |
| $\gamma_c$     | : Zisman critical surface tension   | [mN/m] |
| $\gamma_d$     | : surface tension at air bubble detachment  | [mN/m] |
| $\gamma_L$     | : liquid surface tension  | [mN/m] |
| $\gamma_{12}$  | : interfacial tension   | [mN/m] |
| $\gamma_{ij}$  | : interfacial tension between two components  | [mN/m] |
| $\gamma_{o/w}$ | : oil/water interfacial tension   | [mN/m] |
| $\gamma^d$     | : dispersive component of surface tension   | [mN/m] |
| $\gamma^p$     | : polar component of surface tension  | [mN/m] |
| $\Delta\gamma$ | : difference in interfacial free energy between oil-wetted and water phase-wetted surface | [mN/m] |
| $\theta_1$     | : phase 1 advancing contact angle   | [°]    |
| $\theta_2$     | : phase 2 advancing contact angle   | [°]    |
| $\theta_o$     | : oil phase contact angle   | [°]    |
| $\theta_w$     | : water phase contact angle   | [°]    |
| $\Delta\theta$ | : difference in contact angle between oil and water phase ( $=\theta_o-\theta_w$ )        | [°]    |

## REFERENCES

- 1) Janczuk, B., The effect of n-alcohols on the wettability of hydrophobic solids, *Powder Technol.* 45 (1985) 1-6
- 2) Pyter, R.A., G. Zografi and P. Mukerjee, Wetting of solids by surface-active agents: the effects of unequal adsorption to vapor-liquid and solid-liquid interfaces, *J. Colloid Interface Sci.* 89 (1982) 144-153
- 3) Menezes, J.L., J. Yan and M.M. Sharma, The mechanism of alteration of macroscopic contact angles by the adsorption of surfactants, *Colloids Surfaces* 38 (1989) 365-390
- 4) Somasundaran, P. and L.T. Lee, Polymer-surfactant interactions in flotation of quartz, *Sep. Sci. Technol.* 16 (1981) 1475-1490
- 5) Rao, K.H., B. Antti and E. Forssberg, Mechanism of oleate interaction on salt type minerals. Part I. Adsorption and electrokinetic studies of calcite in the presence of sodium oleate and sodium metasilicate, *Colloids Surfaces* 34 (1988/1989) 227-239
- 6) Lemlich, R. (ed.), *Adsorptive bubble separation techniques*, Academic Press Inc., New York, 1972
- 7) Schwuger, M.J., Effects of adsorption on detergency in: *Anionic Surfactants- physical chemistry of surfactant action*, E.H. Lucassen-Reynders (ed.), *Surfactant Science Series* vol. 11, Marcel Dekker, Inc., New York, 1981
- 8) Paxton, T.R., Adsorption of emulsifier on polystyrene and poly(methylmethacrylate) latex particles, *J. Colloid Interface Sci.* 31 (1969) 19-30
- 9) Sütterlin, N., H.J. Kurth and G. Markert, Ein Beitrag zur Teilchenbildung bei der Emulsionspolymerisation von Acrylsäure- und Methacrylsäureestern, *Makromol. Chem.* 177 (1976) 1549-1565
- 10) Sarada, T., Surfactant treated polyolefinic microporous materials capable of multiple rewetting with aqueous solutions, *Eur. Pat. Appl. EP 129,420*, 1983
- 11) Nakanishi, H., Hydrophilized membrane of porous hydrophobic material, *Eur. Pat. Appl. EP 100,552*, 1982

- 12) Vigo, F., C. Uliana and P. Lupino, The performance of a rotating module in oily emulsions ultrafiltration, *Sep. Sci. Technol.* 20 (1985) 213-230
- 13) Keurentjes, J.T.F., G.I. Doornbusch and K. van 't Riet, The removal of fatty acids from edible oil; removal of the dispersed phase of a water in oil dispersion by a hydrophilic membrane, to be published in *Sep. Sci. Technol.* (1990)
- 14) Chaudhury, J.P., P. Gosh and B.K. Guha, Styrene-grafted cellulose acetate reverse osmosis membrane for ethanol separation, *J. Membrane Sci.* 35 (1988) 301-310
- 15) Tealdo, G.C., P. Canepa and S. Munari, Water-ethanol permeation through grafted PTFE membranes, *J. Membrane Sci.* 9 (1981) 191-196
- 16) Carnell, P.H. and H.G. Cassidy, The preparation of membranes, *J. Polym. Sci.* 55 (1961) 233-249
- 17) Carnell, P.H., Preparation of thin polymer films, *J. Appl. Polym. Sci.* 9 (1965) 1863-1872
- 18) Strobel, M., S. Corn, C.S. Lyons and G.A. Korba, Surface modification of polypropylene with  $\text{CF}_4$ ,  $\text{CF}_3\text{H}$ ,  $\text{CF}_3\text{Cl}$  and  $\text{CF}_3\text{Br}$  plasmas, *J. Polymer Sci., Polymer Chem.* 23 (1985) 1125-1135
- 19) Yagi, T., A.E. Pavlath and A.G. Pittman, Grafting fluorocarbons to polyethylene in glow discharge, *J. Appl. Polymer Sci.* 27 (1982) 4019-4028
- 20) Cadotte, J.E., R.S. King, R.J. Majerle and R.J. Petersen, Interfacial synthesis in the preparation of reverse osmosis membranes, *J. Macromol. Sci. - Chemistry* A15 (1981) 727-755
- 21) Franken, A.C.M., Membrane Distillation, a new approach using composite membranes, PhD thesis University Twente, 1988
- 22) Keurentjes, J.T.F. and K. van 't Riet, Membraan, werkwijze voor het vervaardigen van een membraan, alsmede werkwijze voor het scheiden van mengsels, Dutch Pat. Appl. 90,00082, 1990
- 23) Zisman, W.A., Relation of the equilibrium contact angle to liquid and solid constitution, *Adv. Chem. Ser.* 43 (1964) 1-51
- 24) Keurentjes, J.T.F., J.G. Harbrecht, D. Brinkman, J.H. Hanemaaijer, M.A. Cohen Stuart and K. van 't Riet, Hydrophobicity measurements of MF and UF membranes, *J. Membrane Sci.* 47 (1989) 333-344
- 25) Piirma, I. and S.R. Chen, Adsorption of ionic surfactants on latex particles, *J. Colloid Interface Sci.* 74 (1980) 90-102
- 26) Partyka, S., S. Zaini, M. Lindheimer and B. Brun, The adsorption of non-ionic surfactants on a silica gel, *Colloids Surfaces* 12 (1984) 255-270
- 27) von Rybinski, W. and M.J. Schwuger, in: *Nonionic Surfactants*, M. Schick (ed.), Surfactant Science Series vol. 23, Marcel Dekker Inc., New York, 1987
- 28) Koopal, L.K. and M.R. Böhmer, in: *Fundamentals of Adsorption*, Vol. III, A. Mersmann (ed.), Engineering Foundation, Am. Inst. Chem. Eng., New York, 1990
- 29) Böhmer, M.R. and L.K. Koopal, *Langmuir*, accepted for publication (1990)
- 30) Leermakers, F.A.M. and A. Nelson, Substrate-induced structural changes in electrode adsorbed lipid layers. A self-consistent field theory, *J. Electroanal. Chem.* 278 (1990) 53-72
- 31) Lee, E.M., R.K. Thomas, P.G. Cunnins, E.J. Staples, J. Penfold and A.R. Rennie, Determination of the structure of a surfactant layer adsorbed at the silica/water interface by neutron reflection, *Chem. Phys. Lett.* 162 (1989) 196-202
- 32) Fowkes, F.M., Attractive forces at interfaces, *Ind. Eng. Chem.* 56 (1964) 40-52
- 33) Fowkes, F.M., Determination of interfacial tensions, contact angles, and dispersion forces in surfaces assuming additivity of intermolecular interactions in surfaces, *J. Phys. Chem.* 66 (1962) 382
- 34) Wu, S., Surface and interfacial tensions of polymer melts. II. Poly(methacrylate), poly(n-butylmethacrylate) and polystyrene, *J. Phys. Chem.* 74 (1970) 632-638
- 35) Janczuk, B., T. Białopiotrowicz and W. Wojcik, The surface tension components of aqueous alcohol solutions,

*chapter 5*

Colloids Surfaces 36 (1989) 391-403

## EXTRACTION AND FRACTIONATION OF FATTY ACIDS FROM OIL USING AN ULTRAFILTRATION MEMBRANE

---

### SUMMARY

The removal of fatty acids from oil is an important step in edible oil refining. The classical caustic refining process results in losses of triglycerides, which should preferably be avoided. In this study a membrane based liquid-liquid extraction is used in which these losses can be avoided by the use of a selective extractant. A suitable extractant appears to be 1,2-butanediol. The distribution coefficient for fatty acids varies with alkyl chain length from 0.7 for erucic acid (C22:1) up to 5.5 for caproic acid (C6). The fatty acids can be removed from the 1,2-butanediol solution by the addition of water. The system demixes, and the dispersion can then be separated into pure fatty acids and a fatty acid free 1,2-butanediol/water mixture, to be reused as extractant after dewatering.

Extractions have been performed in cellulose hollow fiber membrane modules. It appears that a major part of the mass transfer resistance is situated inside the membrane wall. The overall mass transfer coefficient varies from  $7 \cdot 10^{-9}$  m/s for erucic acid up to  $5 \cdot 10^{-7}$  m/s for caproic acid. Using these overall mass transfer coefficients, the required membrane surface area for a countercurrent extraction can be calculated. An interesting feature is the fact that the mass transfer coefficients vary with fatty acid chain length, which can be used for the fractionation of a fatty acid mixture. Two mechanisms act in the same direction to obtain selectivity: an increasing mass transfer coefficient and an increasing distribution coefficient with a decrease in fatty acid chain length.

---

J.T.F. Keurentjes, J.T.M. Sluijs, R.J.H. Franssen and K. van 't Riet

This chapter is submitted for publication



## 6.1 INTRODUCTION

Liquid-liquid extraction is usually carried out by dispersing the extraction phase in the feed phase or vice versa. In extraction towers, a large surface area to volume ratio can be obtained. After extraction, the dispersion is allowed to coalesce and the two phases are separated. Coalescence, however, often causes severe problems in case of a very fine dispersion, which occurs at intensive mixing to obtain a large surface area per volume. Less intensive mixing results in a dispersion that can be separated more easily, but also results in a smaller surface area per volume, and hence in a decreased extraction rate. Besides, backmixing or flooding often limits the performance of extraction towers [1,2].

Hollow fiber extractors offer the possibility to perform extractions without the formation of a dispersion [3]. Also, when the fibers are sufficiently small in diameter, a large extraction area per volume can be obtained. Typical values are in the order of  $10^3$ – $10^5$  m<sup>2</sup>/m<sup>3</sup> [4] which is higher than the values found in packed towers [1]. Flooding and backmixing do not occur in hollow fiber extractors.

In most applications of hollow fiber extractors microporous membranes are used [2,3,5–8]. A static pressure is applied on the phase that does not wet the membrane. However, in the case of a low interfacial tension between the two liquid phases, a rather unstable system is obtained because the Laplace pressure in the pores is low. For cylindrical pores this pressure is given by:

$$\Delta P = \frac{2\gamma \cos \theta}{R} \quad (1)$$

where  $\Delta P$  is the pressure difference over the liquid-liquid interface,  $\gamma$  the interfacial tension between the two liquids,  $\theta$  the contact angle with the polymer surface and  $R$  the pore radius. Usually, there is complete wetting of the membrane by one of the phases,  $\cos \theta = 1$ . However, if this is not the case ( $\cos \theta < 1$ ), the pressure which the system can withstand is even lower.

For the separation of free fatty acids from oil, usually sodium hydroxide is added to the oil in order to saponify the fatty acids. Consequently, the soaps are separated from the oil by high speed separators [10,11]. The most important problem occurring in this type of processes is the inclusion of triglycerides into the soapstock. Usually, the amount of triglycerides included equals the amount of fatty acids [12], and these triglycerides have to be considered as a loss. As an alternative, extractions have been proposed. However, the extractants used (mostly alcohols) show a low selectivity [13–16], which also causes losses of triglycerides.

In this study a series of extractants is tested. Factors affecting the extraction of fatty acids from an oil using different homogeneous ultrafiltration membranes are investigated with a suitable extractant.

## 6.2 THEORY

### Overall mass transfer coefficient

Mass balance equations for the oil and the extraction phase can be combined and linearized, resulting in:

$$-\ln \left( \frac{C_{e,eq} - C_e}{C_{e,eq}} \right) = K_o \cdot A \cdot \left( \frac{V_e + \frac{V_o}{m}}{V_e \cdot V_o} \right) \cdot t \quad (2)$$

Here,  $V_o$  and  $V_e$  are the volumes and  $C_o$  and  $C_e$  the concentrations of fatty acid in the oil and extraction phase respectively. The distribution coefficient  $m$  of the fatty acid over oil and the extraction phase is defined by  $m = C_{e,eq}/C_{o,eq}$  where the subscript eq indicates equilibrium.  $A$  is the contact area between the two phases and  $K_o$  the overall mass transfer coefficient. When  $-\ln((C_{e,eq} - C_e)/C_{e,eq})$  is plotted versus  $t$ , a straight line is obtained and  $K_o$  can be calculated from the slope.

### Partial mass transfer coefficients

For a hydrophilic membrane with the extraction phase inside the membrane, the overall mass transfer can be written as [5]:

$$K_o^{-1} = k_o^{-1} + (m \cdot k_m)^{-1} + (m \cdot k_e)^{-1} \quad (3)$$

In this equation the overall mass transfer resistance (the reciprocal of the overall mass transfer coefficient  $K_o$ ) is the sum of the mass transfer resistance in the oil phase inside the fibers ( $k_o^{-1}$ ), the mass transfer resistance in the extraction phase outside the fibers ( $(m \cdot k_e)^{-1}$ ) and the resistance of the extraction phase in the membrane wall ( $(m \cdot k_m)^{-1}$ ).

Since the Reynolds number inside the fibers will be less than 1, mass transfer inside the fibers is described by [17]:

$$\frac{k_o \cdot d_f}{D_o} = 1.64 \left( \frac{d_f^2 \cdot v_o}{l_f \cdot D_o} \right)^{\frac{1}{3}} \quad (4)$$

in which is  $d_f$  the internal fiber diameter,  $l_f$  the fiber length,  $D_o$  the diffusion coefficient of the solute and  $v_o$  the average oil flow velocity.

The resistance in the membrane wall ( $k_m^{-1}$ ) is proportional to the membrane thickness  $d_m$  divided by the diffusivity  $D_e$  of the solute in the liquid filling the pores. With a correction for the effective diffusion distance by the tortuosity  $\tau$  and a correction for the polymer volume by the porosity  $\epsilon$  the resistance in the membrane is given by [18]:

$$k_m^{-1} = \frac{d_m \cdot \tau}{D_e \cdot \epsilon} \quad (5)$$

The mass transfer outside the fibers can be calculated using equations for mass transfer outside fibers or tubes as given in literature. All those equations are of the form

$$\frac{k_e \cdot d}{D_e} = a \left( \frac{d^2 \cdot v_e}{l_f \cdot \nu} \right)^b \cdot \left( \frac{\nu}{D_e} \right)^{\frac{1}{3}} \quad (6)$$

where  $v_e$  is the extractant flow velocity,  $d$  the outer fiber diameter and  $\nu$  the viscosity of the extraction liquid. The constants  $a$  and  $b$  differ with the system investigated [17–20], resulting in  $k_e$  values that may vary by a factor of 100. For this reason the best way for the determination of the  $k_e$  values is to measure  $K_o$ , to determine  $k_o$  and  $k_m$  and calculate  $k_e$  therefrom, using equations (3), (4) and (5).

### Extraction

For a continuous extraction, the amount of fatty acids that can be transferred from the oil phase into the extraction phase is determined by both the distribution coefficient  $m$  and the ratio of the oil phase and extraction phase flow ( $F_o$  and  $F_e$ , respectively), as combined in the stripping factor  $A$ :

$$A = \frac{m \cdot F_e}{F_o} \quad (7)$$

When we consider the extraction to take place by a countercurrent process (which can be relatively easily achieved in a hollow fiber membrane device) the number of theoretical transfer units (NTU) equals the height of the extractor (H) divided by the height of a transfer unit (HTU) [21]. This can be written as:

$$\frac{A}{A-1} \cdot \ln \left[ \left( 1 - \frac{1}{A} \right) \cdot \frac{x_i}{x_o} + \frac{1}{A} \right] = \frac{K_o \cdot A \cdot \rho}{F_o} \quad (\text{NTU} = H/\text{HTU}) \quad (8)$$

with  $x_i/x_o$  as the ratio between the inflow and the outflow concentration in the oil phase and  $\rho$  the density of the oil phase. Once the overall mass transfer coefficient is known it is possible to calculate the required surface area (A) for a given  $A$  and  $x_i/x_o$ .

### 6.3 MATERIALS

Fatty acids with different chain lengths were used. Some relevant characteristics are summarized in table 1. All fatty acids used were reagent grade, except oleic acid, which was technical grade.

Table 1. *Fatty acids used in this study; the fatty acid chain length is calculated using a binding length of 0.154 nm for a C-C bond and a binding angle of 109°*

| fatty acid            | manufacturer | estimated chain length (nm) |
|-----------------------|--------------|-----------------------------|
| caproic acid (C6:0)   | Aldrich      | 0.8                         |
| capric acid (C10:0)   | Unichema     | 1.3                         |
| myristic acid (C14:0) | Aldrich      | 1.8                         |
| oleic acid (C18:1)    | Merck        | 2.5                         |
| erucic acid (C22:1)   | Aldrich      | 3.1                         |

Extractions were carried out in hollow fiber membrane devices containing different membrane materials, provided by ENKA Membrana AG, FRG. The membranes used are given in table 2.

All experiments were carried out at 30 °C. The water used was demineralized and all other reagents were analytical grade and purchased from Merck (FRG). The oil phase was soy bean oil of edible quality (Rhenus Inc. The Netherlands).

## 6.4 EXPERIMENTAL

Distribution coefficients were determined as follows. After intensive mixing of 100 ml fatty acid containing soy bean oil with 100 ml extractant, the fatty acid concentration was determined in both phases and mass balances were set up in order to check the recovery. Fatty acid concentrations were determined by titration of a 1 gram sample in 20 ml ethanol with a 0.5 N sodium hydroxide solution. Water concentrations were measured using an automatic Karl Fisher titration apparatus (Mettler).

Table 2. *Membranes used in extraction experiments*

| membrane          | cut off<br>(D) | surface area<br>m <sup>2</sup> | wall thickness<br>(10 <sup>-6</sup> m) | trade name |
|-------------------|----------------|--------------------------------|--|------------|
| cellulose         | 6,000          | 0.90                           | 6.5                                    | Cuprophane |
| cellulose         | 6,000          | 0.77                           | 8                                      | Cuprophane |
| cellulose         | 6,000          | 0.70                           | 11                                     | Cuprophane |
| mod. cellulose    | 70,000         | 0.177                          | 16                                     | Hemophane  |
| cellulose acetate | 60,000         | 0.144                          | 25                                     | Diaphane   |
| cellulose acetate | 750,000        | 0.062                          | 85                                     | PF 100     |

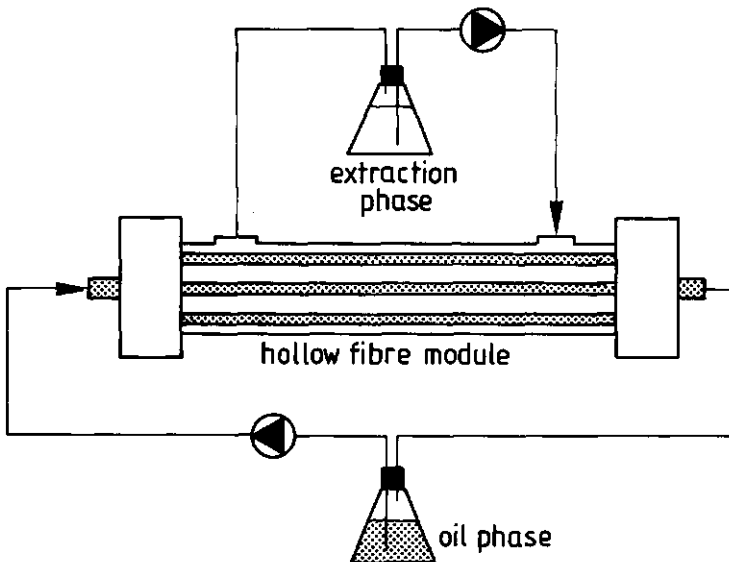


Figure 1. *Experimental set-up for membrane extraction experiments*

Membrane extractions were carried out using hollow fiber membrane modules. The experimental set-up is depicted in figure 1. The oil phase is circulated inside and the extraction phase outside the fibers and the polar extraction phase wets the fiber wall. In order to avoid emulsion formation by extractant permeating into the oil phase, the oil phase was circulated at a static pressure of  $0.5 \cdot 10^5 \text{ Nm}^{-2}$ . Before use the membranes are rinsed with demineralized water.

Fatty acid concentrations in fractionation experiments were determined on a Carlo Erba gas chromatograph with a 5 m CP-Sil 5 CB capillary column (Chrompack, The Netherlands) with a cold on-column injection system using hexadecane as an internal standard.

## 6.5 RESULTS AND DISCUSSION

### Distribution coefficients

For several extractants the distribution coefficient for oleic acid over the extractant and soy bean oil is determined at an oleic acid concentration of 20% (v/v). The results are given in table 3. From table 3 it appears, that several extractants found in the literature, like methanol and mixtures of methanol with water and acetonitrile or furfural, are partially or completely miscible with oil. For an effective extraction, however, it is necessary that the mutual solubility is very low. This requirement, together with the highest distribution coefficient, can be met using 1,2-butanediol.

Table 3. *Distribution coefficients of oleic acid over soy bean oil and different extractants. Miscibility of the extractant with oil is indicated by --: not miscible, +-: partially miscible and ++: completely miscible*

| extractant                                  | m    | miscibility with oil |
|---|------|----------------------|
| formamide                                   | 0.04 | --                   |
| glycerol                                    | 0.16 | --                   |
| 1,3-butanediol                              | 0.29 | --                   |
| 2,3-butanediol                              | -    | ++                   |
| 1,4-butanediol                              | 0.12 | --                   |
| 1,2-butanediol                              | 1.08 | --                   |
| 2-butene-1,4-diol                           | 0.08 | --                   |
| methanol                                    | 1.10 | +-                   |
| methanol/acetonitrile/water 75/20/5 (v/v/v) | 0.45 | +-                   |
| methanol/furfural/water 75/20/5 (v/v/v)     | -    | ++                   |

The distribution coefficient appears to be almost independent of the fatty acid concentration and temperature, but decreases with an increase in water content (figure 2). The chain length of the fatty acid strongly influences the distribution coefficient (figure 3), varying from 0.7 for erucic acid up to 5.5 for caproic acid. It could be expected that short chain fatty acids are more soluble in butanediol than the long chain fatty acids, due to the smaller ratio between hydrophobic tail and hydrophilic head group.

The solubility of soy bean oil in 1,2-butanediol appeared to be below the threshold of detection using refractive indices (i.e.  $<0.1\%$  w/w). The solubility of 1,2-butanediol in soy bean oil was measured to be  $1\%$  (w/w) in the case butanediol is used without water. Since cellulose membranes are not allowed to be used with dry solvents, it is necessary to add some water to the butanediol. When 1,2-butanediol contains  $2\%$  (w/w) water, the solubility of 1,2-butanediol in soy bean oil decreases to a value below the threshold of detection using refractive indices ( $<0.1\%$  w/w).

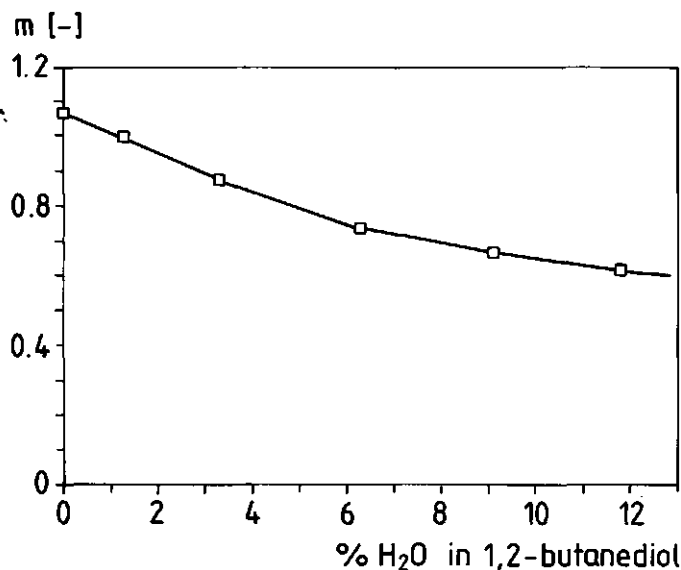


Figure 2. Effect of the water content of 1,2-butanediol on the distribution coefficient of oleic acid over soy bean oil and 1,2-butanediol

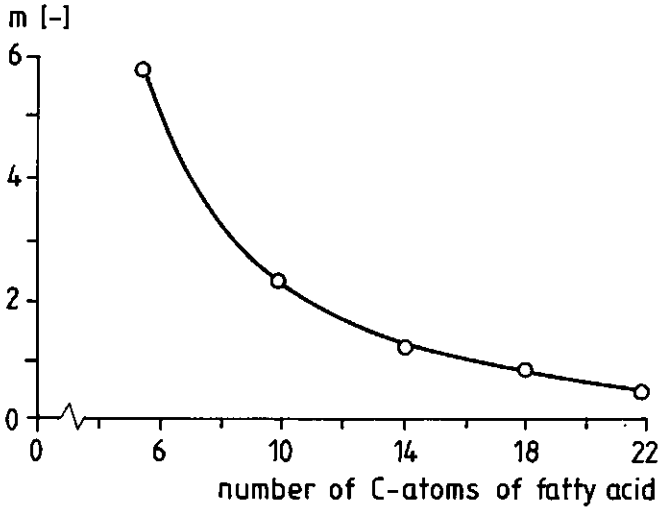


Figure 3. *Effect of the fatty acid alkyl chain length on the distribution coefficient of fatty acids over 1,2 butanediol (containing 2% water) and soy bean oil*

When 1,2-butanediol is used as extractant, extracted oleic acid can be removed from the 1,2-butanediol phase by the addition of water up to 35% (w/w). This water addition results in demixing of the system, yielding a dispersion with fatty acids as the dispersed phase and 1,2-butanediol/water as the continuous phase. The amount of water required for demixing increases up to 55% for capric acid, and is almost independent of the fatty acid content. Below the water content required for demixing, fatty acids are completely miscible with the 1,2-butanediol mixture. After phase separation a fatty acid phase and a 1,2-butanediol/water phase are obtained. The fatty acid phase then contains 2% 1,2-butanediol, whereas the 1,2-butanediol/water mixture contains less than 0.05% of fatty acids. Values that are virtually independent of the nature of the fatty acid, indicating that a higher mutual solubility in the case of shorter fatty acids is compensated by an increased water content required for demixing. After dewatering this stream can be reused as extraction liquid.

#### Mass transfer coefficients

Because of the low interfacial tension between fatty acid containing oil and 1,2-butanediol (which



vanishes to zero at a fatty acid content of 35% (v/v) in the oil phase), and probably also because of incomplete wetting by the water phase, it appeared impossible to use the PF100 cellulose acetate membrane for these extractions. Even at a low static pressure ( $0.05 \cdot 10^5 \text{ N/m}^2$ ) the oil phase permeates through the membrane. Applying the same static pressure on the water circuit results in permeation of the water phase. The other membranes listed in table 2 could be used for the extraction experiments.

For the determination of the overall mass transfer resistance, experiments have been carried out with different fatty acids in soy bean oil and the Cuprophane cellulose membranes. Measuring the concentration of fatty acid in the extraction circuit with time yields figure 4a as a typical result. Linearizing this curve according to equation (2) then yields figure 4b, from which the overall mass transfer coefficient can be calculated. The overall mass transfer coefficient increases with a decrease in fatty acid chain length (figure 5).

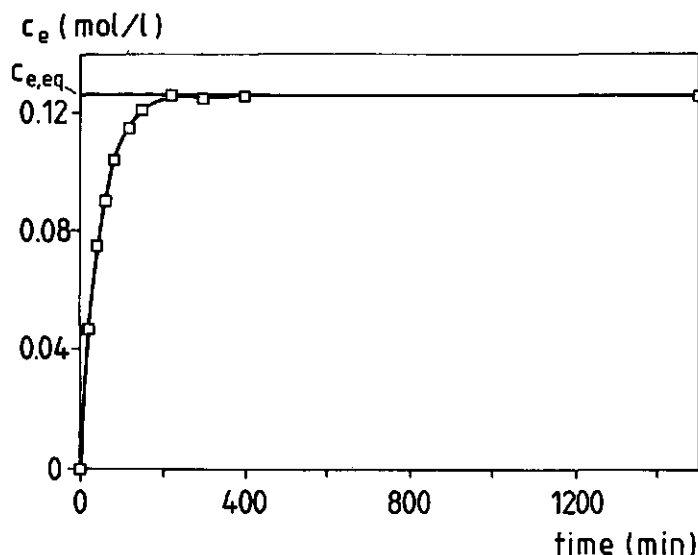


Figure 4a. *Fatty acid concentration versus time in a typical extraction experiment of oleic acid from oil*

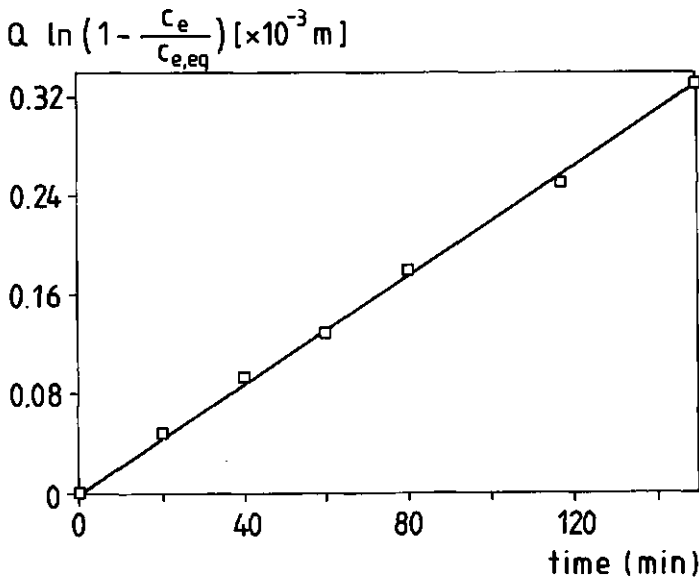


Figure 4b. *Linearized concentration versus time for the determination of  $K_0$ .  $Q$  represents the volume correction term of equation (2)*

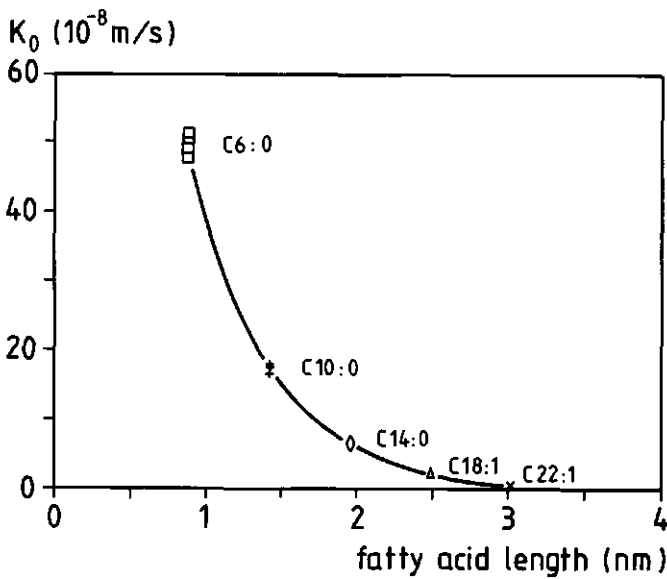


Figure 5. *Overall mass transfer coefficient versus fatty acid chain length*

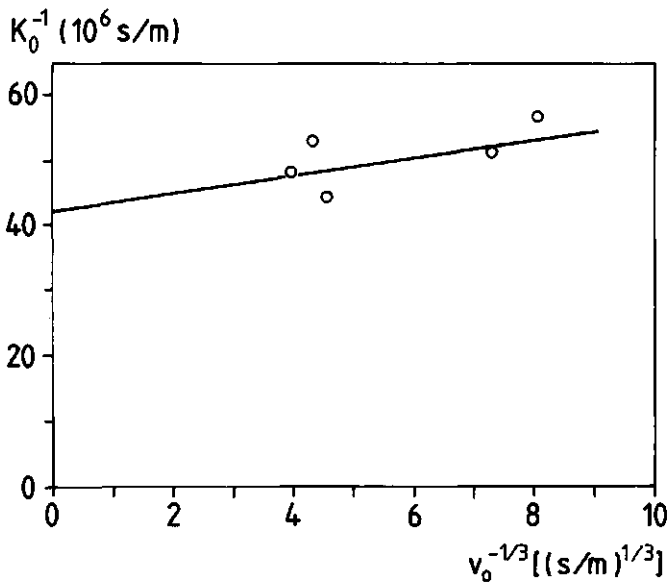


Figure 6.  $1/K_0$  versus  $v_0^{-1/3}$  for the determination of the partial mass transfer resistance inside the fibers

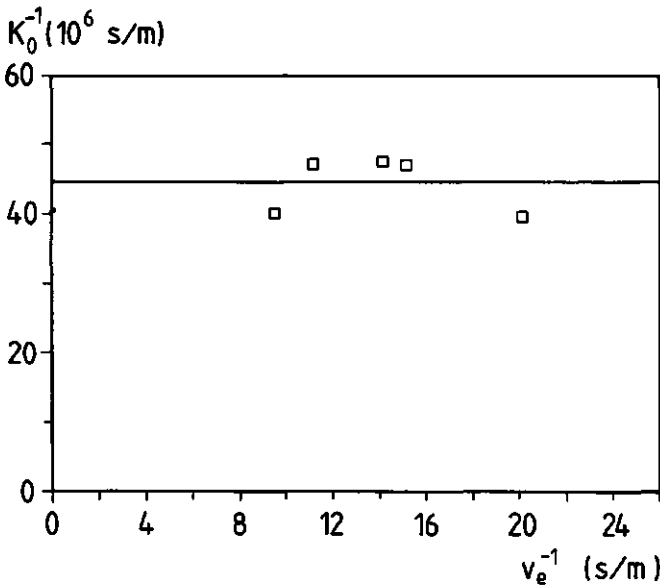


Figure 7.  $1/K_0$  versus  $v_e^{-1}$  for the determination of the partial mass transfer resistance outside the fibers

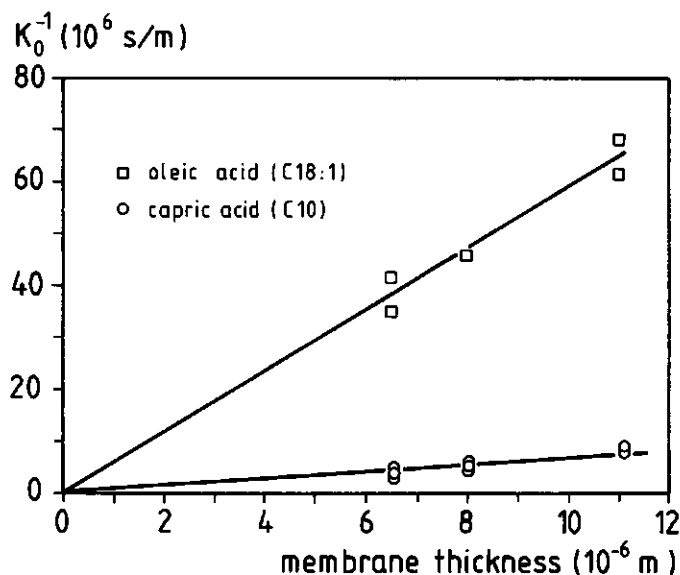


Figure 8.  $1/K_o$  versus the dry membrane thickness

In order to determine the contribution of the partial mass transfer resistance inside the fibers to the overall mass transfer resistance  $1/K_o$  is plotted versus  $v_o^{-1/3}$ , according to equation (4) (figure 6). Only a slight dependence is found, and extrapolation to an infinitely large velocity still yields a significant mass transfer resistance (the intercept represents the sum of the resistances inside the fiber wall and in the extraction phase). When  $1/K_o$  is plotted versus  $v_o^{-1}$  (figure 7) no dependence is found, indicating that no significant resistance is situated outside the fibers. It can therefore be expected, that the intercept of figure 6 represents the mass transfer resistance inside the membrane wall only. Also, a plot of  $1/K_o$  versus the membrane wall thickness (figure 8) gives a straight line through the origin, indicating that indeed almost all resistance against mass transfer is situated inside the membrane wall. This appeared to be the case for all fatty acids used, except for caproic acid (C6:0), where the resistance inside the fiber wall only represents 60% of the overall mass transfer resistance. According to equation 3, the mass transfer resistances inside the fiber wall and at the extractant side of the membrane can be neglected when  $m \rightarrow \infty$ .

#### Diffusion in the membrane matrix

From measurements of the different partial mass transfer resistances, the diffusion coefficients

inside the membrane matrix can be calculated. These are given in figure 9. The diffusion coefficients inside the cellulose membrane matrix obtained for different fatty acids can be compared to the coefficients as obtained from different models that have been proposed in the literature to relate the diffusion coefficient in solution (calculated according to the Wilke–Chang relationship [22]) to the diffusion coefficient inside a homogeneous membrane matrix. The results of these calculations are also included in figure 9. Most models use the porosity, tortuosity and pore diameter of the membrane material (0.65 [23], 1.9 [24] and 3.4 nm [35], respectively), except the model proposed by Peppas and Reinhart [23], which requires information about the molecular structure of the polymer.

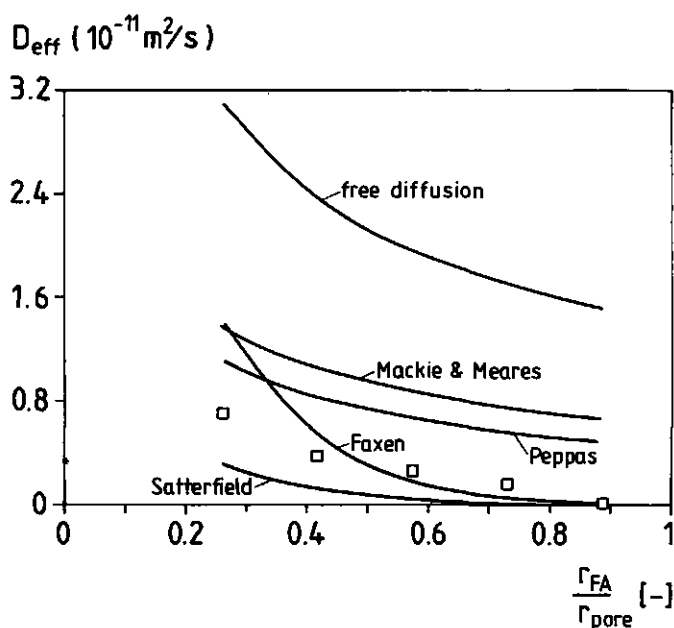


Figure 9. Diffusion inside the membrane matrix. Values are compared to values obtained with diffusion models proposed in literature

It appears, that most models predict the diffusion coefficient within a factor of 4. The curve following from the theory of Faxen [29] is differently shaped and predicts too steep a decrease of the diffusion coefficient with chain length, whereas both the models of Faxen [29] and Satterfield [28] differ more than a factor of 4 for the longest fatty acids. From these results it can

be concluded that all models give predictions in the range of the experimental values for the diffusivity inside the membrane matrix. However, none of them results in an exact fit of the experimental data, which may be partly due to deviations in the estimates for the fatty acid and pore diameter. It seems that the models can, at best, make a reasonable first guess of the diffusion coefficient. Whenever values are needed that are more reliable than that, they will have to be determined experimentally.

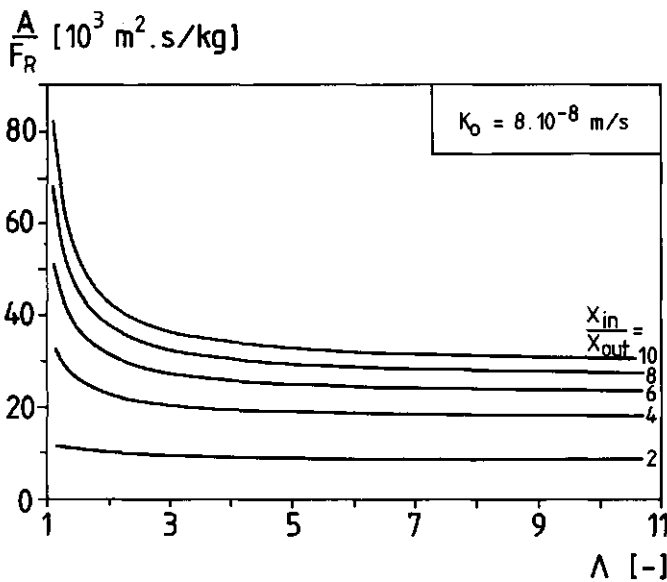


Figure 10. The membrane surface area required for the separation of oleic acid from soy bean oil using the Diaphan membrane as a function of the stripping factor at different required separation efficiencies

#### Countercurrent extraction

Once the overall mass transfer coefficients are obtained, it is possible to calculate the required membrane surface area for a given extraction. As an example, the surface area required for the separation of oleic acid from oil using the Diaphan membrane is calculated for different extraction efficiencies ( $x_1/x_o$ ) versus the stripping factor  $\Lambda$ . The overall mass transfer coefficient

for this separation is the measured one, being  $8 \cdot 10^{-8}$  m/s. The results of these calculations are shown in figure 10. It appears that an increase in the stripping factor has a strong influence on the required surface area up to values of about 3. A further increase does not result in a further decrease in the required surface area.

These data reveal that for a full scale extraction (90% fatty acid removal from 5,000 kg/h oil) about 40,000 m<sup>2</sup> of membrane area are required. The costs for the extraction of copper from oil using the same cellulose hollow fiber membranes as used in this study for a 10,000 m<sup>2</sup> system to treat 5,000 kg/h have been estimated to be between 0.01 and 0.03 \$/kg [30]. The increase of the costs of a membrane plant are estimated to be proportional to  $A^{0.6}$  [31]. These figures indicate that the costs for this fatty acid extraction will be between 0.025 and 0.07 \$/kg.

### Fractionation

Because of the low interfacial tension between oil and 1,2-butanediol it is necessary to use rather 'dense' membranes, i.e. with small pores. For such membranes, mass transfer coefficients are small as compared to transport in solution. This implies that relatively large membrane surface areas are needed for an extraction. However, it yields another opportunity, which is the ability to achieve a fractionation of a fatty acid mixture, since different fatty acids exhibit different mass transfer coefficients, as is clearly shown in figure 5. For this fractionation the selectivity ( $\alpha$ ) with respect to two components A and B can be defined as follows [32]:

$$\alpha_{A,B} = \frac{\left( \frac{x_{i,A}}{x_{o,A}} - 1 \right)}{\left( \frac{x_{i,B}}{x_{o,B}} - 1 \right)} \quad (9)$$

The ratios  $x_{i,A}/x_{o,A}$  and  $x_{i,B}/x_{o,B}$  in this expression can be calculated according to equation (8). In figure 11 calculated selectivities between three different fatty acids (C6, C10 and C18:1) are given as a function of  $A/F_o$  at a stripping factor  $\Lambda=2$  for C18:1. It should be noted, that the stripping factor increases with a decrease in fatty acid chain length as a result of the increased distribution coefficient. This implies that for fractionation two mechanisms act at the same time in the same direction: a difference in retardation by the membrane and a difference in solubility in the extraction liquid. Figure 11 shows that an increase of the permeated amount (which increases with an increase in  $A/F_o$ ) leads to decreased selectivities. Obviously, at 100% permeation no separation is achieved.

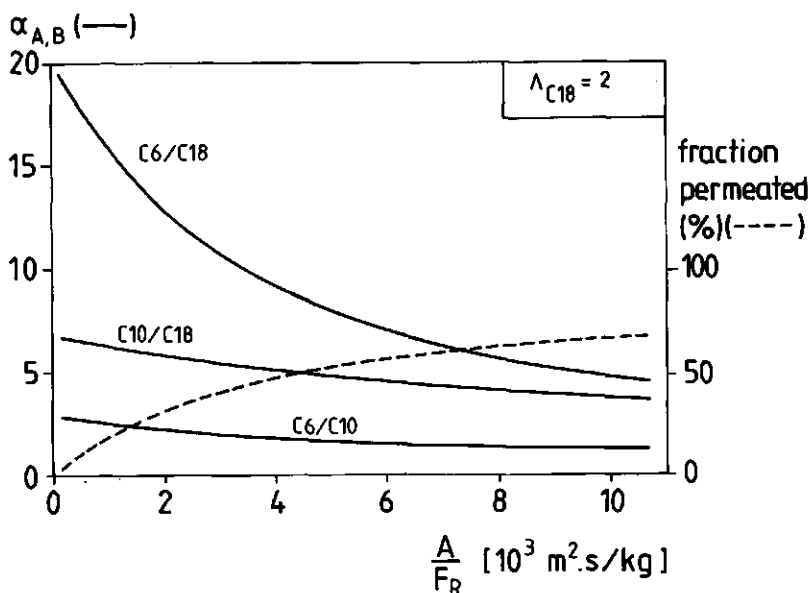


Figure 11. Selectivity between different fatty acid combinations versus the surface area to feed ratio at a stripping factor of 2 for oleic acid

By way of example, we give, in figure 12, the removal of a low concentration C6 from a fatty acid mixture consisting of C10 and C18:1 dissolved in soy bean oil. In this experiment a batch extraction with  $0.77 \text{ m}^2$  membrane area is used. The volumes of the oil and the 1,2-butanediol phase were  $4.9 \cdot 10^{-4}$  and  $4.3 \cdot 10^{-4} \text{ m}^3$ , respectively. It appears that in a relatively short contact time (1 hour) the caproic acid concentration is decreased by 80%, whereas the oleic acid and capric acid concentration are only decreased by 22% and 40%, respectively. The lines in figure 12 are calculated according to equation (2), using mass transfer coefficients from figure 5. The agreement between experimental and predicted values indicates, that the individually measured mass transfer coefficients are not influenced significantly by the presence of other fatty acids.

In this example only one extraction stage is used. More stages will obviously result in almost pure products. Most fatty acid fractionation procedures are based on crystallization (e.g. panning and pressing [33] and the hydrophilization process [34]), which require reaction times of several days



[33]. The major advantage of the present membrane fractionation procedure is found in the time required for separation. Neither of the crystallization processes results in pure products and requires several stages, as does this membrane fractionation, thus stressing the advantage of short reaction times.

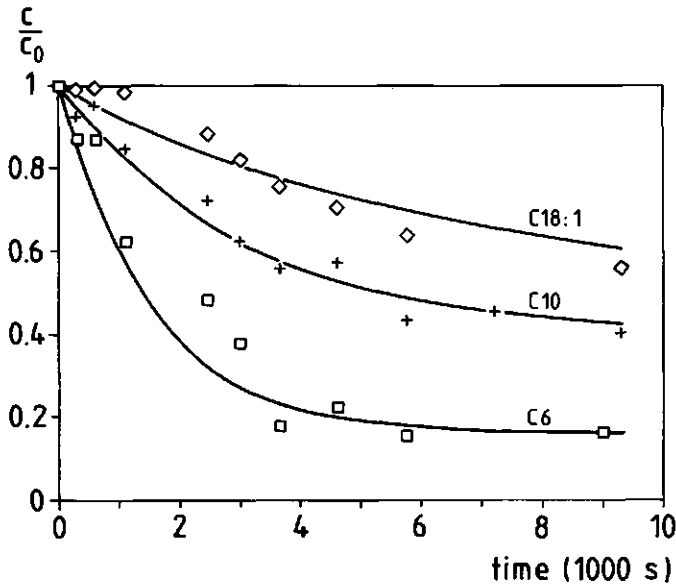


Figure 12. Fractionation of a mixture of C6, C10 and C18:1 (1:5:5) in a batch extraction

Table 4. Concentrations in the different streams as indicated in figure 12 starting with a 1:1:1 ratio in the feed;  $A/F_0=4300 \text{ m}^2\text{s/kg}$ ,  $\Lambda(\text{C18:1})=2$

| stage |                | concentration (%) |     |       |
|-------|----------------|-------------------|-----|-------|
|       |                | C6                | C10 | C18:1 |
| 1     | permeate (P1)  | 60                | 34  | 6     |
|       | retentate (R1) | 8                 | 33  | 59    |
| 2     | permeate (P2)  | 25                | 57  | 18    |
|       | retentate (R2) | 2                 | 21  | 77    |
| 3     | permeate (P3)  | 70                | 22  | 8     |
|       | retentate (R3) | 25                | 57  | 18    |

Using the data of figure 11, a three- membrane countercurrent extraction system (figure 13) can be used to fractionate a 1:1:1 mixture of C6, C10 and C18:1 to produce one stream almost free of

C6 (R2), one stream almost free of C18:1 (P3) and one intermediate stream enriched in C10 (P2 and R3 together). The results are given in table 4.

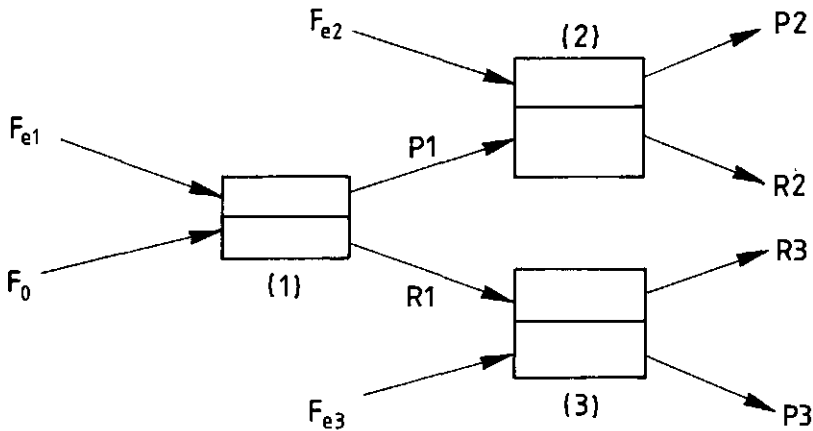


Figure 13. *Three stage membrane system for the fractionation of a fatty acid mixture dissolved in an organic solvent*

However, the two stage extraction is more complicated than shown in figure 13. The fatty acids of the 1,2-butanediol phase have to be reextracted to an other oil phase, since it is not possible to extract fatty acids from 1,2-butanediol to fatty acid free 1,2-butanediol because of a trans-membrane flow due to osmotic effects. Reextraction can easily be achieved by the addition of water to the butanediol phase as described above. This operation yields a fatty acid free butanediol phase and pure fatty acids which then can be dissolved in any organic solvent, thus serving as the feed of stage 3.

## 6.6 CONCLUSIONS

From this work it can be concluded that it is possible to extract fatty acids from an oil stream when a suitable extractant can be found. It appeared that 1,2-butanediol can be used for this purpose. The distribution coefficient varies from 0.7 for erucic acid up to 5.5 for caproic acid.

The mutual solubility of oil and 1,2-butanediol is less than 0.1% in the presence of 2% of water in the system. Recovery of the fatty acids can be achieved by the addition of water, resulting in demixing of the solution into a dispersion containing fatty acids as the dispersed and 1,2-butanediol/water as the continuous phase. The fatty acid phase then contains 2% 1,2-butanediol and the 1,2-butanediol contains less than 0.05% fatty acids.

Extractions have been performed in hollow fiber membrane modules containing cellulose and cellulose acetate membranes. Due to the low interfacial tension between oil and 1,2-butanediol it is necessary to use rather dense membranes. From mass transfer measurements it follows that a major part of the mass transfer resistance is situated inside the membrane matrix. Overall mass transfer coefficients vary significantly for different fatty acids, varying from  $7 \cdot 10^{-9}$  m/s for C22:1 up to  $5 \cdot 10^{-7}$  m/s for C6.

Using the mass transfer data it is possible to calculate the required membrane surface area for a given extraction. As a result of the high mass transfer resistance inside the membrane wall this membrane surface area is large. Fractionation of fatty acid mixtures can be achieved on the basis of differences in overall mass transfer coefficients and differences in solubility in 1,2-butanediol. These two effects act in the same direction: short chain fatty acids have higher mass transfer coefficients and are better soluble in 1,2-butanediol than the long chain fatty acids.

#### ACKNOWLEDGEMENTS

The authors wish to thank the Dutch Program Committee for Industrial Biotechnology (PCIB) for their financial support and B. Hasenack for technical assistance.

#### LIST OF SYMBOLS

|                |                                  |                      |
|----------------|----------------------------------|----------------------|
| A              | membrane surface area            | [m <sup>2</sup> ]    |
| a              | constant                         | [-]                  |
| b              | constant                         | [-]                  |
| C              | fatty acid concentration         | [kg/m <sup>3</sup> ] |
| D              | fatty acid diffusion coefficient | [m <sup>2</sup> /s]  |
| d              | external fiber diameter          | [m]                  |
| d <sub>f</sub> | internal fiber diameter          | [m]                  |
| d <sub>m</sub> | membrane thickness               | [m]                  |
| F              | flow                             | [kg/s]               |

## chapter 6

|            |                                       |                      |
|------------|---------------------------------------|----------------------|
| H          | height of the extractor               | [m]                  |
| HTU        | height of a transfer unit             | [m]                  |
| $K_o$      | overall mass transfer coefficient     | [m/s]                |
| k          | partial mass transfer coefficient     | [m/s]                |
| $l_f$      | fiber length                          | [m]                  |
| m          | distribution coefficient              | [-]                  |
| NTU        | number of theoretical transfer units  | [-]                  |
| $\Delta P$ | Laplace pressure                      | [Pa]                 |
| R          | pore radius                           | [m]                  |
| t          | time                                  | [s]                  |
| V          | volume                                | [m <sup>3</sup> ]    |
| v          | velocity                              | [m/s]                |
| x          | fatty acid concentration in oil phase | [kg/m <sup>3</sup> ] |
| $\alpha$   | selectivity                           | [-]                  |
| $\gamma$   | interfacial tension                   | [N/m]                |
| $\epsilon$ | porosity                              | [-]                  |
| A          | stripping factor                      | [-]                  |
| $\tau$     | tortuosity                            | [-]                  |
| $\theta$   | contact angle                         | [°]                  |
| $\nu$      | viscosity                             | [m <sup>2</sup> /s]  |
| $\rho$     | density                               | [kg/m <sup>3</sup> ] |

## subscripts

|    |                   |
|----|-------------------|
| o  | oil phase         |
| e  | extraction phase  |
| eq | equilibrium state |
| i  | inflow oil phase  |
| o  | outflow oil phase |
| m  | membrane          |
| A  | component A       |
| B  | component B       |

## REFERENCES

- 1) Lo, T.C. and M.H.I. Baird, Liquid-liquid extraction, in: Kirk-Othmer Encyclopedia of Chemical Technology, Vol.

## chapter 6

- 9, 3<sup>rd</sup> edition, M. Grayson (Ed.), J. Wiley and Sons, New York, 1980, 672-721
- 2) D'Elia, N.A., L. Dahuron and E.L. Cussler, Liquid-liquid extractions with microporous hollow fibers, *J. Membrane Sci.* 29 (1986) 309-319
- 3) Prasad, R. and K.K. Sirkar, Dispersion-free solvent extraction with microporous hollow fiber modules, *Am. Inst. Chem. Eng. J.* 34 (1988) 177-188
- 4) Kiani, A., R.R. Bhawe and K.K. Sirkar, Solvent extraction with immobilized interfaces in a microporous hydrophobic membrane, *J. Membrane Sci.* 20 (1984) 125-145
- 5) Alexander, P.R. and R.W. Callahan, Liquid-liquid extraction and stripping of gold with microporous hollow fibers, *J. Membrane Sci.* 35 (1987) 57-71
- 6) Kim, B.M., Membrane-based solvent extraction for selective removal and recovery of metals, *J. Membrane Sci.* 21 (1984) 5-19
- 7) Callahan, R.W., Novel uses of microporous membranes: a case study, *AIChE Symposium Series*, vol 84 no. 261 (1988) 54-65
- 8) Dekker, M., P.H.M. Koenen and K. van 't Riet, Reversed micellar-membrane-extraction of enzymes, *Int. Chem. Eng. Symp. Series* 118 (1990) 7.1-7.12
- 10) Applewhite, T.H., Fats and fatty oils, in: *Kirk-Othmer Encyclopedia of Chemical Technology*, Vol. 9, 3<sup>rd</sup> edition, M. Grayson (Ed.), J. Wiley and Sons, New York, 1980, 795-831
- 11) Edible oils and fats, developments since 1978, *Food Technology Rev.* 57, S. Torrey (Ed.), Noyes Data Corp., Park Ridge NJ, USA 1983
- 12) Braae, B., Degumming and refining practices in Europe, *J. Am. Oil Chem. Soc.* 53 (1976) 353-357
- 13) Shah, K.J. and T.K. Venkatesan, Aqueous isopropyl alcohol for extraction of free fatty acids from oils, *J. Am. Oil Chem. Soc.* 66 (1989) 783-787
- 14) Pons, W.A., P.H. Eaves, Aqueous acetone extraction of cottonseed, *J. Am. Oil Chem. Soc.* 44 (1967) 460-464
- 15) Swern, D. (ed.), *Bailey's industrial oil and fats products*, Vol. 2, 4<sup>th</sup> edition, J. Wiley and Sons, New York, 1982
- 16) Uksila, E., M. Varesmaa and I. Lehtinen, Separation of unsaturated fatty acids of soybean and linseed oils by crystallization and subsequent liquid-liquid extraction, *Acta Chim. Scandinavica* 20 (1966) 1651-1657
- 17) Yang, M.C. and E.L. Cussler, Designing hollow fiber contactors, *Am. Inst. Chem. Eng. J.* 32 (1986) 1910-1916
- 18) Dahuron, L. and E.L. Cussler, Protein extraction with hollow fibers, *Am. Inst. Chem. Eng. J.* 34 (1988) 130-136
- 19) Prasad, R. and K.K. Sirkar, Solvent extraction with hydrophilic and composite membranes, *Am. Inst. Chem. Eng. J.* 33 (1987) 1057-1066
- 20) Kreith, F., *Principles of heat transfer*, Harper and Row, New York, 1973
- 21) Beek, W.J. and K.M.K. Muttzall, *Transport Phenomena*, J. Wiley and Sons, London, 1975
- 22) Wilke, C.R. and P. Chang, Correlation of diffusion coefficients in dilute solutions, *Am. Inst. Chem. Eng. J.* 1 (1955) 264-270
- 23) Peppas, N.A. and C.T. Reinhart, Solute diffusion in swollen membranes. Part I. A new theory, *J. Membrane Sci.* 15 (1983) 275-287
- 24) Sakai, K., S. Takesawa, R. Mimura and H. Ohashi, Structural analysis of hollow fiber dialysis membranes for clinical use, *J. Chem. Eng. Japan* 20 (1987) 351-356
- 27) Mackie, J.S. and P. Meares, The diffusion of electrolytes in a cation exchange resin membrane, *Proc. Roy. Soc. (London)*, A232 (1955) 498-509
- 28) Satterfield, C.N., C.K. Colton and W.H. Pitcher, Restricted diffusion in liquids with fine pores, *Am. Inst. Chem. Eng. J.* 19 (1973) 628-635
- 29) Faxen, H., Die Bewegung einer starren Kugel langs der Achse eines mit zährer Flüssigkeit gefüllten Rohres, *Arkiv. Mat. Astron. Fys.*, 17 (1923) 27
- 30) Keurentjes, J.T.F., Th.G.J. Bosklopper, L.J. van Dorp and K. van 't Riet, The removal of metals from edible oil

*chapter 6*

- by a membrane extraction procedure, *J. Am. Oil Chem. Soc.* 67 (1990) 28-32
- 31) Kloosterman, J., P.D. van Wassenaar and W.J. Bel, Membrane bioreactors, *Fat Sci. Technol.* 89 (1987) 592-597
  - 32) Sandell, E.B., Meaning of the term separation factor, *Anal. Chem.* 4 (1968) 834-835
  - 33) Zilch, K.T., Separation of fatty acids, *J. Am. Oil Chem. Soc.* 56 (1979) 739A-742A
  - 34) Stein, W., The hydrophilization process for the separation of fatty materials, *J. Am. Oil Chem. Soc.* 45 (1968) 471-474
  - 35) Klein E., F.F. Holland and K. Eberle, Comparison of experimental and calculated permeability and rejection coefficients for hemodialysis membranes, *J. Membrane Sci.* 5 (1979) 173-188

## MEMBRANE CASCADES FOR THE SEPARATION OF BINARY MIXTURES

---

### SUMMARY

For the separation of binary mixtures several techniques can be considered, of which is distillation the most widely used. When problems occur in distillation (like the formation of an azeotropic mixture), membrane separation can be an alternative. A cascade of membranes has to be applied in those cases where it is impossible to achieve a complete separation in a single membrane separation process. To calculate the separation in such a cascade, a McCabe-Thiele diagram is used in which the equilibrium curve is determined by the membrane selectivity. Optimization calculations for the cascade have been performed with respect to the total membrane surface area. Because of the large reflux flows around the feed stage, the permeate/retentate ratio in the feed stage has to be chosen carefully, since the required membrane surface area is merely determined by the permeate flows. The membrane characteristics that influence the required membrane surface area are selectivity and permeability: an increased selectivity or permeability reduces the membrane area. However, an increase of the selectivity usually goes with a decrease of the permeability. It appears from this study, that for selectivity and permeability values commonly found for RO membranes, an increase of the permeability influences the required membrane area to a larger extent than an increase in selectivity. This effect is illustrated by simulations for RO membranes used for the separation of water/1,3-butanediol mixtures. The total membrane area can be reduced by 25% when two membranes are available with opposite selectivity, i.e. membranes with a retention for the other component.

---

J.T.F. Keurentjes, L.J.M. Linders, W.A. Beverloo and K. van 't Riet

This chapter is submitted for publication

## 7.1 INTRODUCTION

For the separation of liquid mixtures several techniques such as distillation, liquid-liquid extraction and membrane separations can be employed, of which distillation is the most commonly used [1]. The use of distillation can be limited by the formation of an azeotropic mixture. In most of the membrane separations, differences in molecular size and sorption characteristics determine the selectivity for the components, and since for that case no phase transition is required, the formation of an azeotropic mixture will not influence the separation. Membrane separation processes will also be energetically favourable as compared to distillation [2,3,4], and because of the low temperatures used in membrane processes, thermal or oxidative degradation will be retarded.

For the methods described in this report, reverse osmosis (RO), pervaporation and gas separation are the main applications. Reverse osmosis can be applied to the separation, concentration and fractionation of organic as well as inorganic substances in the liquid phase. The classical application of RO is in desalination of sea and brackish water. Novel applications are found in the separation of liquid mixtures such as water-ethanol [1,7], n-heptane-ethanol [5] and butanol-acetone [6] mixtures. Pervaporation and gas separation can also be used for the separation of binary mixtures. In these processes the membrane material is a dense polymer film and a difference in solubility in the membrane material yields selectivity for one of the components. Pervaporation can be applied to the separation of mixtures consisting of components having rather close boiling points [8]. Although the separation of gas mixtures by membranes has been known for a long time, it has only found application recently due to an increased knowledge of membrane materials [9]. Examples are the separation of helium and methane to produce helium from natural gas and the separation of  $\text{SO}_2$ -nitrogen mixtures [10,11].

Like most separation processes, membranes can not separate mixtures into pure components in one single step. Generally, a feed stream is separated in two product streams with different compositions. Often a series of consecutive stages with membranes is needed to obtain product streams of predetermined specifications. Several configurations have been proposed [12,11,13,14,15], of which a multistage column (figure 1) seems to be the generally accepted configuration.

Descriptions of multistage membrane separations are derived from the graphical description of other multistage separation processes using a McCabe-Thiele diagram. The equilibrium curve is obtained by plotting the retentate concentration versus the permeate concentration. Since it is



impossible to consider a membrane separation process as an equilibrium separation, we would, however, prefer to use the term selectivity curve instead of equilibrium curve.

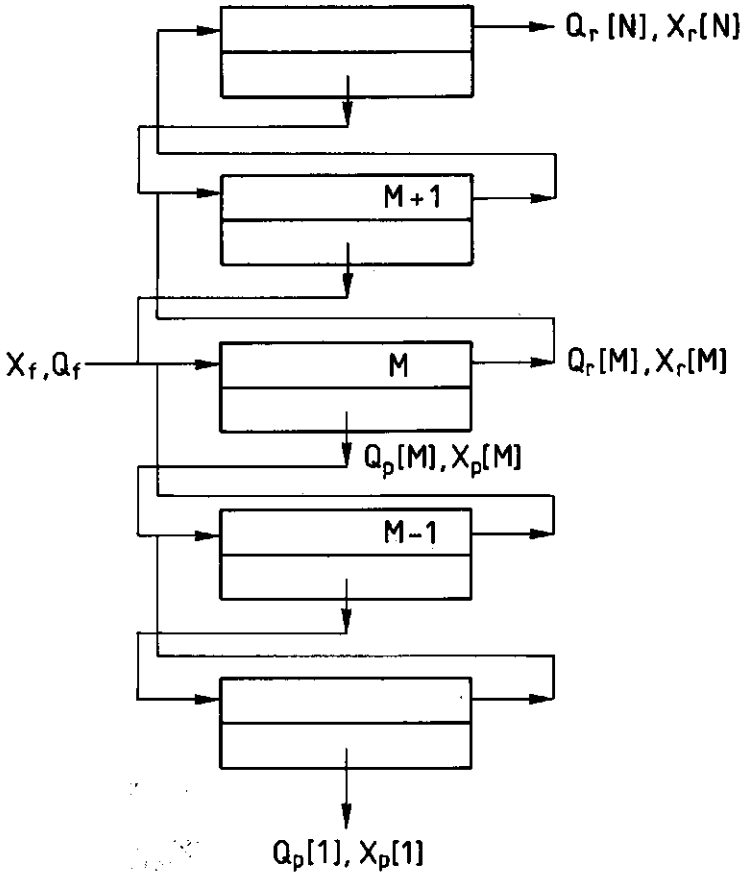


Figure 1. Cascade configuration for the separation of a binary mixture with feed concentration  $X_f$  into a top and bottom stream with concentration  $X[N]$  and  $X[1]$ , respectively

Usually, an operating line is drawn to describe the deviation from an ideal separation process. This line is determined by the concentrations in the two streams in between two consecutive stages. The required number of stages can be determined graphically from this operating line and the selectivity curve. For membrane separations, attempts have been made to give a suitable description of the operating line [14,15]. Hwang and Kammermeyer [14] have given a general

description of the operating line for multistage separations, however, this results in extensive equations and a different operating line for every single stage. They showed that this approach can be worked out graphically for a constant stage cut (the permeate to inflow ratio) or a constant overflow, however, when both change with stage number, the graphical determination of the number of stages is impossible, although it can be calculated numerically. Schulz et al. [12] treated a membrane cascade for gas separations in a similar way, using a constant stage cut. Evangelista [15] constructed a different type of membrane cascade for the separation of liquid solutions: several parallel series of membranes were used without reflux streams. This procedure is of interest to the design of a RO plant for the concentration of a liquid in which one of the streams (permeate or retentate) may be wasted. However, for the separation of binary mixtures in which both components are valuable this configuration is not very suitable (although the model might be extended for this situation). In this study the use of operating lines is avoided, and it will be shown that the number of stages can be determined from the selectivity curve directly. The effect of permeability and selectivity (the two most important membrane characteristics in this respect) and cascade configuration will be investigated.

## 7.2 THEORY

The feed stream of the cascade is a binary mixture with components a and b with a fraction  $X_f$  of component a (figure 1). The feed stream, with a flow rate  $Q_f$ , is led across the feed stage membrane, numbered as M. By applying a static pressure P at the feed side, a part of the stream ( $Q_p[M]$ ) will permeate with fraction  $X_p[M]$ , and is led towards stage [M-1]. The retentate stream ( $Q_r[M]$ ) with fraction  $X_r[M]$  is led towards stage [M+1]. The feed of each stage [I] consists of the retentate flow of the stage below ([I-1]) and the permeate flow of the stage on top ([I+1]), except the feed stage [M] where the feed stream entering the system is added to these flows, and the top and bottom stage (stage [1] and [N], respectively) where the product streams leave the system. For an efficient separation process it is a prerequisite that the composition of the retentate stream of stage [I-1] equals the permeate composition of stage [I+1]. When this requirement is not met, the separation efficiency will decrease, due to the extra entropy production of mixing [14].

For the cascade as a whole and for each separate stage a mass balance can be written:

$$Q_{in} = Q_p + Q_r \quad (1)$$

in which  $Q_{in}$  is the mass flow entering a stage and  $Q_p$  and  $Q_r$  are the permeate and retentate flows, respectively. The same applies for the component balance:

$$Q_{in} X_{in} = Q_p X_p + Q_r X_r \quad (2)$$

The selectivity of a membrane can be defined in several ways [1,6,8,10, 16,17,18]. In this study the selectivity  $\alpha$  is defined in a way similar to the definition generally used in other separation processes:

$$\alpha = \frac{X_p(1 - X_r)}{X_r(1 - X_p)} \quad (3)$$

In gas separations this selectivity is called the actual separation factor, whereas the ideal separation factor as defined for gas separations is the ratio of the two permeability coefficients [11,12,13].

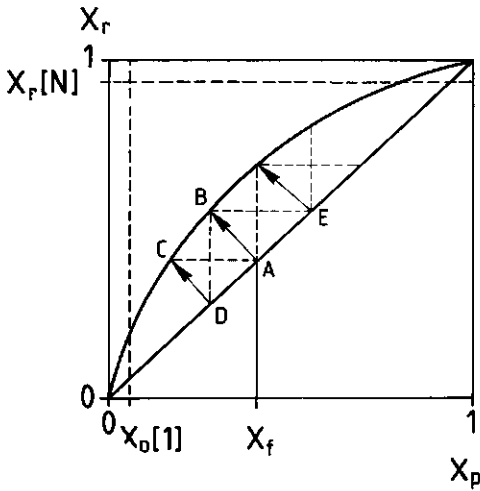


Figure 2. McCabe-Thiele diagram for  $\alpha < 1$ . The curved line is the selectivity curve

Starting point for our calculations on multistage membrane separations is a McCabe-Thiele diagram as shown in figure 2, in which the curved line gives the composition of the retentate plotted against the permeate composition (the selectivity curve) as given by equation (3) at a given and constant value of  $\alpha$ . The effect of incomplete mixing and concentration polarization is incorporated in the selectivity curve when it is determined for the same experimental conditions as applied in the cascade.

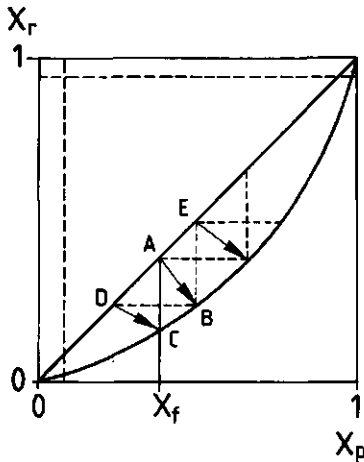


Figure 3. McCabe-Thiele diagram for  $\alpha > 1$

Starting with a feed stream with composition  $X_f$  (point A) a line can be drawn to point B on the selectivity curve. At this point, the retentate and permeate composition of the feed stage are known (E and D, respectively). Now the composition of the permeate and retentate streams throughout the system are known, since  $X_p[I] = X_r[I-2]$  and  $X_r[I] = X_p[I+2]$ . The line AB can be chosen freely, and is given by an equation derived from the balance equation (2) and the selectivity equation (3) as:

$$X_r = -\frac{Q_p}{Q_r}X_p + \left(1 + \frac{Q_p}{Q_r}\right)X_f \quad (4)$$

The tangent of the line AB (written as  $\tan[M]$ ) equals the ratio of the permeate and retentate streams ( $-Q_p/Q_r$ ). The boundary condition of a tangent close to 0 yields a maximum increase in permeate concentration, but with a permeate flow near to 0, whereas the boundary condition of an infinite tangent results in the permeation of the whole mixture. In calculations  $\tan[M]$  is an important parameter, since the line AB determines the permeate and retentate flows of all the other stages. Membrane cascades can be optimized with respect to a minimum membrane surface area (A), but other optimization criteria can be used as well. The total membrane surface area is determined by the permeating streams, since  $A[I]$  is directly related to  $Q_p[I]$ :

$$A[I] = \frac{Q_p[I]}{\phi[I]P} \quad (5)$$

in which is  $\phi[I]$  the permeability of the membrane material for the liquid permeating at stage  $[I]$  and  $P$  the applied pressure. Equation (5) shows that it is necessary to minimize the permeate flows. Similarly to figure 2 one can construct the McCabe-Thiele diagram for a membrane having a selectivity towards the other component  $b$  (figure 3). In this case the selectivity curve is situated below the  $X_p = X_r$  line. The treatment of this diagram is similar to the one described above.

### 7.3 MATERIALS

Permeation experiments have been performed using an Amicon stirred cell device with an effective membrane surface area of  $32.4 \cdot 10^{-4} \text{ m}^2$  at a trans-membrane pressure of  $4 \cdot 10^6 \text{ Pa}$ . Three cellulose acetate RO membranes (table 1) have been used for the determination of separation characteristics and permeabilities for 1,3-butanediol/water mixtures.

Table 1. *Cellulose acetate RO membranes used for permeation experiments*

| Membrane | Manufacturer | NaCl retention (%) |
|----------|--------------|--------------------|
| 1        | Hoechst      | 30                 |
| 2        | DDS          | 55-65              |
| 3        | Toray        | 96                 |

Demineralized water was used, the 1,3-butanediol was reagent grade and purchased from Merck (F.R.G.). The membranes were rinsed thoroughly with water before use, and the temperature was 20 °C throughout.

### 7.4 RESULTS AND DISCUSSION

#### Water/1,3-butanediol separation

The results of permeation experiments with water/1,3-butanediol mixtures using the three RO membranes are given in figure 4a and 4b. In figure 4a, the retentate concentration is plotted versus the permeate concentration. The selectivity calculated according to equation (3) is plotted versus  $X_r$  in the inset. Figure 4b shows the permeation rate versus  $X_p$ . From these figures it

appears that the less selective membrane (membrane 1) has the highest permeability, and the most selective one (membrane 3) has the lowest permeability. All three membranes become less selective upon a decrease in 1,3-butanediol concentration. The selectivities found are comparable to those found in the literature for the separation of organic liquid mixtures using RO membranes [5,6,16,19,20]. The permeabilities increase significantly at low 1,3-butanediol contents, and the difference in permeability is about two decades over the full concentration range. This effect will be due to the fact that water molecules are significantly smaller than 1,3-butanediol molecules, resulting in smaller friction with the membrane material. The permeabilities found here ( $10^{-3}$ – $10^{-5}$  kg/(m<sup>2</sup>.s.bar)) are somewhat higher than the permeabilities usually found for RO ( $10^{-4}$ – $10^{-6}$  kg/(m<sup>2</sup>.s.bar)), which is due to the fact that the RO membranes used here are relatively loose RO membranes with low NaCl retentions.

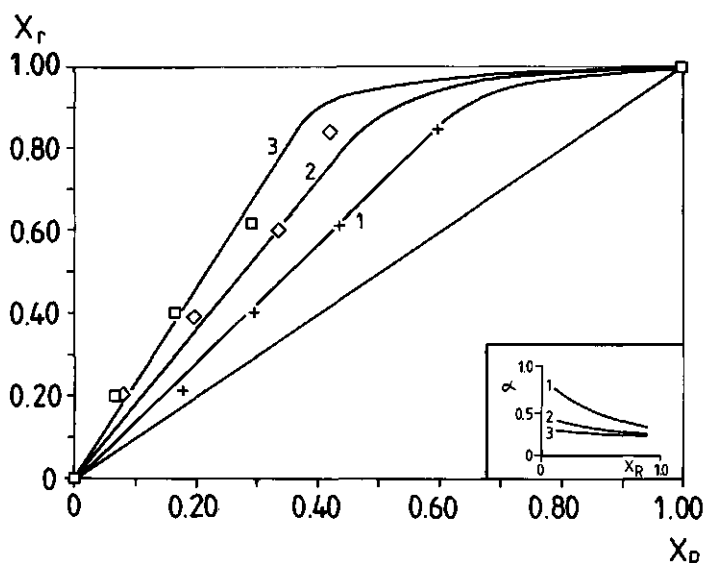


Figure 4a. McCabe-Thiele diagram as measured for different RO membranes for the separation of water/1,3-butanediol mixtures. Concentrations are 1,3-butanediol concentrations. Inset: selectivity  $\alpha$  versus  $X_r$ .

From the foregoing it appeared, that selectivities and permeabilities are not constant over the whole composition range. In the following, however, cascade calculations will be performed using idealized membranes, possessing a constant selectivity and permeability over the whole

concentration range. In that case the selectivity curve is given by equation (3). If necessary, however, it is possible to use the exact values of  $\alpha[I]$  instead of equation (3) and the exact values of  $\phi[I]$  in equation (5). For the separation of the water/1,3-butanediol mixture the exact values are given in figures 4a and 4b. It will be shown that this simplification does not significantly affect the results.

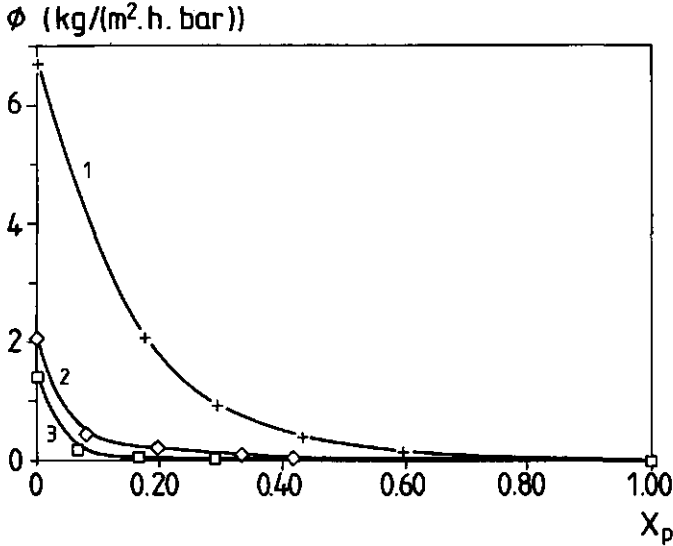


Figure 4b. Permeability of the three RO membranes versus permeate concentration

### Single-membrane type cascade

#### I. Cascade parameters.

Optimization calculations on the cascade are carried out with respect to the required membrane surface area. A membrane with selectivity  $\alpha=0.7$  and permeability  $2 \cdot 10^{-4}$  kg/(m<sup>2</sup>.s.bar) is used, based on the data in figures 4a and 4b. As an example the results for the separation of a feed stream of 1 kg/s with composition  $X_F=0.5$  into product streams with compositions  $X[1]=0.05$  and  $X[N]=0.95$  are presented. The applied pressure is 80 bar. In figure 5 the concentrations in the permeate and retentate streams of each stage through the whole cascade are given. It can be seen that close to the feed stage [M], concentration differences between two stages are significantly larger than close to the top and bottom stage, which is caused by the fact that in the McCabe-Thiele diagram the selectivity curve approaches the line  $X_r=X_p$  near the end points.

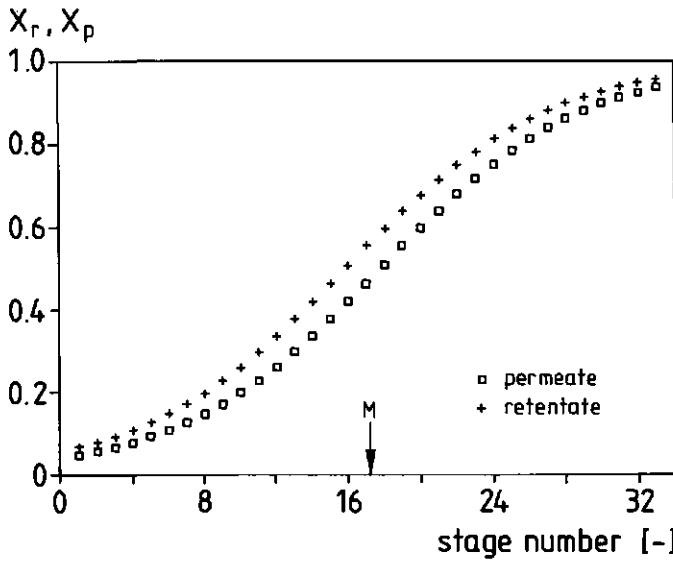


Figure 5. Permeate and retentate concentration for each stage.  $X_f=0.5$ ,  $X[1]=0.05$ ,  $X[N]=0.95$ ,  $\tan[M]=-1.07$ ,  $Q_f=1$  kg/s,  $P=80$  bar,  $\alpha=0.7$  and  $\phi=2 \cdot 10^{-4}$  kg/(m<sup>2</sup>.s.bar)

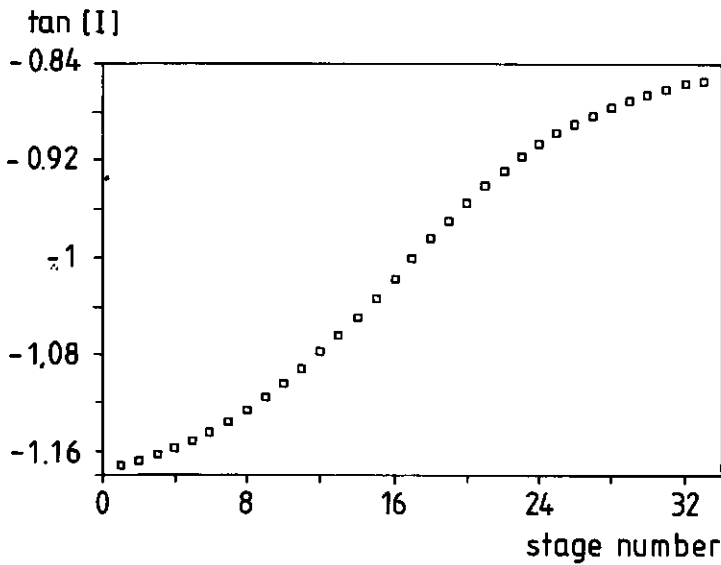


Figure 6. Variation of  $\tan[I]$  with stage number for the conditions of figure 5



Figure 6 shows that  $\tan[I]$  (which is the permeate/retentate flow ratio) varies for each stage. The ratio decreases from the bottom stage upwards. However, the influence on the surface area is small as compared to the effect of reflux flows (figure 7, line a). Reflux flows are smaller towards the top and the bottom of the cascade, which results in a smaller surface area for the stages at the top and the bottom. The choice of a correct permeate/retentate ratio in the feed stage will be an important design parameter, since the volume flow through the feed stage is the largest one. This is shown by line b in figure 7, where an incorrect choice of  $\tan[M]$  results in membrane areas that show a strong variation in consecutive stages. The total membrane surface area for the case of line b in figure 7 is 6655 m<sup>2</sup> versus 5422 m<sup>2</sup> for line a. The total membrane surface area can be decreased when the stages with the large permeate/retentate ratio of line b in figure 7 are replaced by membranes with opposite selectivity, as will be shown in the next paragraph.

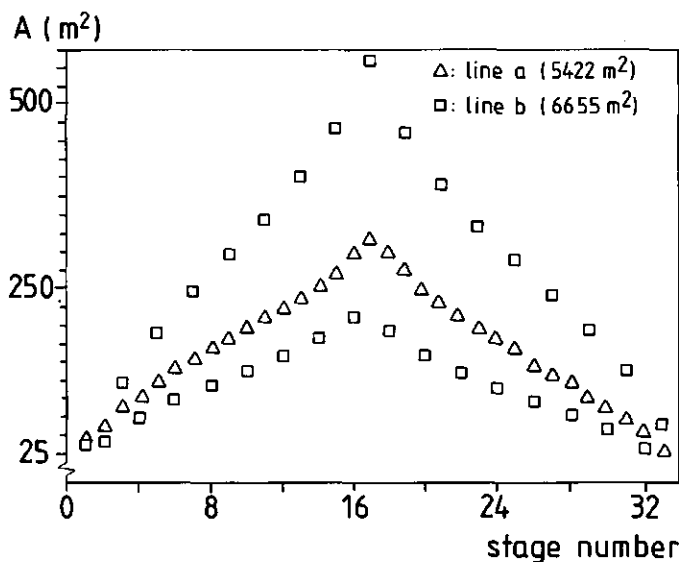


Figure 7. Membrane surface area per stage for the conditions of figure 5. Line a is obtained at the optimum  $\tan[M]$  ( $-1.07$ ), line b is obtained for  $\tan[M] = -2.5$

It turns out, that the optimum permeate/retentate ratio is a function of the feed concentration (figure 8), indicating that at low feed concentrations a relatively large fraction of the feed permeates in the feed stage, whereas a relatively small fraction permeates when the feed concentration is high. This implies that at feed concentrations around 0.5,  $\tan[M]$  will be close to -

1, at higher feed concentrations larger than  $-1$  and at low feed concentrations smaller than  $-1$ . This is, however, a tendency and the exact value of the optimum  $\tan[M]$  also depends on the selectivity  $\alpha$ . The effect of  $X_f$  on the optimum  $\tan[M]$  is smaller at selectivities close to 1 than at selectivities further from 1 (figure 8).

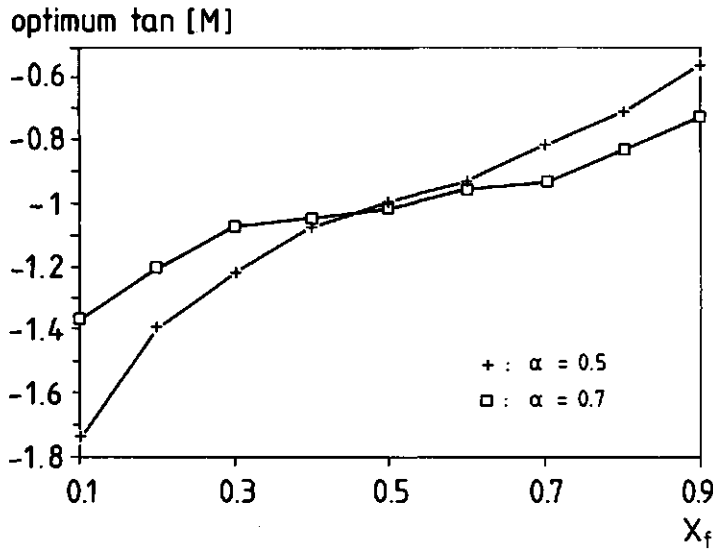


Figure 8. Optimum feed stage permeate/retentate ratio versus feed concentration for  $\alpha=0.5$  and  $\alpha=0.7$  (other conditions as mentioned at figure 5)

## II. Membrane parameters.

Two membrane parameters are important for the separation of a mixture in a cascade: the selectivity ( $\alpha$ ) and permeability ( $\phi$ ). The required number of stages depends on the selectivity (figure 9), and increases when the selectivity becomes close to 1. Also, the required surface area increases with a selectivity coming closer to 1. Since the total surface area is merely determined by the total permeate flow, it will be inversely proportional to the permeability. Although no mathematical relation exists between  $\alpha$  and  $\phi$ , an increase in selectivity usually goes together with a decrease in permeability. The three membranes used for the separation of water/1,3-butanediol mixtures showed this dependence also. The effect of  $\alpha$  and  $\phi$  on the total membrane surface area

is shown in figure 10. Since it is difficult to draw conclusions from this plot, the slope of the 3D-plane is taken in both the  $\alpha$  and  $\phi$  direction. The result of this procedure is shown in figure 11, using some typical values for reverse osmosis membranes. The dotted lines in figure 11 connect points with equal selectivity, whereas the solid lines connect points with equal permeability. The dashed line in figure 11 represents the line where a relative change in permeability has the same effect on the cascade surface area as a relative change in selectivity. From figure 11 it can be concluded that all points are found below the dashed line, indicating that permeability affects the total membrane area to a larger extent than the selectivity. Even when an improvement of the permeability results in a decrease in selectivity, this may often result in a reduced total membrane surface area.

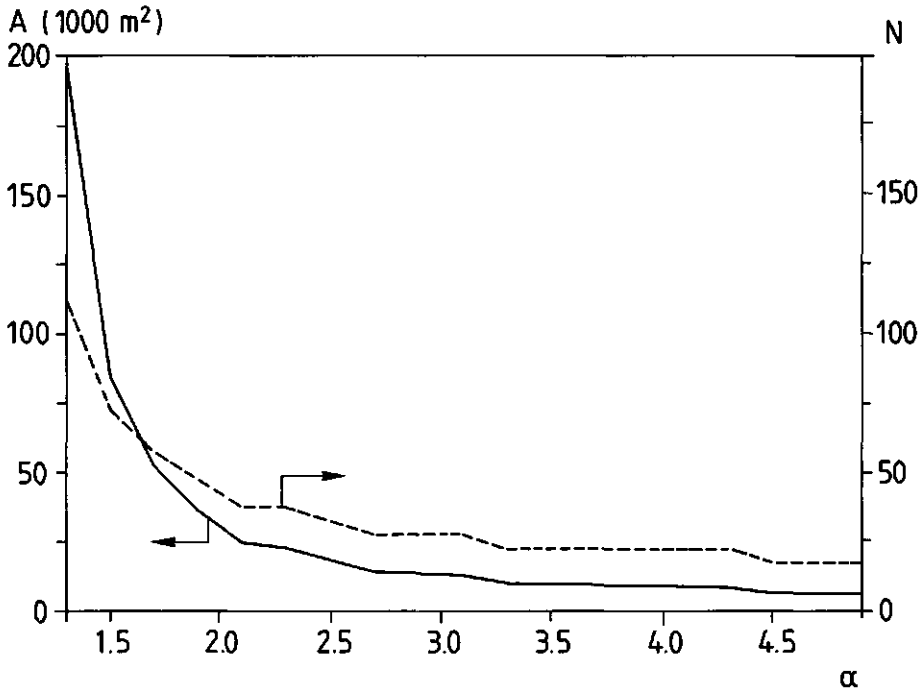


Figure 9. Total number of stages and total membrane surface area versus membrane selectivity (other conditions as mentioned at figure 5)

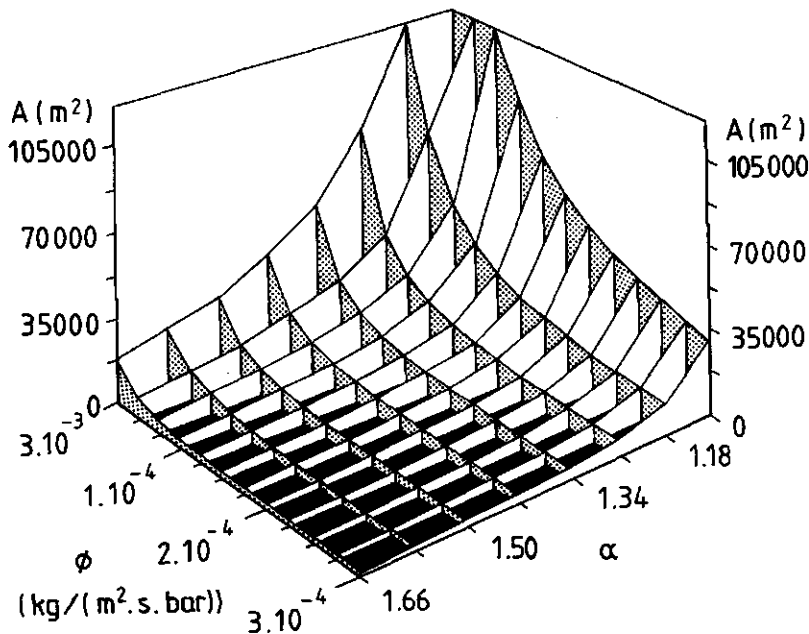


Figure 10. Total membrane surface area versus selectivity and permeability.  $X[1]=0.1$  and  $X[N]=0.9$ , other conditions as mentioned at figure 5

The foregoing can be illustrated for the separation of 1 kg/s water/1,3-butanediol mixture with a 1,3-butanediol concentration of 0.2 into top and bottom streams with concentrations 0.9 and 0.05, respectively. For this calculation,  $\alpha[1]$  and  $\phi[1]$  are adjusted for each stage according to the data of figures 4a and 4b. Using membrane 1 (the less selective one) 894 m<sup>2</sup> are required at a trans-membrane pressure of 80 bar. For this separation 17 stages are required and the feed stage is stage number 9. Performing the same calculations for membrane 3 results in 1499 m<sup>2</sup>, although only 7 stages are required with number 3 as the feed stage. As expected, this calculation shows a smaller total surface area for membrane 1. This does not necessarily mean that this process is the most competitive, since there is a large difference in the total number of stages required for membrane 1 and 3. This difference will introduce other parameters than membrane surface area into the cost analysis.

The data obtained with the exact selectivity and permeability values can now be compared to the surface area obtained for membranes with a constant selectivity and permeability. For this purpose

the permeability used for membrane 1 and 3 is chosen as the permeability belonging to the feed stage composition,  $4.8 \cdot 10^{-4}$  and  $0.4 \cdot 10^{-4}$  kg/(m<sup>2</sup>.s.bar), respectively. This choice is based on the fact that at the feed stage the largest reflux flows are found, resulting in the largest membrane area at the feed stage. For the selectivity the average values are used (i.e. 0.6 and 0.28 for membrane 1 and 3, respectively). Using these values, the total surface area for membrane 1 and 3 is 813 and 1861 m<sup>2</sup>, respectively. Those values can be compared to the values obtained when selectivity and permeability are varied with stage number. From these results it can be concluded, that the use of an idealized membrane with constant selectivity and permeability influences the results only to a minor extent.

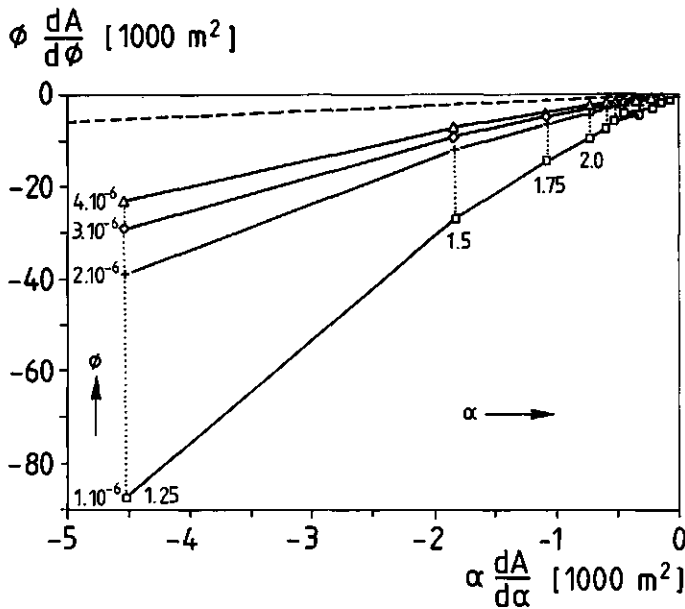


Figure 11. *Derivative of the membrane surface area to the selectivity versus the derivative to the permeability. The dashed line represents an equal effect of both permeability and selectivity on the cascade surface area*

### Two-membrane cascade

For the separation of organic liquid mixtures, the separation characteristics strongly depend on the solubility of the two components in the membrane material. Using different materials, it is possible to obtain selectivities both below and above unity [20]. When we consider a cascade

consisting of two membranes with opposite selectivity (e.g. 0.1 and 10) and equal permeability, the same calculations as described above can be carried out. The McCabe-Thiele diagram then contains two selectivity curves, one below and one above the line  $X_r = X_p$ . For every stage membrane 1 or membrane 2 can be chosen. It can be shown graphically, that this operation will result in a decrease of the total membrane surface area. As it was shown in figure 6, choosing a small permeate to retentate ratio results in a small surface area in the feed stage. However, for this situation  $\tan[I]$  switches between small and large for consecutive stages. The second membrane can now be installed at the stages where a large part of the inflow has to permeate (i.e. A-B2 instead of A-B1 in figure 12). For the situation of exactly opposite selectivities (e.g. 0.1 and 10) the permeate/retentate ratio belonging to membrane 1 becomes the retentate/permeate ratio of membrane 2. This finally results in a reduced surface area for all stages.

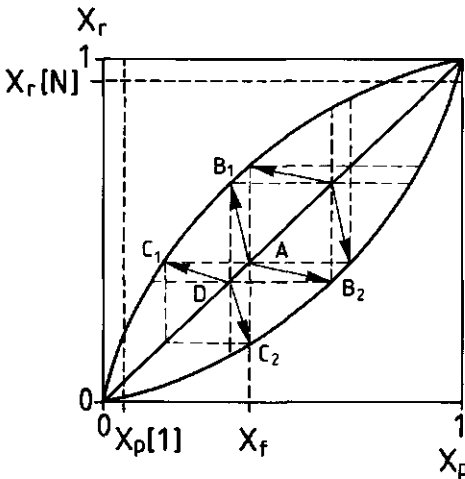


Figure 12. McCabe-Thiele diagram for two membranes having opposite selectivities

The calculations showed that at very high or very low feed concentrations (when the feed stage is the top or the bottom one) the optimum configuration consists of one block of stages containing membrane 1 and one block containing membrane two. The block of stages near the feed stage merely consists of the membrane that retains the component present in a high concentration, whereas the block of stages at the other end of the cascade merely contains the membrane with retention for the component with a low concentration in the feed. This will result in a rather small reduction of surface area, as is shown in figure 13 for  $X_f = 0.1$  or  $0.9$ . When the feed stage is not

the bottom or the top stage this finally results in a minimum surface area when membrane 1 and 2 are used alternately. It can be seen in figure 13 that this procedure can result in a reduction of 25% in membrane area. It has to be noted, that in the case of opposite selectivities the number of stages will not change as compared to the use of one membrane.

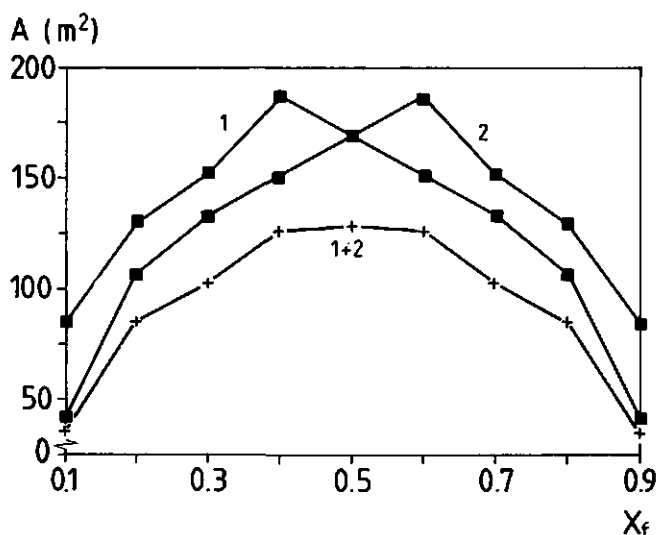


Figure 13. Membrane surface area versus feed concentration of a cascade constructed with membrane 1, membrane 2 and the optimum combination of membrane 1 and 2.  $\alpha_1=0.1$ ,  $\alpha_2=10$ , other conditions as mentioned at figure 5

## 7.5 CONCLUSIONS

Using a McCabe-Thiele diagram a cascade of membranes for the separation of a binary liquid mixture can be designed. Calculations have been carried out using an idealized membrane with a constant selectivity and permeability over the whole concentration range. Optimization of the cascade is performed using the total membrane surface area as criterion, although it has to be noted that especially for cascades consisting of many stages other factors may govern the choice of optimization criteria. It appeared, that in the feed stage the largest surface area is required, due to large reflux streams. Because of these large reflux streams, the permeate/retentate ratio of the feed stage has to be chosen carefully. The selectivity  $\alpha$  and permeability  $\phi$  influence the required

membrane surface area to a large extent: an increased selectivity (larger deviation from 1) and increased permeability result in a decreased surface area. However, an improved selectivity often goes with a decreased permeability. It appears, that for fluxes and permeabilities commonly found for RO membranes, an improvement of the permeability leads to a significantly larger decrease in membrane surface area than an improvement made on the selectivity. These effects were illustrated using different RO membranes for the separation of water/1,3-butanediol mixtures. A decrease of 25% of the total membrane surface area can be achieved using two membrane materials having the same permeability but an opposite selectivity, i.e. membranes that are selective for either one of the two components of the mixture. In this situation each stage can be equipped with the membrane with the appropriate selectivity.

## ACKNOWLEDGEMENTS

The authors wish to thank the Dutch Program Committee for Industrial Biotechnology (PCIB) for their financial support, B. Hasenack for performing the experiments and T. Robbertsen (NIZO) for the lab-scale RO module.

## LIST OF SYMBOLS

|                         |                          |                              |
|-------------------------|--------------------------|------------------------------|
| a                       | component a              |                              |
| b                       | component b              |                              |
| A                       | membrane surface area    | [m <sup>2</sup> ]            |
| Q                       | mass flow                | [kg/s]                       |
| $\text{tan} = -Q_p/Q_r$ | permeate/retentate ratio | [-]                          |
| X                       | mass fraction            | [-]                          |
| P                       | trans-membrane pressure  | [Pa]                         |
| [I]                     | stage number             |                              |
| [M]                     | feed stage               |                              |
| [1]                     | bottom stage             |                              |
| [N]                     | top stage                |                              |
| $\alpha$                | selectivity              | [-]                          |
| $\phi$                  | permeability             | [kg/(m <sup>2</sup> .s.bar)] |

subscripts



## chapter 7

|    |                          |
|----|--------------------------|
| f  | feed of the cascade      |
| p  | permeate                 |
| r  | retentate                |
| in | inflow of a single stage |

## REFERENCES

- 1) Metha, G.D., Comparison of membrane processes with distillation for alcohol-water separation, *J. Membrane Sci.* 12 (1982) 1-26
- 2) Tusel, G.F. and A. Ballweg, Verfahren und Vorrichtung zur Entwässerung von Gemischen aus organischen Flüssigkeiten und Wasser, German patent DE 3037736, 1980
- 3) Sourirajan, S. (ed.), *Reverse Osmosis: Theory, Technology, Engineering*, Ottawa, National Research Council, Canada, 1977
- 4) Cheryan, M., *Ultrafiltration Handbook*, Technomic Publishing Company, Inc., Lancaster, 1986
- 5) Sourirajan, S. and T. Matsuura, *Reverse Osmosis/Ultrafiltration Process Principles*, Ottawa, National Research Council, Canada, 1985
- 6) Garcia, A. III, E.L. Iannotti and J.L. Fischer, Butanol fermentation liquor production and separation by reverse osmosis, *Biotechnol. Bioeng.* 28 (1986) 785-791
- 7) Adam, W.J., B. Luke and P. Meares, The separation of mixtures of organic liquids by hyperfiltration, *J. Membrane Sci.* 13 (1983) 127-149
- 8) Mulder, M., Pervaporation, separation of ethanol-water and of isomeric xylenes, Thesis Twente University, 1984
- 9) Ward, W.J. III, Membrane gas separations - why and how, in: *Synthetic Membranes: Science, Engineering and Applications* (P.M. Bungay, H.K. Lonsdale and M.N. de Pinho (eds.)), NATO ASI Series, Series C: Mathematical and Physical Sciences, Vol. 181, D. Reidel Publishing Comp., Dordrecht, 1986
- 10) Agrawal, J.P. and S. Sourirajan, High flux freeze-dried cellulose-acetate reverse osmosis membranes as microporous barriers in gas permeation and separation, *J. Appl. Polymer Sci.* 14 (1970) 1303-1321
- 11) Weller, S. and W.A. Steiner, Engineering aspects of separation of gases: fractional permeation through membranes, *Chem. Eng. Progress* 46 (1950) 585-590
- 12) Schulz, G., H. Michele and U. Werner, Membrane rectification columns for gas separation and determination of the operating lines using the McCabe-Thiele diagram, *J. Membrane Sci.* 12 (1982) 183-194
- 13) Benedict, M., Multistage separation processes, *Trans. Am. Inst. Chem. Eng.* 2 (1947) 41-60
- 14) Hwang, S.T. and K. Kammermeyer, Operating lines in cascade separation of binary mixtures, *Canadian J. Chem. Eng.* 43 (1965) 36-39
- 15) Evangelista, F., Approximate design method for reverse osmosis plants equipped with imperfectly rejecting membranes, *Ind. Eng. Chem. Research* 26 (1987) 1109-1116
- 16) Choudhury, J.P., P. Ghosh and B.K. Guha, Separation of ethanol from ethanol-water mixture by reverse osmosis, *Biotechnol. Bioeng.* 27 (1985) 1081-1084
- 17) Tusel, G.F. and H.E.A. Bruschke, Use of pervaporation systems in the chemical industry, *Desalination* 53 (1985) 327-338
- 18) Thiel, S.W. and D.R. Lloyd, Multicomponent effects in the pressure driven membrane separation of dilute solutions of non-electrolytes, *J. Membrane Sci.* 42 (1989) 285-302
- 19) Kopecek, J. and S. Sourirajan, Performance of porous cellulose acetate membranes for the reverse osmosis

*chapter 7*

separation of mixtures of organic liquids, Ind. Eng. Chem. Proc. Des. Dev. 9 (1970) 5-12

- 20) Sourirajan, S., Separation of hydrocarbon liquids by flow under pressure through porous membranes, Nature 203 (1964) 1348-1349

## **CONCLUDING REMARKS; THE IMPROVEMENT OF MEMBRANE PERFORMANCE**

---

### **8.1 INTRODUCTION**

In this thesis, two processes for the removal of fatty acids from oil have been investigated. A characteristic property of both systems is the application of membranes in a two-phase environment. The process described in chapters 2 to 5 includes the separation of an emulsion, and the process described in chapters 6 and 7 is based on a membrane liquid-liquid extraction. The latter system also has to be completed with the separation of an emulsion, but this has not been investigated in detail.

In this last chapter, the methods described in this thesis for the separation of fat/fatty acid mixtures will be compared to other systems that serve the same purpose and that can be found in the literature. In order to assess the progress that has been made, the more generalized application of the principles described in this thesis applied to other membrane separation processes will be discussed. Since part of this thesis was concerned with the separation of an emulsion, factors affecting the separation of such systems will be discussed, this in relation to the wetting properties of the membrane. Finally, possible applications of membrane modifications will be discussed.

### **8.2 FAT/FATTY ACID SEPARATION**

The classical method for the separation of fatty acids from edible oil is the caustic refining process [1,2]. To compare the two membrane-based processes for fat/fatty acid separations with the caustic refining process on other than economical considerations, three parameters are of importance: losses of triglycerides, temperature and selectivity. In the caustic refining process, losses of triglycerides can be due to the saponification of triglycerides or can be due to inclusion of triglycerides into the soapstock [1,3,5]. For an application in the refining of edible oils, saponification of triglycerides should always be avoided, since a maximum yield of triglycerides is required. In order to reduce the losses due to saponification of triglycerides, a rather small

surplus of alkali should be applied [2]. The relatively low temperature used in the membrane process (20 °C versus 90 °C) also minimizes saponification losses. However, for an application in the (enzymatic) hydrolysis of oils, "losses" due to saponification can even be favorable for the process, since it results in an enhanced production rate of fatty acids. Inclusion of triglycerides into the soapstock should, however, for both applications be avoided. It was shown for the membrane separation systems that losses due to inclusion do not occur, resulting in rather pure product streams. In the classical caustic refining process a fatty acid free oil can be obtained. However, the soapstock usually contains about 50% triglycerides [1], which are difficult to regain.

Temperature is a factor of importance for the physical refining (distillation) of oils [5] and for the fractionation of fatty acid mixtures by distillation techniques [4]. High temperatures mainly affect unsaturated fatty acids, resulting in oxidation and/or polymerization reactions [4,6,7], a problem that can be avoided by the use of mild fractionation techniques such as panning and pressing [8,9] and solvent fractionation [10,11]. Disadvantages of those techniques are the extremely long reaction times (several days in the case of panning and pressing) and the relatively poor product quality. This introduces the factor selectivity, since pure product streams are required. It was shown in chapter 7, that the application of a membrane-based fractionation may result in rather pure product streams after relatively short times. Selectivity is due to differences in mobility inside the membrane matrix with a variation in fatty acid chain length. A clear disadvantage of the membrane fractionation is that it will be difficult to distinguish between fatty acids with the same number of carbon atoms but with different degrees of saturation. For this purpose, other mild separation techniques have to be developed. One example is the fractionation of fatty acid mixtures using cyclodextrin inclusion [12].

It can be concluded that the membrane-based separations as proposed in this thesis may offer advantages as compared to the classical fat/fatty acid separation processes in terms of reduced losses of triglycerides and mild process conditions. It has nevertheless to be noted that economical or safety considerations may change the feasibility of these processes.

### 8.3 EMULSION SEPARATIONS

In chapters 2 to 5 a system for the separation of a two-phase system has been described, resulting in relatively high fluxes over a broad range in phase composition. We should emphasize, however, that the emulsion used in those chapters has a phase behaviour that is not commonly found. In order to broaden the scope of applications of the knowledge generated here, the relation between

the phase characteristics of an emulsion and its permeation behaviour will be the first issue to be considered.

It was shown in chapter 5 that preferential wetting of the membrane was necessary to achieve separation of the oil phase from the emulsion. This condition was only fulfilled in the absence of adsorption of surfactant onto the membrane surface. If the surface is not completely wetted by only one of the two phases (i.e. the contact angle at the three phase boundary is larger than  $0^\circ$ ), it is difficult to retain the non-wetting liquid, as it can easily be forced through the pores. This is because the Laplace pressure over the liquid-liquid interface, which must prevent the non-wetting phase from entering the pores, decreases as the contact angle and, hence, the curvature of the interface decreases. In the case of a small Laplace pressure it can easily be exceeded by the pressure used for permeation of the continuous phase. It is advantageous to use a membrane with small pores, however, the permeation flux will then be reduced also.

#### Removal of the continuous phase

It appeared from chapter 2, that the permeation rate of the water phase strongly decreases at the transition from a continuous into a discrete water phase. We have performed similar experiments with emulsions with a known phase behaviour. Figure 1 shows an example where an emulsion of water in soy bean oil containing 1% Span 80 as emulsifier is used. The permeation rate of the oil through a PVDF ultrafiltration membrane (IRIS 3065, provided by Rhone Poulenc) is plotted versus the emulsion composition. At the transition from a continuous into a discrete oil phase, the flux drops almost stepwise to a value close to zero. Other experiments showed the same trends. These experiments reveal that this permeation behaviour is not only a property of the system studied in chapter 2, but is a more general property for the permeation through a membrane of one of the two phases of an emulsion.

Although this composition-flux relation may seem an important difficulty for an efficient separation, it does not prevent separation, since most emulsions show some hysteresis in their phase behaviour [13,14]. Hysteresis means that the history of the emulsion determines which of the two phases is the continuous one and which is the dispersed one. When the electrical conductivity of an emulsion containing water as the water phase and soy bean oil containing 1% Span 80 as the oil phase is measured, figure 2 is obtained. This figure indicates that hysteresis is found over a large composition interval. Starting with an oil in water emulsion with the composition belonging to concentration O in figure 2, the continuous water phase can be removed using a hydrophilic membrane up to the composition belonging to concentration B. Here the

emulsion changes from an oil in water (o/w) into a water in oil (w/o) emulsion (C), and now the continuous oil phase can be removed using a hydrophobic membrane until D is reached, where the emulsion changes back from w/o into o/w (A).

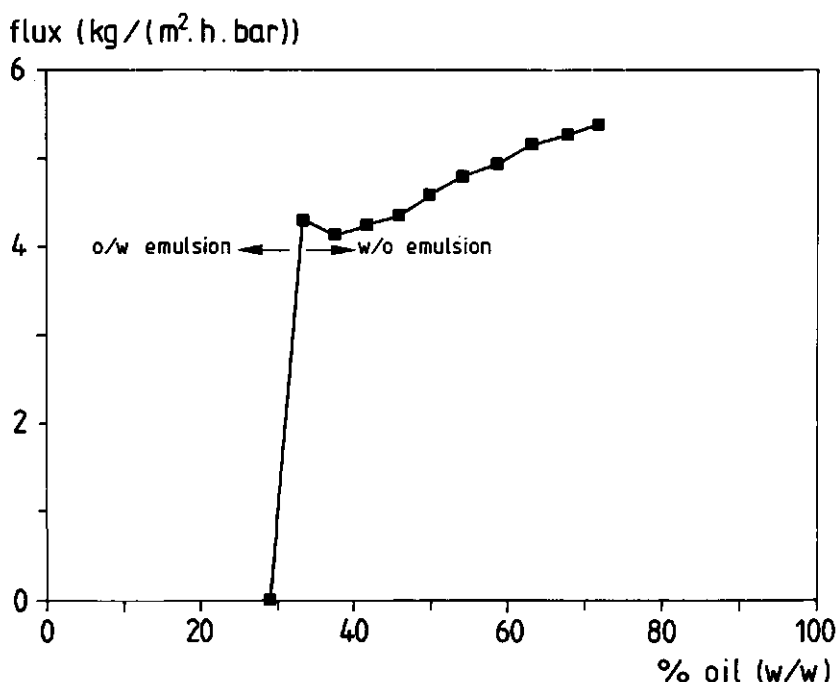


Figure 1. Permeation of the oil phase of a water-in-oil emulsion containing 1% Span 80 in the oil phase through a PVDF ultrafiltration membrane

#### Removal of the dispersed phase

In the literature several publications on the separation of emulsions are found, however, they are mainly concerned with the removal of the continuous (water) phase, resulting in a more concentrated emulsion [15,16]. It may, however, be preferable to remove the dispersed phase from an emulsion, especially when one is dealing with a particularly small volume of dispersed phase. One example one can think of is the removal of a trace amount of oil droplets from a waste water stream. For the permeation of the (continuous) water phase a large membrane area would be

required whereas the selective permeation of the dispersed oil phase would result in a significant reduction of the required surface area.

log (conductivity)

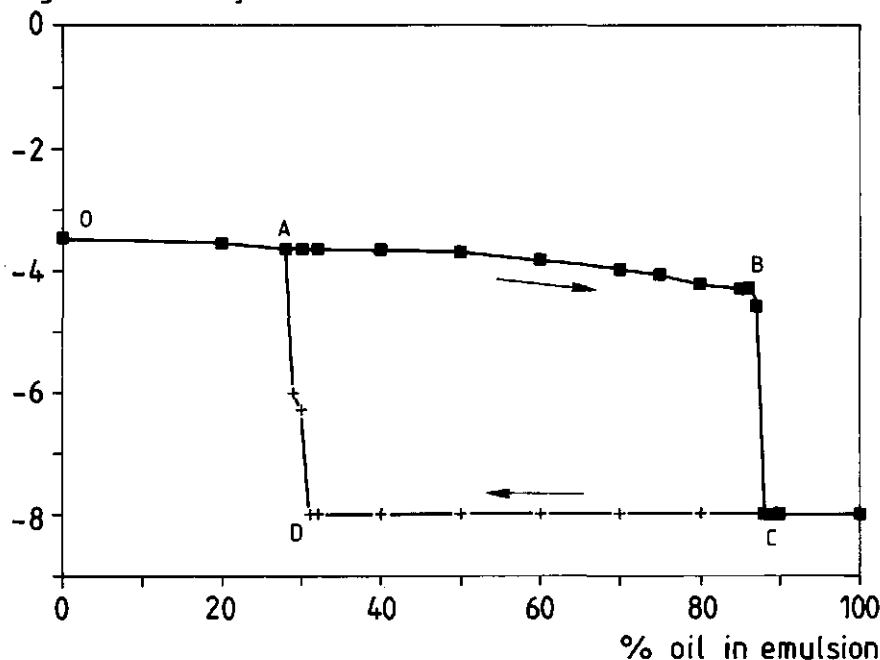


Figure 2. Conductivity of an emulsion containing 1% Span 80 in the oil phase versus composition

If the dispersed phase is to pass the membrane selectively, it must first of all preferentially wet the membrane material. This may appear simple at first sight, but the presence of surfactant in the system may lead to some surprises. We demonstrated the effect of surfactant adsorption on the wettability of a hydrophobic membrane for the separation of the oil phase from an emulsion in chapter 5.

The wetting condition being met, one has to consider the rate of separation. Two rate-determining steps can be recognised. The first step is transport of the dispersed droplets from the bulk to the membrane surface. Secondly, once a droplet has arrived at the membrane surface, it has to coalesce with the membrane or the liquid inside the membrane. Transport of (solid) particles from the bulk to the membrane surface is an important phenomenon in membrane fouling, and several publications deal with this subject [17,18]. They reveal that in a laminar flow, dispersed particles will not move towards the membrane surface, but will migrate towards the center of the duct, an

effect known as "tubular pinch" [19,20]. It is obvious that this phenomenon will reduce the droplet flux towards the membrane and that one must try to drive the droplets towards the membrane surface by an external field. Since emulsion droplets are usually charged, an electrical field will probably do [21].

A second point of interest is the rate of coalescence at the membrane surface. Although emulsion stability has been subject to extensive investigations [21,22], relations for stability and coalescence have mainly been derived for particles approaching a flat surface in a non-flowing medium [23]. Before coalescence, drainage of the film of continuous phase between two droplets (or a droplet and a surface) must occur. Once the film has reached a critical thickness, rupture occurs, followed by coalescence (figure 3a). When coalescence is the rate determining step, a fully occupied membrane surface can be obtained (figure 3b). For this situation Hartland and Vohra [24] determined the following relation for the time (t) required for coalescence:

$$t \propto \frac{a^2}{F} \quad (1)$$

where  $a$  is the area of the film where coalescence has to occur and  $F$  the force acting on the droplet. From this relationship it follows, that lateral coalescence (i.e. between adjacent drops) increases the time required for coalescence in the normal direction, since the liquid between the droplet and the membrane surface has to drain over a longer distance, due to an increased film area  $a$ . This implies, that coalescence with the membrane surface should be enhanced, whereas coalescence between adjacent droplets should be avoided.

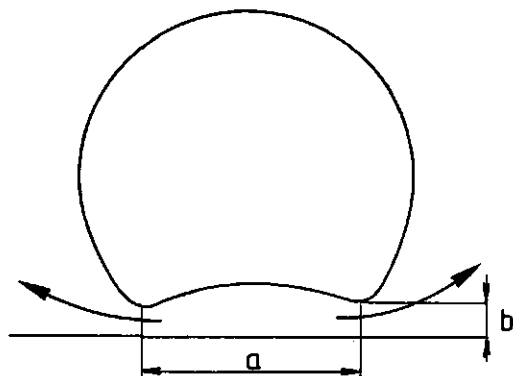


Figure 3a. *Approximate shape of a droplet at the oil/water interface*



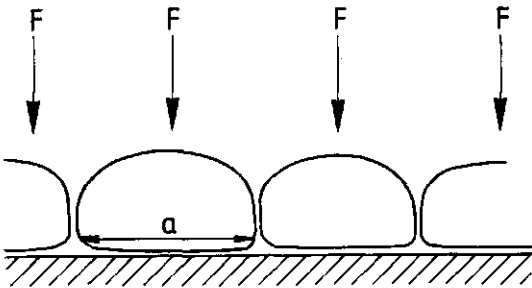


Figure 3b. *Emulsion droplets approaching the interface, subject to a vertical force*

Summarizing this section, it can be concluded that the removal of the continuous phase from an emulsion can be achieved easily when the membrane is preferentially wetted by this phase. For the removal of the dispersed phase, however, two phenomena that require further study can be recognized. Firstly, hydrodynamics of dispersion flow are important for the transport of emulsion droplets from the bulk towards the membrane. Secondly, the coalescence mechanisms are important once a droplet has arrived at the membrane surface. Which of the two is the rate determining process is difficult to predict, however, it certainly will depend on the nature of the emulsion.

#### 8.4 FOULING REDUCTION

For the system described in chapter 5 it appeared possible to avoid adsorption of the surfactant onto the membrane surface by adjusting the hydrophobicity of the surface. When adsorption of surface active agents could be avoided by adjusting the nature of the surface, this would offer the possibility to tailor membranes for a given application [29,30]. Modifying the membrane surface for the separation of an emulsion was already discussed in chapter 5. A second important application could be avoiding or minimizing fouling. Fouling of membrane materials is often due to the adsorption of proteins [27,28,43] or other surface active agents [31] and results in a decreased permeation rate.

In chapter 5 it also appeared possible to describe the adsorption of sodium oleate onto polymer surfaces in terms of hydrophobicity of the membrane surface. The adsorption of non-ionic surfactants onto polysulfone membranes was shown to be due to hydrophobic interactions [32,33]. For the adsorption of charged or very large molecules, however, other than hydrophobic

interactions may be important [41].

For the adsorption of proteins, van Oss et al. [34,35] showed that the adsorption and desorption behaviour merely depends on the hydrophobicity of the protein and the polymer surface, and they stressed that other effects can be neglected. On the other hand, Norde [36] and Grainger [37] showed that under many conditions, adsorption is driven by an increased entropy, which is partly due to conformation changes of the protein upon adsorption and partly due to the solvent. Others [38,39] showed that the amount of protein adsorbed onto various substrates strongly depends on pH, and thus on electrostatic interactions.

Tailoring the membrane surface would make it possible to obtain surfaces with relatively low fouling potential. Since it will often be impossible to adjust the nature of the solvent, it is generally impossible to avoid adsorption by choosing the proper solvent. Fouling may, however, be minimized by the use of a membrane material or coating that closely resembles the solvent. This means, that in order to minimize fouling from aqueous solutions a very hydrophilic material has to be used. This mechanism could be applied in order to minimize protein-membrane interactions by adjusting surface hydrophobicity [37,40], using copolymers in a way similar to the one described in chapter 5. The underlying mechanism has not yet been understood completely.

Electrostatic repulsion can also be used to minimize adsorption [41]. In the case of electrostatic repulsion it is usually impossible to avoid adsorption completely. The reason for this is that unfavorable electrostatic interactions are screened by a transfer of ions from solution to the adsorbed protein [42].

From these considerations it will be obvious, that it is difficult to avoid adsorption by adjusting only one parameter. Using an appropriate combination, however, one may perhaps obtain a significant decrease in fouling due to protein adsorption.

## 8.5 LIQUID-LIQUID EXTRACTIONS

For liquid-liquid extraction systems, where the function of the membrane is to stabilize the liquid-liquid interface, a low interfacial tension gives rise to problems. The Laplace pressure (which keeps the interface in place) is easily exceeded by an external pressure. This was shown for a membrane extraction of  $\alpha$ -amylase with a reversed micellar solution [25]. Reversed micellar systems exhibit an interfacial tension of  $10^{-4}$ – $10^{-7}$  mN/m [26], so that even in the case of a  $0^\circ$

contact angle, the maximum pressure the system can withstand is  $400 \text{ N/m}^2$  at a (maximum) pore size of  $1 \cdot 10^{-6} \text{ m}$ . It can be concluded, that the application of membrane-based liquid-liquid extractions will be limited by the Laplace pressure (which is determined by the maximum pore size) and by the size of the molecules to be extracted: molecules larger than the pore size will not be able to pass the membrane. It was shown in chapter 6 that a rather dense membrane matrix had to be used for the extraction of fatty acids from oil using 1,2-butanediol as extractant. These membranes, however, have too small pores for the extraction of proteins.

Modifications of the membrane surface can also be used in order to improve the stability of solid-supported liquid membranes (SLM's). Instability of this type of membranes is mainly caused by the disappearance of the membrane liquid from the pores of the support. This results in a reduced permeability of the membrane due to lost carrier, or in a disappearance of the membrane function [44,45,46]. Several methods have been proposed to solve this problem, most of them attempting to replenish the liquid that has been lost from the pores [47,48]. Since these methods tend to conceal leakage of the membrane liquid only, the method proposed by Neplenbroek [49] has to be preferred. He used a (partially) gelled membrane liquid in order to prevent leakage of the membrane liquid. Indeed, an improved stability was observed, however, this gel layer may constitute a supplementary barrier to mass transport, especially when large molecules such as proteins have to be transported.

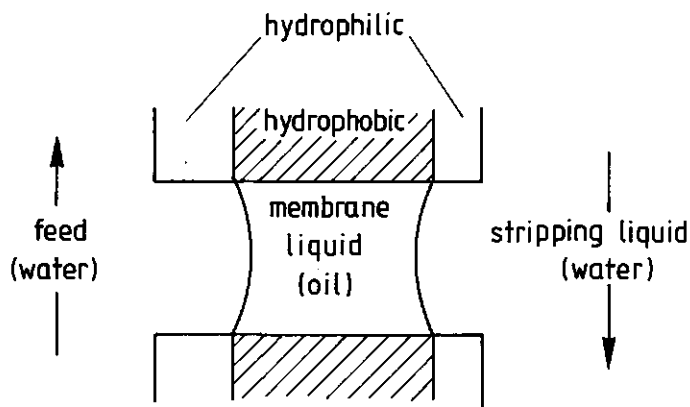


Figure 4a. *Solid-supported liquid membrane in a three-layer sandwich membrane. The membrane consists of a hydrophobic polymer membrane which contains the membrane liquid and two hydrophilic layers on top of the hydrophobic membrane*

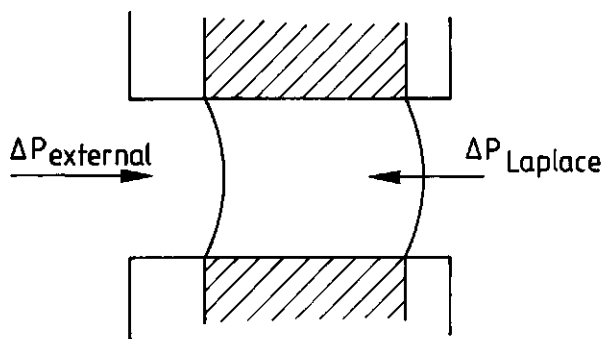


Figure 4b. *The liquid membrane of figure 4a when subject to an external force*

Instabilities of solid-supported liquid membranes are mainly caused by two effects. Firstly, liquid may be forced out of the supporting membrane [50,51] by too high trans-membrane pressures. This may e.g. occur as a result of the pressure drop over the length of the fibers in hollow fiber systems. Secondly, shear forces may result in emulsification of the membrane liquid into the feed or stripping solution [52]. In order to avoid these two effects, we would suggest to modify a microporous support as follows. When both sides of the (usually hydrophobic) membrane are coated with a hydrophilic layer, a composite membrane as shown schematically in figure 4a is obtained. Since the liquid-liquid interface is situated inside the pores, shear forces will hardly affect it and emulsion formation will be retarded significantly. More important, however, is the fact that such a system is self-correcting with respect to pressure variations. When an excess pressure is applied onto one of the two sides (figure 4b), the membrane liquid is forced towards the hydrophilic part of the pore. Since the hydrophilic part is poorly wetted by the membrane liquid (i.e. exhibits a contact angle close to  $0^\circ$ ), the Laplace pressure will counteract the external pressure. In this way a pressure of  $5 \cdot 10^5 \text{ N/m}^2$  can be withstood for pores with a  $0.1 \text{ }\mu\text{m}$  pore radius and a liquid-liquid interfacial tension of  $25 \text{ mN/m}$ . Even though the gelled liquid membrane was apparently capable to withstand larger pressure differences, one may expect that already before breakthrough a significant part of the membrane liquid will have spread over the membrane surface, and will be lost due to emulsification.

## 8.6 CONCLUSIONS

In this chapter some implications of the fat/fatty acid separation processes as described in this

## chapter 8

thesis are discussed. It can be concluded, that for the separation of an emulsion it is often more interesting to remove the dispersed phase instead of the continuous phase, although new problems will occur, due to hydrodynamic and physico-chemical effects. Adsorption onto the membrane is an important parameter in fouling, which might be minimized or even completely avoided by modifications of the membrane surface. It can also be concluded that mechanisms other than size exclusion are important for the use of membranes in separation processes. Liquid membranes and membrane-based extractions illustrate this in many ways.

## REFERENCES

- 1) Braae, B., Degumming and refining practices in Europe, *J. Am. Oil Chem. Soc.* 53 (1976) 353-357
- 2) Carr, R.A., Degumming and refining practices in the U.S., *J. Am. Oil Chem. Soc.* 53 (1976) 347-352
- 3) Forster, Physical refining, *J. Am. Oil Chem. Soc.* 60 (1983) 217A-223A
- 4) Stage, H., Fatty acid fractionation by column distillation: purity, energy consumption and operating conditions, *J. Am. Oil Chem. Soc.* 61 (1984) 204-214
- 5) Francois, R. (ed.), *Les Industries des Corps Gras*, Soc. P.I.C., Genève, 1974
- 6) D. Swern, J.T. Scanlan and H.B. Knight, Mechanism of the reactions of oxygen with fatty materials. Advances from 1941 to 1946, *J. Am. Oil Chem. Soc.* 25 (1948) 193-200
- 7) Tsuchiya, T., Biochemistry of fish oil, in: *Fish as Food*, G. Borgstrom (ed.), 1961
- 8) Combs, D.L., Processing for industrial fatty acids-I, *J. Am. Oil Chem. Soc.* 62 (1985) 327-330
- 9) Zilch, K.T., Separation of fatty acids, *J. Am. Oil Chem. Soc.* 56 (1979) 739A-742A
- 10) Demunerle, R.L., Emersol process- a staff report, *Ind. Eng. Chem.* 39 (1947) 126-131
- 11) Gloyer, S.W., Furans in vegetable oil refining, *Ind. Eng. Chem.*, 40 (1948) 228-236
- 12) Boswinkel, G., B. van der Meer, J.T.F. Keurentjes and K. van 't Riet, Membrane Techniques in Biotechnology, in: *Agricultural Biotechnology in Focus in the Netherlands*, J.J. Dekkers et al. (eds.), Pudoc, 1990
- 13) Salager, J.-L., Phase transformation and emulsion inversion on the basis of catastrophe theory, in: *Encyclopedia of Emulsion Technology*, Vol 3, Basic theory, Measurement, Applications, P. Becher (ed.), Marcel Dekker, Inc. New York, 1988
- 14) Becher, P., The effect of the nature of the emulsifying agent on emulsion inversion, *J. Soc. Cosm. Chem.* 1 (1950) 141-148
- 15) Lipp, P., C.H. Lee, A.G. Fane and C.J.D. Fell, A fundamental study of the ultrafiltration of oil-water emulsions, *J. Membrane Sci.* 36 (1988) 161-177
- 16) Kutowy, O., W.L. Thayer, J. Tigner and S. Sourirajan, Tubular cellulose acetate reverse osmosis membranes for treatment of oily wastewaters, *Ind. Eng. Chem., Prod. Res. Dev.* 20 (1981) 354-361
- 17) Altena, F.W. and G. Belfort, Lateral migration of spherical particles in porous flow channels: application to membrane filtration, *Chem. Eng. Sci.* 39 (1984) 343-355
- 18) Bentría, M. and D.A. Drew, Fouling layer growth and distribution at the interface of pressure-driven membranes, *Chem. Eng. Sci.* 45 (1990) 1223-1235
- 19) Segré, G. and A. Silberberg, Radial particle displacements in Poiseuille flow of suspensions, *Nature* 189 (1961) 209-210
- 20) Segré, G. and A. Silberberg, Behaviour of macroscopic rigid spheres in Poiseuille flow. Part 2, Experimental results and interpretation, *J. Fluid Mech.* 14 (1962) 136-157
- 21) Allan, R.S. and S.G. Mason, effects of electric fields on coalescence in liquid-liquid systems, *Trans. Faraday Soc.*

- 57 (1961) 2027-2040
- 22) Chappelaer, D.C., Models for a liquid drop approaching an interface, *J. Colloid Sci.*, 16 (1961) 186-190
- 23) Tadros, Th.F. and B. Vincent, Emulsion Stability, in: *Encyclopedia of Emulsion Technology*, Vol 1, Basic theory, P. Becher (ed.), Marcel Dekker, New York, 1983
- 24) Hartland, S. and D.K. Vohra, Effect of interdrop forces on the coalescence of drops in close-packed dispersions, *J. Colloid Interface Sci.* 77 (1980) 295-316
- 25) Dekker, M., P.H.M. Koenen and K. van 't Riet, Reversed micellar-membrane-extraction of enzymes, *Inst. Chem. Eng. Symp. Series, Advances in separation processes* (1990) 7.01-7.12
- 26) Kahlweit, M. et al., How to study microemulsions, *J. Colloid Interface Sci.* 118 (1987) 436-453
- 27) Horst, H.C. van der and J.H. Hanemaaijer, Cross-flow microfiltration in the food industry. State of the art, *Desalination* 77 (1990) 235-258
- 28) Aimar, P., S. Bahlonti and V. Sanchez, Membrane-solute interactions: influence on pure solvent transfer during ultrafiltration, *J. Membrane Sci.* 29 (1986) 207-224
- 29) Baier, R.E., Modifications of surfaces to reduce fouling and/or reduce cleaning, *Proc. Workshop Fund. and Appl. of Surface Phenomena associated with Fouling and Cleaning in Food Processing*, Tylösand, Halmstad, Sweden, 1981
- 30) Bauser, H., H. Chmiel, N. Stroh and E. Walitza, Control of concentration polarization and fouling of membranes in medical, food and biotechnical applications, *J. Membrane Sci.* 27 (1986) 195-202
- 31) P.M. van der Velden and C.A. Smolders, Solute/membrane interactions of sodium dodecyl sulfate with uncharged and cation exchange membranes, *J. Colloid Interface Sci.* 61 (1977) 446-454
- 32) Wolff, J., H. Steinhauser and G. Ellinghorst, Tailoring of ultrafiltration membranes by plasma treatment and their application for the desalination and concentration of water-soluble organic substances, *J. Membrane Sci.* 36 (1988) 207-214
- 33) Fontyn, M., J.A.M. Stoots, M.F.J.M. Verhagen, M.A. Geluk, K.van 't Riet and B.H. Bijsterbosch, Characterization of polymer adsorption on ultrafiltration membranes by permeation and adsorption, submitted
- 34) Van Oss, C.J., D.R. Absolom, A.W. Neumann and W. Zingg, Determination of the surface tension of proteins. I. Surface tension of native serum proteins in aqueous media, *Biochimica Biophysica Acta* 670 (1981) 64-73
- 35) Absolom, D.R. and A.W. Neumann, Modification of substrate surface properties through protein adsorption, *Colloids Surfaces* 30 (1988) 25-45
- 36) W. Norde, Adsorption of proteins from solution at the solid-liquid interface, *Adv. Colloid Interface Sci.* 25 (1986) 267-340
- 37) Grainger, D.W., T. Okano and S.W. Kim, Protein adsorption from buffer and plasma onto hydrophilic-hydrophobic poly(ethylene oxide)-polystyrene multiblock copolymers, *J. Colloid Interface Sci.* 132 (1989) 161-175
- 38) Matthiasson, E., The role of macromolecular adsorption in fouling of ultrafiltration membranes, *J. Membrane Sci.* 16 (1983) 23-36
- 39) Fane, A.G., C.J.D. Fell and A. Suki, The effect of pH and ionic environment on the ultrafiltration of protein solutions with retentive membranes, *J. Membrane Sci.* 16 (1983) 195-210
- 40) Horbett, T.A., Adsorption of blood proteins from plasma to a series of hydrophilic-hydrophobic copolymers. II Compositional analysis with the prelabeled protein technique, *J. Biomed. Mater. Res.* 15 (1981) 673-695
- 41) Fraaije, J.G.E.M., Interfacial thermodynamics and electrochemistry of protein partitioning in two-phase systems, Thesis, Wageningen Agricultural Univ., 1987
- 42) Norde, W., Ion participation in protein adsorption at solid surfaces, *Colloids Surfaces* 10 (1984) 21-31
- 43) Hanemaaijer, J.H., T. Robbertsen, T.H. van de Boomgaard and J.W. Gunnink, Fouling of ultrafiltration membranes. The role of protein adsorption and salt precipitation, *J. Membrane Sci.* 40 (1989) 199-217
- 44) Danesi, P.R., Supported liquid membranes in 1986: new technology or scientific curiosity?, *Int. Solvent Extr. Conf. Munich* 11-16 september, 1986

## *chapter 8*

- 45) Gallagher, P.M., A.L. Athayde and C.F. Ivory, Electrochemical coupling in carrier-mediated membrane transport, *J. Membrane Sci.* 29 (1986) 49-67
- 46) Tanigaki, M., M. Ueda and W. Eguchi, Facilitated transport of zinc chloride through hollow fiber supported liquid membrane. Part II. Membrane stability, *Sep. Sci. Technol.* 23 (1988) 1161-1169
- 47) Danesi, P.R. and P.G. Rickert, Some observations on the performance of hollow-fiber supported liquid membranes for cobalt-nickel separations, *Solvent Extr. Ion Exch.* 4 (1986) 149-164
- 48) Nakano, M., K. Takahashi and H. Takeuchi, A method for continuous operation of supported liquid membranes, *J. Chem. Eng. Japan* 20 (1987) 326-328
- 49) Neplenbroek, A.M., Stability of supported liquid membranes, Thesis, Twente University, 1989
- 50) Dworzak, W.R. and A.J. Naser, Pilot-scale evaluation of supported liquid membranes, *Sep. Sci. Technol.* 22 (1987) 677-689
- 51) Takeuchi, H., K. Takahashi and W. Goto, Some observations on the stability of supported liquid membranes, *J. Membrane Sci.* 34 (1987) 19-31
- 52) Walstra, P., Formation of emulsions, in: *Encyclopedia of Emulsion Technology*, Vol.1, Basic Theory, P. Becher (ed.) Marcel Dekker Inc., New York, 1988

## SUMMARY

---

Fatty acids have to be removed from non-mineral oil for several purposes. In the refining of edible oils and fats they have to be removed as a contaminant. In the enzymatic hydrolysis of oils, a high content in fatty acids results in a reduced conversion rate. In order to maintain a sufficiently high reaction rate they will have to be removed, preferably in-line. The conventional separation method is the caustic refining process, in which alkali is added to the fatty acid containing oil, resulting in the formation of the sodium salts of the fatty acids (soapstock). Then the soapstock is separated from the oil by centrifugation. However, this soapstock contains considerable amounts of triglycerides (about 50%), which have to be considered as a loss. For this reason, caustic refining of oils containing high concentrations of fatty acids is not an economical process.

In this thesis two alternative processes for the separation of fatty acids from oil are presented, with the common feature that membranes are used in a two-phase environment. It is the aim of this thesis to study the engineering and physico-chemical phenomena that are relevant for the operation of these processes.

In the first process, alkali is added to the oil in order to form the sodium salts of the fatty acids. Additionally, 2-propanol is added to solubilize the soapstock thus formed, resulting in a two-phase system. The water phase contains the fatty acid salts dissolved in a water/2-propanol mixture and the oil phase merely contains triglycerides and a trace amount of 2-propanol. This two-phase system can be separated into its two phases by a hydrophilic and a hydrophobic membrane in series.

In chapter 2 the nature of the two-phase system and the permeation behaviour of the water phase through the hydrophilic membrane have been investigated. It appears, that both the oil and the water phase are present as a continuous phase between 20 and 65% water phase in the dispersion. Above 20% water phase, the flux through the membrane is merely determined by the hydrodynamic membrane resistance, provided that the membrane is entirely wetted by the water phase. Below 20% water phase, the water phase is present as dispersed droplets in oil. At the transition from a continuous into a discrete water phase the permeation flux drops almost stepwise to a value close to zero.



### *summary*

When in the system described in chapter 2, a concentrated NaCl solution is circulated at the permeate side of the cellulose membrane, initially a flux reversed to the normal permeation flux is observed. After some time the flux changes direction and becomes 2 to 10 times larger than it would be based on the pressure difference over the membrane. These effects cannot be accounted for using the classical Fickian diffusion theory. In chapter 3 it is shown that the flux changes can be explained qualitatively using the Maxwell-Stefan diffusion theory.

It appeared, that commercially available hydrophobic membranes were incapable of separating the oil phase from this dispersion. As the preliminary requirement to solve this problem, chapter 4 describes a method that has been developed to measure hydrophobicities of membranes. When a piece of membrane is submerged in a liquid, air bubbles will adhere to the membrane when the surface tension of the liquid is high. Decreasing the surface tension of the liquid yields a transition from adhesion to non-adhesion. The surface tension of the liquid at which this transition occurs can be compared to the critical surface tension as is commonly used to characterize polymeric surfaces.

In chapter 5 the adsorption is measured of a surfactant in water/2-propanol mixtures onto surfaces that vary in hydrophobicity. Adsorption appears to occur in three regions: "tail down" adsorption on hydrophobic surfaces, "head down" adsorption on hydrophilic surfaces, and a very small region in between, where adsorption is absent. A membrane that possesses a hydrophobicity belonging to this region appears to be capable of separating the oil phase from the dispersion selectively.

The second system for the removal of fatty acids from oil consists of a membrane extraction step, using 1,2-butanediol as a selective extractant. When water is added to the fatty acid containing 1,2-butanediol, the system demixes in a fatty acid phase dispersed in a 1,2-butanediol/water mixture. After phase separation, water has to be removed from the 1,2-butanediol, which can be reused as extractant. In chapter 6 extraction of fatty acids from oil has been investigated. In order to obtain a stable system, it is necessary to use rather dense membranes. This results in relatively high mass transfer resistances and hence in large surface areas for extraction. Due to the fact that the mass transfer coefficients vary significantly with fatty acid chain length, it appears to be possible to fractionate a fatty acid mixture.

In chapter 7 membrane cascades for the separation of binary mixtures have been investigated. Calculations based on a McCabe-Thiele diagram show that, for permeabilities and selectivities commonly found for reverse osmosis membranes, permeability is the parameter on which improvements have to be made when a minimum total membrane surface area is required.

### *summary*

Finally, in chapter 8 some implications of the work described in this thesis have been discussed. The two systems described for the separation of fatty acids from oil are capable to perform this separation selectively and at mild conditions. Two future implications that require further investigations are discussed. The first one is the separation of emulsions using membranes. Secondly, tailoring membranes for special applications and in order to reduce fouling are possible applications that require further investigations.

## **SAMENVATTING**

---

Vetzuren dienen uit eetbare olie te worden verwijderd om verschillende redenen. Bij de raffinage van oliën en vetten dienen ze te worden verwijderd als ongewenste component, terwijl bij de enzymatische hydrolyse van oliën en vetten de vetzuren als gewenst produkt moeten worden geïsoleerd. Dit omdat bij de hydrolyse een hoog vetzuurgehalte de reactiesnelheid sterk verlaagt. De klassieke ontzuring van olie vindt plaats in het zogenaamde "caustic refining" proces. Hierbij wordt een loogoplossing aan de olie toegevoegd waarbij de natriumzouten van de vetzuren worden gevormd, de zogeheten soapstock. Deze wordt vervolgens afgescheiden van de olie met behulp van centrifuges. Deze methode resulteert in verliezen van triglyceriden, omdat de zeepmassa na afscheiding uit de olie nog een aanzienlijke hoeveelheid triglyceriden bevat (ongeveer 50%). Om deze reden is dit proces niet geschikt voor het ontzuren van olie met een hoog vetzuurgehalte. In dit proefschrift worden twee processen beschreven voor het afscheiden van vetzuren uit olie waarbij deze verliezen geminimaliseerd worden. De twee processen hebben als gemeenschappelijk kenmerk, dat membranen worden gebruikt in combinatie met twee niet mengbare vloeistoffasen. Het doel van het werk zoals beschreven in dit proefschrift is het bestuderen van procestechnologische en fysisch chemische parameters die van belang zijn voor het bedrijven van deze twee processen.

In het eerste proces wordt, analoog aan het klassieke proces, een loogoplossing toegevoegd aan de olie. Vervolgens wordt ook 2-propanol toegevoegd, waarbij de gevormde zeep weer in oplossing gaat en een emulsie wordt gevormd. De waterfase bevat dan de zeep opgelost in een water/2-propanol mengsel en de oliefase bestaat uit olie met een spoortje 2-propanol. Dit tweefasen systeem kan worden gescheiden in de twee afzonderlijke fasen met behulp van een hydrofoob en een hydrofiel membraan.

In hoofdstuk 2 is het gevormde tweefasen systeem gekarakteriseerd, alsmede het permeatiegedrag van de waterfase door het hydrofiel membraan. Het blijkt, dat zowel de waterfase als de oliefase, als continue fase aanwezig zijn tussen 20 en 65% waterfase in de emulsie. Wanneer het membraan volledig door de waterfase wordt bevochtigd wordt boven 20% waterfase in de emulsie de flux door het membraan louter bepaald door de hydrodynamische weerstand van het membraan. Beneden 20% waterfase in de emulsie is de waterfase aanwezig als gedispergeerde deeltjes in olie. Bij de overgang van een continue naar een disperse waterfase neemt de flux nagenoeg stapsgewijs af tot een waarde van ongeveer nul. In hoofdstuk 3 zijn multicomponent diffusieverschijnselen

### *samenvatting*

in cellulose membranen bestudeerd. Wanneer een geconcentreerde NaCl-oplossing wordt gecirculeerd aan de permeaatzijde van het membraan, wordt in eerste instantie een flux tegen de transmembraandruk in waargenomen. Deze verandert na enige tijd van richting en wordt dan 2 tot 10 keer groter dan de flux die hoort bij de aangelegde transmembraandruk. Deze effecten kunnen niet verklaard worden wanneer de klassieke Fick diffusietheorie wordt gebruikt, echter wel met behulp van de Maxwell-Stefan diffusietheorie.

Het is gebleken, dat geen commercieel verkrijgbaar hydrofoob membraan in staat is om de oliefase selectief uit de emulsie af te scheiden. Om dit probleem op te lossen is allereerst een methode ontwikkeld om de hydrofobiciteit van membranen te meten, als beschreven in hoofdstuk 4. Wanneer een stukje hydrofoob membraan wordt ondergedompeld in een vloeistof en luchtbellen worden in contact gebracht met het oppervlak, dan zullen deze hechten wanneer de oppervlaktespanning van de vloeistof hoog is. Wordt de oppervlaktespanning van de vloeistof verlaagd, dan wordt een punt gepasseerd waarbeneden geen hechting meer plaatsvindt. De oppervlaktespanning die behoort bij deze overgang kan vergeleken worden met de kritische oppervlaktespanning die vaak gebruikt wordt om polymeeroppervlakken te karakteriseren.

In hoofdstuk 5 is adsorptie van zeep aan oppervlakken met verschillende hydrofobiciteiten gemeten, vanuit water/2-propanol mengsels. Adsorptie blijkt plaats te vinden in drie gebieden: met de staarten naar het oppervlak op hydrofobe oppervlakken; met de koppen naar het oppervlak bij hydrofiële oppervlakken en een zeer klein gebiedje daartussen waarin geen adsorptie optreedt. Wanneer een membraan wordt gemaakt met de hydrofobiciteit die behoort bij dit kleine gebiedje kan de oliefase selectief worden afgescheiden uit de emulsie.

Het tweede systeem bestaat uit een extractie met behulp van een membraan met 1,2-butaandiol als extractiemiddel. Wanneer water wordt toegevoegd aan de vetzuurbevattende 1,2-butaandiol, ontmengt het systeem en wordt een dispersie van vetzuren in 1,2-butaandiol/water gevormd. Na fasescheiding moet het water worden verwijderd uit de 1,2-butaandiol, hetgeen dan weer als extractiemiddel gebruikt kan worden. In hoofdstuk 6 is de extractie van vetzuren uit olie bestudeerd. Om een stabiel systeem te verkrijgen is het nodig relatief dichte membranen te gebruiken, hetgeen resulteert in hoge stofoverdrachtsweerstand en daardoor in grote membraanoppervlakken voor extractie. Omdat de stofoverdrachtscoëfficiënten sterk variëren met de lengte van de vetzuurketen kan een vetzuurmengsel gefractioneerd worden. In hoofdstuk 7 zijn berekeningen aan membraancascades voor de scheiding van binaire mengsels gedaan op basis van een McCabe-Thiele diagram. Het blijkt, voor selectiviteiten en permeabiliteiten die gevonden worden voor omgekeerde osmose, dat de permeabiliteit de belangrijkste parameter is wanneer een

### *samenvatting*

minimaal oppervlak van de cascade gewenst is.

In hoofdstuk 8 worden enkele implicaties van het in dit proefschrift beschreven werk besproken. De twee systemen voor de afscheiding van vetzuren uit olie zijn in staat dit selectief en onder milde condities te doen. Emulsiescheidingen met behulp van membranen en het aanpassen van membraanoppervlakken om vervuiling te verminderen of geheel te voorkomen zijn mogelijke toepassingen die verder onderzoek behoeven.

## CURRICULUM VITAE

---

Johannes Theodorus Faustinus Keurentjes werd geboren op 15 februari 1963 te Rheden. In 1981 behaalde hij het VWO-diploma aan het Thomas a Kempis College te Arnhem. In datzelfde jaar begon hij met zijn studie aan de toenmalige Landbouwhogeschool in Wageningen.

In 1984 legde hij het kandidaatsexamen in de richting Milieuhygiëne/Waterzuivering met lof af. Het vakkenpakket in de doctoraalfase omvatte Waterzuivering (verzwaard hoofdvak) en Kolloïdchemie (hoofdvak). Zijn stageperiode bracht hij door bij het Zuiveringsschap Hollandse Eilanden en Waarden in Dordrecht en een gecombineerde afstudeeropdracht/stage voerde hij uit aan de Ecole Nationale de la Santé Publique in Rennes, Frankrijk. In september 1986 studeerde hij met lof af.

Van oktober 1986 tot oktober 1990 was hij werkzaam aan de sectie Proceskunde van de Landbouwniversiteit in Wageningen waar het onderzoek zoals beschreven in dit proefschrift werd uitgevoerd.

In 1990 werd hem een DSM prijs voor Chemie en Technologie uitgereikt. Vanaf oktober 1990 is hij werkzaam bij de afdeling Fysische en Chemische Technologie van AKZO Research in Arnhem.